

**Application of Non-Linear Time Series  
Models to Power Risk Management:  
A Case Study for Germany**

Inauguraldissertation

zur

Erlangung des Doktgrades

der

Wirtschafts- und Sozialwissenschaftlichen Fakultät

der

Universität zu Köln

2007

vorgelegt

von

Diplom-Volkswirt Peter Kosater

aus

Berent/Polen

**Referent: Prof. Dr. Karl Mosler**

**Korreferent: Prof. Dr. Eckart Bomsdorf**

**Tag der Promotion: 9.02.07**

## Vorwort

Diese Arbeit ist das Ergebnis eines Projektes im Rahmen des Graduiertenkollegs Risikomanagement an der Universität zu Köln, an dem ich das Glück hatte, in den Jahren 2003 bis 2006 teilnehmen zu dürfen.

Wie im täglichen Leben allgemein wäre diese Arbeit nicht ohne die Hilfe anderer zustande gekommen. Als erste und wichtigste Bezugsperson möchte ich meinen Doktorvater Prof.Dr.Karl Mosler danken für die fachliche und finanzielle Unterstützung als auch insbesondere die kritischen Kommentare zu den Arbeitspapieren, die im Verlauf der Dissertation entstanden sind.

Weiterhin danke ich Prof.Dr.Alexander Kempf stellvertretend für die das Graduiertenkolleg tragenden Professoren sowie die DFG, die in einer gemeinsamen Kraftanstrengung das Graduiertenkolleg aus der Taufe gehoben haben. Im Rahmen der Promotion innerhalb des Kollegs habe ich inhaltliche und persönliche Qualifikationen erworben, die mir auch im beruflichen Alltag nach Abschluss der Promotion hilfreich sind, obwohl ich selbst während der Promotionsphase nicht daran geglaubt hatte.

Schließlich möchte ich noch Prof.Dr.Eckart Bomsdorf für die Übernahme des Korreferats und die kritischen Kommentare sowie Prof.Dr.Dieter Hess für die Übernahme des Vorsitzes bei meiner Disputation danken.

Ferner möchte ich meinen Kollegen aus den verschiedenen Kohorten danken. Besonders erwähnt seien Daniel Mayston für die Nachhilfe im Verfassen englischsprachiger Zeitschriftenartikel sowie Martin Honal und Tanja Thiele für viele Gespräche, die geholfen haben über die vielen Selbstzweifel während der Arbeit hinwegzukommen. Den Teilnehmern des Oberseminars der beiden Statistiklehrstühle danke ich für die hilfreichen Kommentare.

Eine gute Promotion ist offen für Impulse von außerhalb. Deshalb möchte ich stellvertretend vor allem Dr. Cyriel de Jong von der Erasmus Universität in Rotterdam für seine Hilfe danken. Bedankt voor jouw hulp, Cyriel. Hoe je ziet, ik heb nu toch een beetje Nederlands geleerd.

Eine Promotion wirkt sich bis in den privaten Bereich aus. Deshalb möchte ich im speziellen Anna Cellarova für Ihren seelischen Beistand danken. Ďakujem ti a prajem ti ťsetko najlepšie.

Abschliessend möchte ich meiner Familie und da vor allem meiner Mutter für die Unterstützung danken.

## Abstract

As a consequence of the ongoing liberalization process, sensible management in the electricity sector has to take into account the market price risk as well as volume risks.

Market price risk mainly arises due to the scarce storability of electricity which causes spot prices to be highly volatile. Secondly, the demand for electricity strongly depends on weather conditions. Electricity suppliers sell less power during mild winters than expected beforehand. Consequently, the suppliers are faced with volume risks.

To cope with the market price risk suitable models of the spot price are required. These models can be exploited for pricing of derivatives on the electricity spot price as the underlying on one hand and the short term optimization of the production schedule on the other hand.

In the first part of the thesis, the author discusses some of the existing approaches to the modelling of spot prices and puts forward a new approach. In addition, he examines the impact of weather on electricity spot prices.

In the second part of the thesis, the author discusses bivariate modelling of temperature time series which is crucial for cross-city hedging with weather derivatives. Weather derivatives are financial instruments which allow to hedge against volume risks emerging from unforeseen weather conditions.

## Zusammenfassung

Die Liberalisierung des Energiesektors stellt Energiemanager vor neue Aufgaben. Sie müssen sich mit Marktpreis- und Mengenrisiken auseinandersetzen.

Marktpreisrisiken spiegeln sich in der hohen Volatilität der Spotpreise wider, die hauptsächlich in der Nichtspeicherbarkeit von Strom begründet ist. Ferner ist die Nachfrage nach Strom stark wetterabhängig. Während milder Winter wird weniger Strom abgesetzt als erwartet. Folglich sind Stromproduzenten auch einem Mengenrisiko ausgesetzt.

Um sich gegen Marktpreisrisiken abzusichern, sind geeignete Modelle für den Spotpreis notwendig. Diese Modelle können zur Bewertung von Derivaten auf dem Spotpreis als dem Underlying einerseits und zur operationalen Kurzfristoptimierung andererseits eingesetzt werden.

Im ersten Teil der Arbeit diskutiert der Verfasser ausgewählte bestehende Ansätze zur Spotpreismodellierung und stellt einen neuen Ansatz vor. Außerdem untersucht der Verfasser den Einfluss von Wetter auf die Spotpreise.

Im zweiten Teil der Arbeit, wird die Bivariate Modellierung von Temperaturzeitreihen diskutiert. Dies ist von Bedeutung für Cross-city hedging mit Wetterderivaten. Wetterderivate sind Finanzinstrumente, die es erlauben sich gegen Mengenrisiken hervorgerufen durch unvorhergesehene Wetterbedingungen abzusichern.

# Contents

<b>1</b>	<b>Introduction</b>	<b>11</b>
<b>2</b>	<b>Markov Regime-Switching Models for Electricity Spot Prices</b>	<b>14</b>
2.1	Review of Literature on Electricity Spot Prices . . . . .	14
2.2	Data and Descriptive Statistics . . . . .	16
2.3	Stochastic Models for Power Prices . . . . .	20
2.3.1	AR(1) Process with Drift . . . . .	20
2.3.2	The Jump Model . . . . .	20
2.3.3	A Markov Regime-Switching Model for Spot Prices: Ethier and Mount(1998) . . . . .	22
2.3.4	Two-Regime Model with Independent Spikes : De Jong and Huisman (2003) . . . . .	23
2.3.5	Estimation of Markov Regime-Switching Models . . . . .	24
2.3.6	Regime-Switching Models with Day-Dependent Spikes: Kosater and Mosler (2006) . . . . .	26
2.4	A Forecast Comparison Study . . . . .	31
2.4.1	Theoretical Preliminaries . . . . .	32
2.4.2	Results of the Study . . . . .	34
2.5	Regime-Switching Models and GARCH . . . . .	38
2.5.1	Two-Regime Switching Model with GARCH(1,1) Errors . . . . .	40
2.5.2	Two-Regime- Switching Model with ARCH(1) Errors . . . . .	42
2.5.3	Two-Regime-Switching Model with Independent Spikes and ARCH(1) Errors . . . . .	42
2.6	Summary . . . . .	46
<b>3</b>	<b>The Impact of Weather on German Hourly Electricity Prices</b>	<b>47</b>
3.1	Introduction . . . . .	47
3.2	Data and Descriptive statistics . . . . .	48
3.3	Choice of the Weather Variables . . . . .	55
3.4	The Empirical Study . . . . .	57
3.4.1	Results on Model Fit . . . . .	58
3.4.2	A Forecasting Experiment . . . . .	71
3.4.3	Results of the Forecasting Study . . . . .	72
3.4.4	An Additional Small Forecasting Study . . . . .	76
3.5	Summary . . . . .	78

<b>4</b>	<b>Cross-City Hedging with Weather Derivatives using Bivariate GARCH Models with Dynamic Conditional Correlations</b>	<b>80</b>
4.1	Introduction and Literature Review . . . . .	80
4.2	Data . . . . .	84
4.3	Univariate Modelling . . . . .	87
4.3.1	Results on Model Fit . . . . .	91
4.3.2	Examining the Departure from Normality . . . . .	96
4.3.3	Out-of-sample Forecasting Study . . . . .	97
4.4	Bivariate Modelling . . . . .	101
4.4.1	The DCC Model Class . . . . .	102
4.4.2	Flexible Dynamic Correlations models . . . . .	104
4.4.3	Two-Step Estimation Procedure . . . . .	104
4.4.4	Results on Model fit . . . . .	105
4.5	Forecasting Conditional Correlations . . . . .	113
4.5.1	Forecasting Correlations in Asymmetric DCC Models . . . . .	113
4.5.2	Forecasting Correlations in the Flexible Dynamic Correlation Models. . . . .	114
4.6	Cross-City Hedging . . . . .	119
4.7	Summary . . . . .	120
<b>5</b>	<b>Conclusion</b>	<b>122</b>

# List of Figures

2.2.1 Plots for baseload spot prices, the logarithm of baseload spot prices, log(baseload), and the traded volume at the EEX. . . . .	18
2.2.2 Quantile-quantile plots for baseload spot prices at the EEX. . . . .	19
2.2.3 Weekly seasonality of baseload spot prices at the EEX. . . . .	19
2.3.1 Plots showing smoothed spike regime probabilities for the following models: (a) Ethier and Mount (1998), (b) De Jong and Huisman (2003), (c) Kosater and Mosler (2006)( <i>without independent spikes</i> ), (d) Kosater and Mosler (2006) ( <i>with independent spikes</i> ). . . . .	29
2.3.2 Quantile-quantile plots for log(baseload) from which the deterministic effects have been removed against the estimated models: (a) Ethier and Mount (1998), (b) De Jong and Huisman (2003), (c) Kosater and Mosler (2006)( <i>without independent spikes</i> ), (d) Kosater and Mosler (2006) ( <i>with independent spikes</i> ), ( <i>Note: To guarantee comparability, two elements in each simulated series throughout the four plots are set equal to 1 and 6, respectively</i> ). . . . .	30
2.3.3 Forecast horizon : 25 <sup>th</sup> August 2002 to 28 <sup>th</sup> July 2004. . . . .	31
2.4.1 Results of all models for the log(baseload) time series ( RMSE means root mean square error and MAE means mean absolute error). . .	36
2.4.2 Results of all models for the log(peakload) time series ( RMSE means root mean square error and MAE means mean absolute error). .	37
2.5.1 Histograms for log(baseload) from which the deterministic effects have been removed are plotted together with the estimated normal probability densities for the models I to IIIb, <i>according to section 2.4</i> . .	39
2.5.2 Smoothed probabilities for the spike regime and quantile-quantile plots for log(baseload) from which the deterministic effects have been removed against the estimated models: ((a),(b)) MS Model with GARCH(1,1), ((c)(d)) Two-Regime Model with ARCH(1), ((e)(f)) Two- Regime Model with Independent Spikes and ARCH(1), ( <i>Note: To guarantee comparability, two elements in each simulated series throughout the three quantile-quantile plots (b,d,f) are set equal to -0.1 and 5, respectively</i> ). . . . .	45
3.2.1 (a) Hourly power price series of the EEX, (b) Measured hourly wind velocity of Holzdorf, (c) Measured hourly temperature of Ulm, (d) Boxplot for hourly wind velocities, all data ranges from June 16 <sup>th</sup> 2000 to December 31 <sup>th</sup> 2004. . . . .	51

3.2.2 Scatter plots for hourly temperature from Ulm and the hourly average wind velocity of Holzdorf and Hamburg with the logarithm of the hourly price series (a,b), one day-ahead forecasts for temperature from Ulm and for wind velocity from Holzdorf (c,d), for 7 a.m. 1/05/2005 until 6 a.m. 1/06/2005, Correlation of measured temperature from Ulm and wind velocity from Holzdorf as well as its one day-ahead forecasts with the hourly price for 7 a.m. 1/05/2005 until 6 a.m. 1/06/2005 (e,f).	54
3.3.1 Coefficients of determination $R^2$ : (a) equation (3.3.1), (b) equation (3.3.2), (c) equation (3.3.3), (d) equation (3.3.4), (e) equation (3.3.2) for the average of three or four stations, (f) equation (3.3.4) for the average of three or four stations.	56
3.4.1 Measured temperature from Ulm (a),(c) and measured wind velocity (b),(d) together with their two and three days ahead forecasts from hour 7 a.m. 1/05/2005 until hour 6 a.m. 1/06/2005.	73
3.4.2 Results of the forecasting study (a,b), (c,d) $R^2$ of equations (3.4.9) and (3.4.10).	75
4.2.1 Daily average temperature from Echterdingen( 01/01/1991 until 04/29/2005 (a), Histogram for Echterdingen (b), Autocorrelation function ( ACF ) for Echterdingen (c), Partial autocorrelation function ( PACF )for Echterdingen (d).	86
4.3.1 ACF of the residuals from equation(4.3.9) (a), PACF of the residuals from equation(4.3.9) (b), ACF of the squared residuals from equation(4.3.9) (c), PACF of the squared residuals from equation(4.3.9)(d), plot of the standardised squared residuals from equation (4.3.9)(e), histogram of the residuals from equation(4.3.9)(f).	90
4.3.2 $\sigma_t^2$ : Model III (a), $\sigma_t^2$ : Model IV (b), $h_t$ : Model III (c), $h_t$ : Model IV (d), all series for Echterdingen.	95
4.3.3 $h_t$ : Model III and IIIb (a), $h_t$ : Model III and Model IV (b), $h_t$ : Model IV and IVb (c), $h_t$ : Model IIIb and Model IVb (d), all series for Echterdingen.	99
4.4.1 Conditional correlations estimated by QML: DCC and Asymmetric DCC Echterdingen-Berlin (a),FDC Echterdingen-Berlin (b), DCC and Asymmetric DCC Hamburg-Berlin (c), FDC Hamburg-Berlin (d).	112
4.5.1 Point and interval forecasts ( 99 %) for the HDD period 11/01/2004 until 03/31/2005 for Hamburg from : the symmetric DCC (a), the asymmetric DCC (b), FDC of Christodoulakis and Satchell (2002) (c), FDC of Baur (2006) (d), FDC of Kosater (2006)(e).	116
4.5.2 Point forecasts of the conditional correlations for the HDD period 11/01/2004 until 03/31/2005 for Echterdingen-Berlin from : the symmetric DCC (Forecast Q correponds to equation (4.5.2) and Forecast R corresponds to equation (4.5.3) )(a), the asymmetric DCC (b), FDC of Christodoulakis and Satchell (2002) (c), FDC of Baur (2006) (d), FDC of Kosater (2006)(e).	117

4.5.3 Point forecasts of conditional correlations for the HDD period 11/01/2004  
to 03/31/2005 for Hamburg-Berlin from : the symmetric DCC  
(Forecast Q correponds to equation (4.5.2) and Forecast R corre-  
sponds to equation (4.5.3) )(a), the asymmetric DCC (b), FDC of  
Christodoulakis and Satchell (2002) (c), FDC of Baur (2006) (d),  
FDC of Kosater (2006)(e). . . . . 118

# List of Tables

2.2.1 Descriptive Statistics on Baseload and Peakload in Euro/MWh. . .	16
2.3.1 Results on the AR(1) Model, equation(2.3.1), and the Jump Model, equation (2.3.2). . . . .	21
2.3.2 Results on the Two-Regime Switching Models, see equations (2.3.4- 2.3.8). . . . .	24
2.3.3 Results on Two- Regime Models with Day-Dependent Spikes, see equations (2.3.17-2.3.21). . . . .	28
2.5.1 Results on the Jump Model and the Two-Regime Switching Model with GARCH(1,1) Errors, see equations(2.5.1-2.5.7). . . . .	41
2.5.2 Results on Two-Regime Models with ARCH(1) errors, see equations (2.5.8-2.5.21). . . . .	44
3.2.1 Descriptive Statistics on Hourly Spot Prices at the EEX in Euro/MWh.	52
3.2.2 Descriptive Statistics on Temperature in $C^{\circ}$ . . . . .	53
3.2.3 Descriptive Statistics on Wind Velocity in meter/second. . . . .	53
3.4.1 Results on the Stochastic Component and Model Selection Criteria. (I) . . . . .	60
3.4.2 Results on the Stochastic Component and Model Selection Criteria (II). . . . .	61
3.4.3 Summary in-sample fit and the Schwartz Criterion (SC) for all 24 hours. . . . .	62
3.4.4 Results on the Deterministic Component, see equation (3.4.2), (I). . . . .	63
3.4.5 Results on the Deterministic Component, see equation (3.4.2), (II). . . . .	64
3.4.6 Results on the Deterministic Component, see equation (3.4.2), (III). . . . .	65
3.4.7 Results on the Deterministic Component, see equation (3.4.2), (IV). . . . .	66
3.4.8 Results on the Weather Component $w_t$ , see equation (3.4.3) . . . . .	67
3.4.9 Results on Constant Transition Probabilities, see equation(3.4.4) . . . . .	68
3.4.10 Summary of results for the time-varying transition probabilities (I), see equation (3.4.4) . . . . .	69
3.4.11 Summary of results for the time-varying transition probabilities (II), see equation (3.4.4). . . . .	70
3.4.12 Summary Out-Of-Sample Forecasting Study. (Best results are emphasized in bold.) . . . . .	74
3.4.13 RMSE for The Three Selected Hours.( Best results are empha- sized in bold.) . . . . .	77
3.4.14 MAE for The Three Selected Hours.( Best results are emphasized in bold.) . . . . .	78

3.4.15 RMSE for The Three Selected Hours.( Best results are emphasized in bold.) . . . . .	78
3.4.16 MAE for The Three Selected Hours. ( Best results are emphasized in bold.) . . . . .	79
4.2.1 Descriptive Statistics on Temperature Series in $C^{\circ}$ from The Three Selected Stations. . . . .	85
4.2.2 Correlations of Temperature Series in $C^{\circ}$ from The Three Selected Stations. . . . .	87
4.3.1 Summary In-Sample Fit : Echterdingen. . . . .	91
4.3.2 Summary In-Sample Fit : Berlin. . . . .	92
4.3.3 Summary In-Sample Fit : Hamburg. . . . .	92
4.3.4 Estimates of Models I and II (equations (4.3.9),(4.3.10) and (4.3.13)).	93
4.3.5 Estimates of Models III and IV, (equations (4.3.14) and (4.3.15)).	94
4.3.6 Summary In-Sample Fit: Model IIIb. . . . .	97
4.3.7 Summary In-Sample Fit: Model IVb. . . . .	97
4.3.8 Results on The Out-Of-Sample Forecasting Study.( Best results are emphasized in bold.) . . . . .	101
4.4.1 Summary In-Sample Fit : DCC Models by Engle (2002) and Capiello et al. (2003), ( Two- step estimation ). . . . .	107
4.4.2 Summary In-Sample Fit : DCC Models by Engle (2002) and Capiello et al. (2003), ( Two- step estimation ). . . . .	107
4.4.3 Summary In-Sample Fit: DCC Models by Engle (2002) and Capiello et al. (2003), ( QML ). . . . .	107
4.4.4 Summary In-Sample Fit: DCC Models by Engle (2002) and Capiello et al. (2003), ( QML ). . . . .	108
4.4.5 Summary In-Sample Fit : Satchell and Christodoulakis (2002), equation(4.4.11). . . . .	108
4.4.6 Summary In-Sample Fit : Satchell and Christodoulakis (2002), equation(4.4.11). . . . .	109
4.4.7 Summary In-Sample Fit : Baur (2006), equation(4.4.12). . . . .	109
4.4.8 Summary In-Sample Fit : Baur (2006), equation(4.4.12). . . . .	110
4.4.9 Summary In-Sample Fit : Kosater (2006), equation(4.4.13). . . . .	110
4.4.10 Summary In-Sample Fit : Kosater (2006), equation(4.4.13). . . . .	111

# Chapter 1

## Introduction

Until recently, the electricity sector has been a vertically integrated industry and prices have been fixed by regulators. The rapidly progressing deregulation is now leading to gradually privatised electricity markets. These markets divide into forward markets, on one hand, and spot markets on the other hand. Especially in spot markets, market participants are exposed to very volatile prices and high uncertainty. Since storability of electricity is limited, spot and forward prices cannot be easily linked. Consequently, forward and spot prices require a separate analysis. In this thesis, we focus on electricity spot markets, since spot prices are more challenging in modelling than forward prices. Our empirical investigations focus on the spot market at the European Energy Exchange in Leipzig.

As in the commodity and financial markets, derivatives can be used to cope with the large uncertainty due to highly volatile prices. However, pricing of derivatives with the spot price as the underlying asset has to take into account the salient characteristics of electricity spot prices. These features are several seasonality cycles, mean reversion and extreme price spikes. Spikes are a direct consequence of the non-storable nature of electricity and are usually explained either by unexpected outages of large power plants or unpredicted changes of weather conditions. In most cases, spikes are very short-lived but they can also last for several days in a row.

Besides derivative pricing, short-term price forecasting is of crucial interest for spot market participants. Since spot prices are typically determined through an auction, market participants are requested to express their bids in terms of prices and quantities. Consequently, market participants who are able to accurately forecast spot prices can adjust their production schedule to maximize their profits.

Derivative pricing as well as short-term price forecasting require a suitable spot price model. Time series models are capable of capturing the salient characteristics of electricity prices. However, spikes induce non-linearities into the price process. Therefore, we especially focus on non-linear time series approaches. Among several non-linear time series approaches, we opt for Markov regime-switching models in spirit to Hamilton (1989). Markov regime-switching models are tailor-made for spot prices and very flexible in modelling non-linearities. In addition, forecasting

can be easily carried out following Hamilton (1989).

The second chapter is dedicated to the application of Markov regime-switching models to spot prices. More precisely, we start with a discussion and application of two established Markov regime-switching models. In a second step, we extend these models by introducing day-dependent spikes. With the inclusion of day-dependent spikes, we take into account that large sized upward spikes are not to be expected on days such as weekends or holidays when demand is usually low. In a forecasting study, we show that our model extensions do not only successfully capture main characteristics of electricity prices but are also an asset in terms of forecasting.

We conclude with a presentation of model extensions of the models with day-dependent spikes which take into account autoregressive conditional heteroscedasticity dynamics.

Hence, the contribution to the literature in the first part of the thesis is the introduction of new models which are an asset in derivative pricing and forecasting.

In the third chapter, the relation between weather, represented by temperature and wind velocity, and hourly electricity prices from the European Energy Exchange in Leipzig is investigated. Furthermore, we assess whether the relation between weather and prices can be successfully exploited for short-term forecasting. Thereby, we proceed in the framework of a Markov regime-switching model with day-dependent spikes.

The additional input to existing literature is the examination of the relationship between temperature and wind, on one hand, and hourly power prices from the EEX on the other. Moreover, we prove that transition probabilities, which govern the transition between the regimes, can be successfully modelled as functions of temperature and wind velocity for a couple of hours. Finally, we assess the significance of the relation between weather variables and hourly prices for forecasting hourly prices at the EEX.

As monopolies gave their way to competitive wholesale electricity markets, volumetric risk came into play. Therefore in the fourth chapter, we turn to a discussion of weather derivatives which can be bought by electricity suppliers to protect from revenue uncertainties due to unexpected weather conditions. Our focus is on temperature derivatives. Yet, exchange-based trading of temperature derivatives mainly takes place at the Chicago Mercantile Exchange. Since temperature contracts at the Chicago Mercantile Exchange can only be struck for weather variables measured at few selected locations, electricity supplier who wish to hedge their risk at non-traded locations have to correlate their risk with the risk at tradeable locations.

We examine the usefulness of bivariate GARCH models with dynamic conditional correlations in modelling the correlation between non-traded and traded temperature time series.

The knowledge of correlation dynamics between these temperature time series enables an electricity supplier to correlate his risk with the risk of a traded city and to construct a sensible hedge.

The contribution to the existing literature can be described as follows. We extend

the existing univariate GARCH framework for temperature time series to the bivariate case. Bivariate GARCH models allow us to explicitly address and model conditional correlation dynamics between two temperature time series. Knowing the conditional correlation dynamics is the key to construct a cross-city hedge. In chapter five, we summarize our work and highlight the contributions of these thesis. Finally, we outline hints for further research.

## Chapter 2

# Markov Regime-Switching Models for Electricity Spot Prices

### 2.1 Review of Literature on Electricity Spot Prices

To highlight the contribution to the literature made in this chapter, we have to summarize previous work, first. Here, we especially outline important articles on electricity spot prices. However, we also mention parts of our own work which have already been evaluated and quoted by other authors in the meantime.

To start with, important initial articles are those of Knittel and Roberts (2005) and of Lucia and Schwartz (2002). Knittel and Roberts (2005) evaluate the forecast performance of several univariate models using Californian power prices. Moreover, they successfully include temperature as covariate. Lucia and Schwartz (2002) present analytic formulas for the pricing of power derivatives. In addition, they take seasonality and mean reversion into account. Escribano et al. (2002) suggest a very general jump model approach. They incorporate mean reversion, spikes and generalized autoregressive conditional heteroscedasticity (GARCH) in their approach for the modelling of electricity spot prices. Moreover, Cuaresma et al. (2004) carry out a forecast study with several linear univariate time series models. They use data from the European Energy Exchange (EEX) in Germany. Angeles et al., forthcoming in (2007), provide empirical evidence of periodic extensions of regression models with autoregressive fractionally integrated moving average disturbances for the analysis of daily spot prices. They apply their models to four different markets. Burger et al. (2004) derive a spot market model for hourly power prices at the EEX. They base their model on economic fundamentals of power prices in combination with a seasonal autoregressive integrated moving average approach. Rambharat et al. (2005) propose a threshold autoregressive model for daily spot prices from Pennsylvania. They incorporate a flexible mean reversion rate depending on temperature and spikes. More recently, Misoi et al. (2006) found that threshold autoregressive regime-switching models clearly outperformed linear approaches in terms of interval forecasts for data from the

California Power Exchange.

Basic idea behind non-linear Markov regime-switching approaches in spirit to Hamilton (1989) is to model spikes as a separate regime. Modelling approaches based on regime-switching have been suggested and successfully applied for instance by Ethier and Mount (1998), Huisman and Mahieu (2003), De Jong and Huisman (2003), Kosater and Mosler (2006). The latter focussed on the forecasting ability of Markov regime-switching models, whereas the remaining authors stressed applicability in derivative pricing. In addition, Mount et al. (2006) show that daily price spikes in the Pennsylvania-New Jersey-Maryland (PJM) Power Pool can be very accurately predicted one day-ahead if load and the reserve margin are included in the model specification and transition probabilities are modelled as functions of load and the reserve margin. Finally, De Jong (2006) tests several spot price models on day-ahead markets in Europe and the USA. The author finds that regime-switching models outperform GARCH(1,1) and Poisson jump models. Furthermore, De Jong argues that especially regime-switching models with day-dependent spikes as suggested by Kosater and Mosler (2006) are very well suited to capture dynamics in many markets.

In the remainder of the chapter, we discuss and apply selected spot price models to data from the EEX. In addition, we assess the out-of-sample forecast ability of some selected Markov regime-switching models. Finally, we give an outlook on further research.

## 2.2 Data and Descriptive Statistics

The European Energy Exchange (EEX) in Leipzig is the largest national power exchange in Europe. EEX wholesale electricity prices for 24 hours of the following day are determined through an auction. These day-ahead prices are typically referred to as spot prices. Besides hourly prices, so-called baseload and peakload prices are traded. The exchange EEX defines baseload prices as an equally weighted average of the 24 individual hourly prices, while peakload prices are determined by the equally weighted average of prices from 9 am to 8 pm. For our investigations on baseload and peakload, we use data including baseload and peakload price series which range from June 16<sup>th</sup> 2000 to July 28<sup>th</sup> 2004. Figure 2.2.1 shows the baseload series that exhibits typical features of power prices like mean reversion and spikes. Table 2.2.1 presents some descriptive statistics for the baseload and peakload series given in Euro/MWh, respectively. Obviously, the descriptive statistics tell us that daily average spot prices are far from being normally distributed. Spot prices tend to fluctuate around a long term equilibrium.

Table 2.2.1: Descriptive Statistics on Baseload and Peakload in Euro/MWh.

	Baseload	Peakload
Mean	24.77	30.84
Median	23.62	28.53
Maximum	240.26	445.09
Minimum	3.12	0.80
Std. Dev.	11.872	19.302
Skewness	6.908	10.059
Kurtosis	103.82	180.00

This fluctuation is due to shifts in demand caused by weather, for example. Thus, the expression mean reversion describes the tendency of spot prices to revert to a long term equilibrium. Let  $P_t$  with time-index  $t \in \{1, \dots, T\}$  be the spot price. A standard mean reverting process has the following specification.

$$P_t = P_{t-1} + \rho \cdot (\mu - P_{t-1}) + \epsilon_t \quad \epsilon_t \sim \mathcal{N}(0, \sigma^2) \quad (2.2.1)$$

In equation (2.2.1) the parameter  $\mu$  is the long term equilibrium for the spot price, whereas  $\alpha$  measures the speed of reversion from the current to the long term equilibrium. The parameter  $\rho$  can be related to the concept of half-life in physics. The lower  $\rho$ , the longer is the half-life. In time series analysis, we model mean reversion in the context of autoregressive processes  $AR(p)$ . Equation (2.2.2) shows the specification of an  $AR(p)$  process for spot prices.

$$P_t = \rho_1 \cdot P_{t-1} + \rho_2 \cdot P_{t-2} + \dots + \rho_p \cdot P_{t-p} + \epsilon_t \quad \epsilon_t \sim \mathcal{N}(0, \sigma^2) \quad (2.2.2)$$

The concept of mean reversion in equation (2.2.1) is a special case of an autoregressive process with  $p = 1$ . Furthermore, we have to include the drift parameter  $\mu_M$  since in equation (2.2.2) we assume a long-run level  $\mu_M = 0$ . Power prices

usually rather seem to follow a lognormal than a normal distribution. Therefore, most authors, e.g. Escribano et al. (2002), Burger et al.(2004), and de Jong and Huisman (2003), prefer working with the logarithm of power prices instead of the original price series. Here, we follow their approach. Furthermore, Figure 2.2.2 shows the quantile-quantile plots of baseload against a normal distribution and a lognormal distribution, respectively. The superimposed lines in subfigures 2.2.2a and 2.2.2b pass through the first and third quartile and help to assess the deviation from the straight line.

According to e.g. Escribano et al. (2002) and de Jong and Huisman (2003) the logarithm of power prices  $\log(P_t)$  will be assumed to consist of two parts, a deterministic part denoted by  $f_t$  and a stochastic part  $X_t$ ,

$$\log(P_t) = f_t + X_t. \quad (2.2.3)$$

Figure 2.2.3 shows the weekly seasonality. In order to take into account the weekly seasonality, weekend dummy variables for Saturdays and Sundays as well as a dummy variable for holidays are included. Moreover, since the range of the data covers more than four years, we include a deterministic linear trend and a sinusoidal term to consider yearly seasonality.

The deterministic part of the logarithm of the power price  $f_t$  is specified as,

$$\begin{aligned} f_t = & \beta_1 \cdot dummy_{sat} + \beta_2 \cdot dummy_{sun} + \beta_3 \cdot dummy_{hol} + \beta_4 \cdot t \\ & + \gamma_1 \cdot \sin\left((\gamma_2 + t) \cdot \frac{2\pi}{365}\right). \end{aligned} \quad (2.2.4)$$

More precisely,  $dummy_{sat}$  is the dummy variable for Saturdays, whereas  $dummy_{sun}$  is the dummy variable for Sundays. The dummy variable for holidays is denoted  $dummy_{hol}$ . Finally,  $t$  is linear trend measured in days. The deterministic component  $f_t$  is estimated jointly with the parameters of the stochastic model of interest.

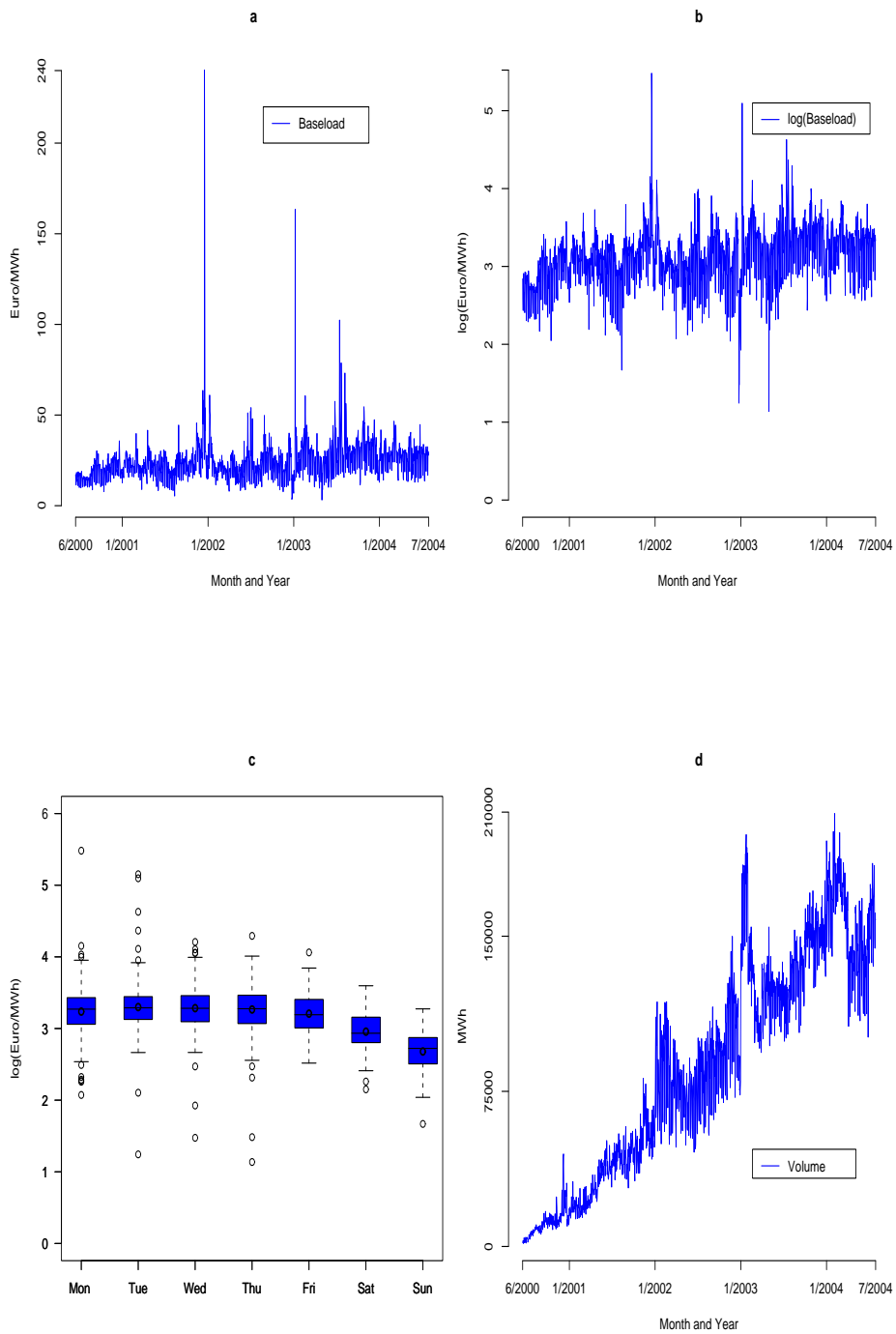


Figure 2.2.1: Plots for baseload spot prices, the logarithm of baseload spot prices,  $\log(\text{baseload})$ , and the traded volume at the EEX.

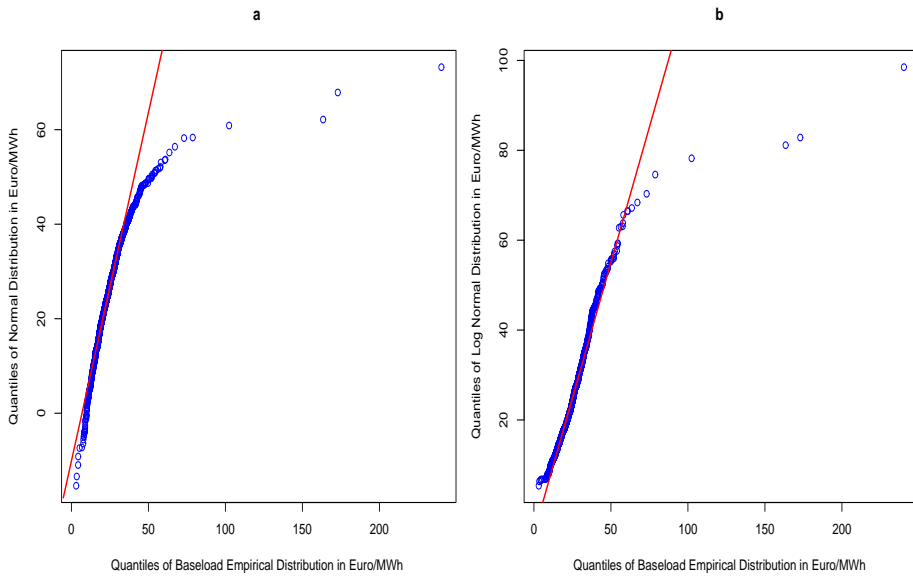


Figure 2.2.2: Quantile-quantile plots for baseload spot prices at the EEX.

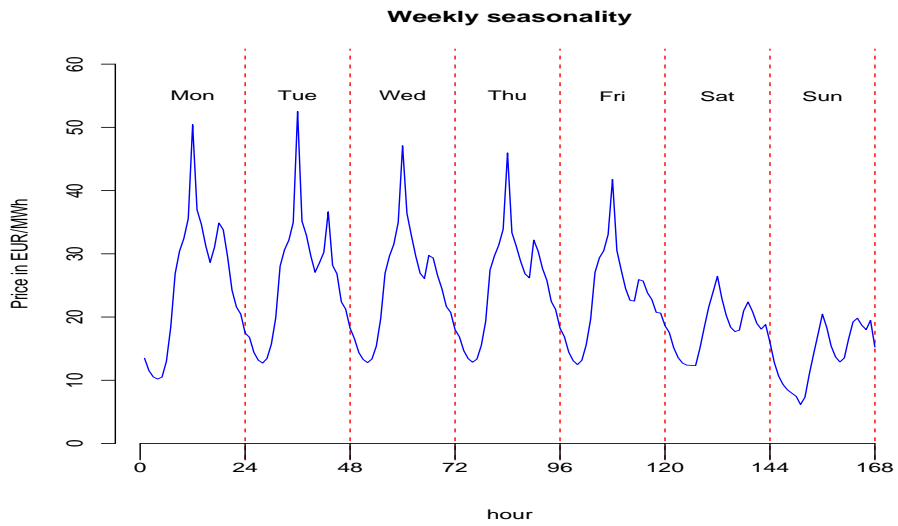


Figure 2.2.3: Weekly seasonality of baseload spot prices at the EEX.

## 2.3 Stochastic Models for Power Prices

In this section, we discuss some of the models for the stochastic part of electricity spot prices with a special focus on Markov regime-switching models.

### 2.3.1 AR(1) Process with Drift

We include the AR(1) process as a linear benchmark model. Although this process captures mean reversion, which is a main stylized fact of electricity prices, it cannot take into account spikes. The mean to which the process reverts is  $\mu_M$ .  $M$  refers to mean reversion in the remainder of the thesis.

$$X_t = \rho \cdot \mu_M + (1 - \rho) \cdot X_{t-1} + \epsilon_{M,t}, \quad \epsilon_{M,t} \sim \mathcal{N}(0, \sigma_M^2). \quad (2.3.1)$$

### 2.3.2 The Jump Model

Stochastic jump diffusion models with mean reversion are a very popular approach for the modelling of electricity prices. The mean reversion component is used to force prices to revert to a normal level after a spike has occurred. We find two procedures to cope with spikes in jump models.

In the first approach, spikes are extracted if they exceed an arbitrarily set threshold. The extracted prices are then replaced by the arithmetic average of the neighboring prices, for example. This kind of preprocessing procedure is advocated by Cuaresma et al. (2004) and Weron (2006). The extracted spikes are then exploited to specify a spike distribution. The intensity of the jump process is determined by the frequency of detected spikes in the data. The data, from which spikes have been extracted, is used to estimate the remaining parameters.

Secondly, we can simply specify a model which allows to simultaneously estimate all model parameters by means of maximum likelihood. The second procedure is applied by Escibano et al. (2002), Huisman and Mahieu (2003) as well as by Knittel and Roberts (2005). Here, we follow the approach presented in Huisman and Mahieu (2003). Hence, we model mean reversion similar to equation (2.3.1). The jumps  $J_t$  are assumed to be each the sum of independently and identically distributed normals  $Z_{i,t}$ . In addition, we assume  $Z_{i,t} \sim \mathcal{N}(\mu_S, \sigma_S^2)$  with  $i = 1, \dots, n_t$ , mean  $\mu_S$  and variance  $\sigma_S^2$ . The arrival process of the compound jumps is modelled by a Poisson distribution with intensity  $\lambda$ ,

$$X_t = \rho \cdot \mu_M + (1 - \rho) \cdot X_{t-1} + \epsilon_{M,t} + \sum_{i=1}^{n_t} Z_{i,t}, \quad \epsilon_{M,t} \sim \mathcal{N}(0, \sigma_M^2). \quad (2.3.2)$$

Let  $LL$  denote the logarithmic likelihood,

$LL =$

$$-T \cdot \lambda - \frac{T}{2} \ln(2\pi) + \sum_{t=1}^T \ln \left[ \sum_{j=0}^{\infty} \frac{\lambda^j}{j! \sqrt{\sigma_M^2 + j\sigma_S^2}} \exp \left( -\frac{(X_t - \rho \cdot \mu_M + (1 - \rho) \cdot X_{t-1} - j\mu_S)^2}{2(\sigma_M^2 + j\sigma_S^2)} \right) \right]. \quad (2.3.3)$$

Following Huisman and Mahieu (2003), we compute the sum  $\sum_{j=0}^{\infty} \dots$  up to  $j = 10$ . Estimation is carried out by maximizing  $LL$  with respect to the model parameters.

We gauge models by means of information criteria. The information criteria of Akaike (AC) and Schwartz (SC) are computed as follows throughout the thesis,

$$AC = \frac{-2 \cdot LL + 2k}{T} \quad SC = \frac{-2 \cdot LL + k \log(T)}{T}.$$

Moreover,  $k$  denotes the number of estimated parameters and  $T$  the number of observations. The jump model provides a notably better fit than the AR(1) model

Table 2.3.1: Results on the AR(1) Model, equation(2.3.1), and the Jump Model, equation (2.3.2).

	AR(1)		Jump Model	
	log(baseload)	log(peakload)	log(baseload)	log(peakload)
$\beta_1$	-0.285 (0.014)	-0.360 (0.021)	-0.270 (0.009)	-0.337 (0.012)
$\beta_2$	-0.579 (0.014)	-0.682 (0.019)	-0.556 (0.010)	-0.645 (0.012)
$\beta_3$	-0.597 (0.018)	-0.812 (0.021)	-0.507 (0.017)	-0.638 (0.020)
$\beta_4$	0.0003 ( $4.5 \cdot 10^{-7}$ )	0.0003 ( $4.5 \cdot 10^{-7}$ )	0.0003 ( $3 \cdot 10^{-7}$ )	0.0003 ( $3 \cdot 10^{-7}$ )
$\gamma_1$	0.099 (0.020)	0.098 (0.022)	-0.124 (0.016)	0.112 (0.015)
$\gamma_2$	-90.18 (15.341)	-67.57 (14.304)	-87.141 (8.680)	-79.940 (8.680)
$\mu_M$	3.041 (0.039)	3.259 (0.038)	3.021 (0.026)	3.228 (0.023)
$\rho$	0.337 (0.011)	0.428 (0.010)	0.327 (0.013)	0.414 (0.014)
$\sigma_M$	0.194 (0.001)	0.237 (0.002)	0.141 (0.003)	0.156 (0.004)
$\lambda$	-	-	0.066 (0.013)	0.091 (0.016)
$\mu_S$	-	-	0.036* (0.058)	0.079* (0.050)
$\sigma_S$	-	-	0.506 (0.040)	0.556 (0.036)
LL	333.83	32.20	543.68	317.89
AC	-0.4322	-0.0309	-0.7075	-0.4070
SC	-0.4004	0.0010	-0.6651	-0.3646

Note that \* means not significant at the 5 % level.

for the logarithm of baseload and peakload, respectively. Moreover, all parameter estimates in table 2.3.1 are highly significant except for the estimate of  $\mu_s$ , which is not significant at the 5 % level. In Figure 2.2.1c, we see that upward and downward deviations are inherent in the logarithm of daily spot prices. This may explain why the estimate of  $\mu_s$  is not significant at the 5 % level. All results are presented in table 2.3.1.

Jump models are a very popular approach with derivative valuation based on spot prices. However, jump models have certain shortcomings. As pointed out by Huisman and Mahieu (2003), it is not easy to disentangle jumps from the estimation of the parameter  $\rho$  which governs the degree of mean reversion. Secondly, these models are not suitable for forecasting. Albeit, a successful attempt to predict spot prices with jump models has been undertaken by Cuaresma et al. (2004), their implemented forecasting procedure is rather heuristic and should be treated with caution.

### 2.3.3 A Markov Regime-Switching Model for Spot Prices: Ethier and Mount(1998)

Besides the jump model, Markov regime-switching approaches are widely considered as tailor-made to model spot prices. These models are based on the Markov regime-switching model of Hamilton (1989) which has originally been put forward to model the business cycle of the economy in the USA. The basic idea of the model is that the economy switches between one or more different regimes. For example, we can assume a boom regime and a recession regime. Furthermore in the basic approach, we assume that the regime-switching mechanism is exogenous and the prevailing regime is latent. By this, we presume that we do not know exactly which regime prevails at a certain point in time. However, we can at least express a certain regime probability. Moreover, we presume to know the probability of transition from one regime to another.

Indeed, it seems very convincing to classify occasional spikes and normal prices in different regimes. To the best of our knowledge, the first attempt to model spot prices with Markov regime-switching models has been undertaken by Ethier and Mount (1998). Analogously to the original model, Ethier and Mount specify a two- regime model. One regime to model normal prices and the second to capture spikes. Contrary to the basic model proposed by Hamilton (1989), they assume heteroscedasticity. By this, each regime is assigned its own variance. The prevailing regime at time  $t$  is denoted  $S_t$ . In the remainder of the thesis, we set  $S_t = M$  when power prices are in the normal regime and  $S_t = S$  else. Additionally, we refer to the normal regime as the stable regime in the remainder of the thesis. We present the model of Ethier and Mount (1998) in equations (2.3.4 - 2.3.6)

$$X_{M,t} = \mu_M + (1 - \rho) \cdot (X_{\{S_{t-1}=i\},t-1} - \mu_{\{S_{t-1}=i\}}) + \epsilon_{M,t}, \quad (2.3.4)$$

$$X_{S,t} = \mu_S + (1 - \rho) \cdot (X_{\{S_{t-1}=i\},t-1} - \mu_{\{S_{t-1}=i\}}) + \epsilon_{S,t}, \quad (2.3.5)$$

with  $i \in \{M, S\}$ ,  $\epsilon_{M,t} \sim \mathcal{N}(0, \sigma_M^2)$ ,  $\epsilon_{S,t} \sim \mathcal{N}(0, \sigma_S^2)$ . Transition between the regimes is governed by the transition matrix  $\Pi$ ,

$$\Pi = \begin{pmatrix} q & 1-p \\ 1-q & p \end{pmatrix}, \quad (2.3.6)$$

where,  $q$  denotes the probability to stay in the stable regime, and  $p$  denotes the probability to stay in the spike regime. In addition,  $X_{M,t}$  denotes the value of  $X_t$  provided that  $S_t = M$  and  $X_{S,t}$  the same with  $S_t = S$ .

### 2.3.4 Two-Regime Model with Independent Spikes : De Jong and Huisman (2003)

The second attempt to model spot prices with Markov regime-switching models has been made by Huisman and Mahieu (2003). These authors put forward a three-regime model. They propose two spike regimes where one spike regime is designed to pull the price process back to the stable regime after a spike has occurred. This three-regime model is conceived to better disentangle spikes from the stable regime than a jump model does. A shortcoming of this model is that it does not allow for consecutive spikes. Hence, the price process cannot stay in the spike regime. However, consecutive spikes are convenient with the fact that unforced outages can have a longer impact on spot prices than one day. To overcome this disadvantage and to allow consecutive spikes, De Jong and Huisman (2003) advocate a two-regime model with independent spikes. The authors assume one spike regime and one stable regime. The stable regime is modelled as follows,

$$X_{M,t} = X_{M,t-1} + \rho \cdot (\mu_M - X_{M,t-1}) + \epsilon_{M,t}, \quad \epsilon_{M,t} \sim \mathcal{N}(0, \sigma_M^2), \quad (2.3.7)$$

whereas for the spike regime, the authors assume,

$$X_{S,t} = \mu_S + \epsilon_{S,t}, \quad \epsilon_{S,t} \sim \mathcal{N}(0, \sigma_S^2). \quad (2.3.8)$$

Transition between the states is governed by the same transition matrix  $\Pi$  as in the Model of Ethier and Mount (1998), which is given in equation (2.3.6).

Up to now, it is not clear why spikes in this model are called independent. This is the peculiarity of the model. The authors assume that the stable regime latently evolves untouched through time, while a spike occurs. Hence, they assume two stochastic processes which independently evolve next to each other through time. However, at each point in time, we can only observe the realization of one of the two processes. For example, we may observe a spike at  $t$  and a normal price at  $t - 1$ . To obtain an unbiased estimation of the stable regime process, we have to include the latent value of the stable regime at  $t$ , which we did not observe. To solve the problem, De Jong and Huisman (2003) suggest to go back to  $t - 1$ , where we assume the price to originate from the stable regime and to approximate the latent value of the stable regime at  $t$  by its forecast based on the normal price at  $t - 1$ . It sounds easy, but, as a result, a very complex logarithmic likelihood has to be constructed.

The aim of De Jong and Huisman (2003) is to disentangle spikes from the stable regime as well as possible, without having to include an additional regime to pull prices back to the stable regime, as suggested by Huisman and Mahieu (2003). In fact, if we compare the results of the two regime model of Ethier and Mount (1998) in table 2.3.2 with the results of De Jong and Huisman (2003), we observe that the estimate of  $\rho$  is smaller in the two regime model of De Jong and Huisman (2003) than in the model of Ethier and Mount (1998) for both considered time series. Moreover, the estimate of  $p$  is also smaller, whereas the estimate of  $q$  is larger in the De Jong and Huisman (2003) model than in the model of Ethier and Mount (1998). All these results indicate that the approach of De Jong and Huisman (2003) is capable of better disentangling spikes from the stable regime

than the model put forward by Ethier and Mount (1998). This is especially true for the logarithm of baseload. By contrast, for the logarithm of peakload the difference between the model results is smaller.

Table 2.3.2: Results on the Two-Regime Switching Models, see equations (2.3.4-2.3.8).

	Ethier and Mount (1998)		De Jong and Huisman (2003)	
	log(baseload)	log(peakload)	log(baseload)	log(peakload)
$\beta_1$	-0.272 (0.009)	-0.342 (0.011)	-0.279 (0.009)	-0.348 (0.011)
$\beta_2$	-0.554 (0.009)	-0.648 (0.011)	-0.565 (0.009)	-0.655 (0.011)
$\beta_3$	-0.482 (0.016)	-0.637 (0.019)	-0.496 (0.015)	-0.634 (0.017)
$\beta_4$	0.0003 ( $2.8 \cdot 10^{-5}$ )	0.0003 ( $2.7 \cdot 10^{-5}$ )	0.0003 ( $3.5 \cdot 10^{-5}$ )	0.0003 ( $3.1 \cdot 10^{-5}$ )
$\gamma_1$	-0.123 (0.016)	0.107 (0.015)	-0.107 (0.018)	0.107 (0.017)
$\gamma_2$	87.031 (8.110)	-80.018 (8.728)	90.815 (11.747)	-77.521 (9.921)
$\mu_M$	3.018 (0.024)	3.230 (0.022)	3.033 (0.031)	3.234 (0.026)
$\rho$	0.327 (0.017)	0.397 (0.019)	0.260 (0.017)	0.321 (0.019)
$\sigma_M$	0.134 (0.003)	0.153 (0.003)	0.140 (0.003)	0.154 (0.003)
$\mu_S$	2.918 (0.061)	3.462 (0.064)	3.057 (0.083)	3.432 (0.073)
$\sigma_S$	0.453 (0.016)	0.584 (0.018)	0.725 (0.054)	0.751 (0.034)
$p$	0.779 (0.046)	0.758 (0.048)	0.600 (0.076)	0.722 (0.054)
$q$	0.973 (0.007)	0.973 (0.006)	0.976 (0.005)	0.975 (0.005)
LL	579.92	356.60	544.82	340.15
AC	-0.7544	-0.4572	-0.7100	-0.4368
SC	-0.7084	-0.4112	-0.6639	-0.3907

### 2.3.5 Estimation of Markov Regime-Switching Models

Here, we explain how the logarithmic likelihoods for the models of interest can be constructed. Let  $LL = \sum_{t=1}^T \ln f(X_t | \mathcal{F}_{t-1})$  be the logarithmic likelihood. Here,  $\mathcal{F}_{t-1}$  denotes the information set at  $t-1$ . The conditional density is expressed as follows:

$$\begin{aligned}
f(X_t | \mathcal{F}_{t-1}) &= f(X_t, S_t = M | \mathcal{F}_{t-1}) + f(X_t, S_t = S | \mathcal{F}_{t-1}) \quad (2.3.9) \\
&= f(X_t | S_t = M, \mathcal{F}_{t-1}) \cdot f(S_t = M | \mathcal{F}_{t-1}) + \\
&\quad f(X_t | S_t = S, \mathcal{F}_{t-1}) \cdot f(S_t = S | \mathcal{F}_{t-1})
\end{aligned}$$

Moreover, the density  $f(S_t = i|\mathcal{F}_{t-1})$ ,  $i \in \{M, S\}$ , has to be determined. It holds ( $j \in \{M, S\}$ ),

$$\begin{aligned} f(S_t = j|\mathcal{F}_{t-1}) &= f(S_t = j, S_{t-1} = M|\mathcal{F}_{t-1}) + f(S_t = j, S_{t-1} = S|\mathcal{F}_{t-1}) \\ &= f(S_t = j|S_{t-1} = M) \cdot f(S_{t-1} = M|\mathcal{F}_{t-1}) \\ &\quad + f(S_t = j|S_{t-1} = S) \cdot f(S_{t-1} = S|\mathcal{F}_{t-1}). \end{aligned} \quad (2.3.10)$$

The terms  $f(S_t = j|S_{t-1} = i)$  are the one-step transition probabilities.

Conditional probabilities of type  $f(S_{t-1} = j|\mathcal{F}_{t-1})$  are recursively calculated.

Due to  $\mathcal{F}_{t-1} = \{\mathcal{F}_{t-2}, X_{t-1}\}$  it holds

$$\begin{aligned} f(S_{t-1} = j|\mathcal{F}_{t-1}) &= f(S_{t-1} = j|\mathcal{F}_{t-2}, X_{t-1}) = \frac{f(S_{t-1} = j, X_{t-1}|\mathcal{F}_{t-2})}{f(X_{t-1}|\mathcal{F}_{t-2})} \quad (2.3.11) \\ &= \frac{f(X_{t-1}|S_{t-1} = j, \mathcal{F}_{t-2}) \cdot f(S_{t-1} = j|\mathcal{F}_{t-2})}{\sum_{i \in \{M, S\}} f(X_{t-1}|S_{t-1} = i, \mathcal{F}_{t-2}) \cdot f(S_{t-1} = i|\mathcal{F}_{t-2})}. \end{aligned}$$

According to Hamilton (1989), we can further decompose the densities in equation (2.3.9),  $f(X_t|S_t = M, \mathcal{F}_{t-1})$ ,  $f(X_t|S_t = S, \mathcal{F}_{t-1})$ , and compute  $f(X_t|\mathcal{F}_{t-1})$  as given in equation (2.3.12),

$f(X_t|\mathcal{F}_{t-1}) =$

$$\begin{aligned} &f(X_t|S_t = M, S_{t-1} = M|\mathcal{F}_{t-1}) \cdot f(S_t = M, S_{t-1} = M|\mathcal{F}_{t-1}) \quad (2.3.12) \\ &+ f(X_t|S_t = M, S_{t-1} = S|\mathcal{F}_{t-1}) \cdot f(S_t = M, S_{t-1} = S|\mathcal{F}_{t-1}) \\ &+ f(X_t|S_t = S, S_{t-1} = M|\mathcal{F}_{t-1}) \cdot f(S_t = S, S_{t-1} = M|\mathcal{F}_{t-1}) \\ &+ f(X_t|S_t = S, S_{t-1} = S|\mathcal{F}_{t-1}) \cdot f(S_t = S, S_{t-1} = S|\mathcal{F}_{t-1}). \end{aligned}$$

Note that in this case spikes enter the stable regime due to  $f(X_t|S_t = M, S_{t-1} = S|\mathcal{F}_{t-1})$ . De Jong and Huisman (2003) want to avoid this effect. Therefore, they do not decompose  $f(X_t|S_t = M, \mathcal{F}_{t-1})$  as in equation (2.3.12) but replace the part of the conditional density that represents the stable regime  $f(X_t|S_t = M, \mathcal{F}_{t-1})$  by an approximation,

$$f(X_t|S_t = M, \mathcal{F}_{t-1}) \approx \sum_{i=1}^K \text{Prob}[S_{t-i} = M \wedge S_{t-j} \neq M \text{ for } j < i] \cdot f(X_t|S_t = M, \mathcal{F}_{t-i})$$

The key problem in calibrating this conditional density is the determination of the value of  $X_{M,t-i}$ , where  $i = 1, \dots, K$ , because the last spot price originating from the stable regime is not known.  $K$  denotes how far we maximally go back to find the last spot price originating from the stable regime.

$$f(X_t|S_t = M, \mathcal{F}_{t-i}) \approx \frac{1}{\text{Var}[X_{M,t}|\mathcal{F}_{t-i}] \cdot \sqrt{2\pi}} \cdot \exp\left(-\frac{(X_{M,t} - E[X_{M,t}|\mathcal{F}_{t-i}])^2}{2 \cdot \text{Var}[X_{M,t}|\mathcal{F}_{t-i}]}\right)$$

with

$$E[X_{M,t}|\mathcal{F}_{t-i}] = \rho \cdot \mu_M + (1 - \rho) \cdot E[X_{M,t-1}|\mathcal{F}_{t-i}], \quad (2.3.13)$$

$$\text{Var}[X_{M,t}|\mathcal{F}_{t-i}] = \sigma_M^2 + (1 - \rho)^2 \cdot \text{Var}[X_{M,t-1}|\mathcal{F}_{t-i}]. \quad (2.3.14)$$

Applying these equations for the conditional expectations and variances yields

$$E[X_{M,t}|\mathcal{F}_{t-i}] = (1 - \rho)^i \cdot X_{M,t-i} + \mu_M \cdot (1 - (1 - \rho)^i), \quad (2.3.15)$$

$$\text{Var}[X_{M,t}|\mathcal{F}_{t-i}] = \sigma_M^2 \cdot \frac{(1 - \rho)^{2 \cdot i} - 1}{(1 - \rho)^2 - 1}. \quad (2.3.16)$$

The expression  $\text{Prob}[S_{t-i} = M \wedge S_{t-j} \neq M \text{ for } j < i]$  is the probability of the logarithm of the spot price  $X_{t-i}$  to be the last logarithm of the spot price before  $X_t$  originating from the stable regime.  $X_{t-j}$  with  $j < i$ , whereas, are supposed to be spikes. The remaining problem is to determine the right  $K$ . De Jong and Huisman (2003) propose  $K = 5$ . In our calculations,  $K = 5$  appears to be sufficient, too.

### 2.3.6 Regime-Switching Models with Day-Dependent Spikes: Kosater and Mosler (2006)

The models proposed by Ethier and Mount (1998) and De Jong and Huisman (2003) assume that deviations from the stable regime are independent of the type of the day. However, it seems more sensible to distinguish between working days on one hand and weekends and holidays on the other. Very low demand is typical of weekends and holidays. Therefore, upward directed spikes are rather not to be expected, whereas we can detect downward directed deviations from the stable regime in our German data. In order to take into account different types of days, Kosater and Mosler (2006) put forward to distinguish between high spikes and low spikes.

Practically, they decompose spikes by introducing an indicator function  $\mathbf{1}_H$  which takes the value zero on holidays, weekend days, and two days before and after a holiday. All remaining days are candidates for high spikes only, therefore for these days the indicator function takes value 1. The decomposition fits well to observed German data. However, weekends, at least Sundays, and holidays are days of low demand not only in Germany. In fact, De Jong (2006) finds that the decomposition put forward by Kosater and Mosler (2006) works well for a number of international markets, too.

$$\mathbf{1}_H = \begin{cases} 0 & \text{holiday, weekend, two days before and after a holiday,} \\ 1 & \text{else.} \end{cases} \quad (2.3.17)$$

Since for both two-regime models, the authors only modify the spike regime, the stable regime is left unchanged with respect to the original models. Moreover, transition between the regimes is assumed to be governed by the transition matrix  $\Pi$ . The authors extend the spike regime in De Jong and Huisman (2003) as follows,

$$X_{S,t} = \mathbf{1}_H \cdot (\mu_{S,H} + \epsilon_{S,H,t}) + (\mathbf{1} - \mathbf{1}_H) \cdot (\mu_{S,L} + \epsilon_{S,L,t}) \quad \text{spike regime.} \quad (2.3.18)$$

Additionally, they assume that the disturbances in the high spike regime denoted  $\epsilon_{S,H,t}$  and the low spike regime denoted  $\epsilon_{S,L,t}$  are both normally distributed with possibly different variances,  $\epsilon_{S,H,t} \sim \mathcal{N}(0, \sigma_{S,H}^2)$  and  $\epsilon_{S,L,t} \sim \mathcal{N}(0, \sigma_{S,L}^2)$ .

Kosater and Mosler (2006) analogously extend the model of Ethier and Mount

(1998),

$$X_{S,t} = \mu_S + (1 - \rho) \cdot (X_{\{S_{t-1}=i\},t-1} - \mu_{\{S_{t-1}=i\}}) + \epsilon_{S,t}, \quad (2.3.19)$$

$$\mu_S = \mathbf{1}_H \cdot (\mu_{S,H}) + (\mathbf{1} - \mathbf{1}_H) \cdot (\mu_{S,L}), \quad (2.3.20)$$

$$\epsilon_{S,t} = \mathbf{1}_H \cdot (\epsilon_{S,H,t}) + (\mathbf{1} - \mathbf{1}_H) \cdot (\epsilon_{S,L,t}), \quad (2.3.21)$$

where  $j, i \in \{M, S\}$ ,  $\epsilon_{M,t} \sim \mathcal{N}(0, \sigma^2)$ ,  $\epsilon_{S,H,t} \sim \mathcal{N}(0, \sigma_{S,H}^2)$ ,  $\epsilon_{S,L,t} \sim \mathcal{N}(0, \sigma_{S,L}^2)$ .

The results for the two- regime models with a day-dependent spike regime are collected in table 2.3.3. More precisely, table 2.3.3 shows that the modified models put forward by Kosater and Mosler (2006) outperform the original versions of Ethier and Mount (1998) and De Jong and Huisman (2003) in terms of fit. This result is also clearly confirmed by both information criteria. All parameter estimates are significant. Hence, the introduction of day-dependent spikes is a worthwhile extension.

In addition to the estimation results presented in tables 2.3.2-2.3.3, Figure 2.3.1 presents the smoothed probabilities for the considered Markov regime-switching approaches. Furthermore, Figure 2.3.2 shows quantile-quantile plots for the logarithm of baseload series from which the deterministic effects have been removed against simulated series from the discussed Markov regime-switching approaches. In more detail, the smoothed probabilities are computed as follows. Let  $\xi_{t|t}$  be the vector of filtered regime probabilities at time  $t$  given the information at time  $t$ . We calculate the smoothed regime probabilities at time  $t$  given the information at time  $T$ ,  $\xi_{t|T}$ , according to Kim (1994):

$$\xi_{t|T} = \xi_{t|t} \odot \{\Pi' [\xi_{t+1|T} \div \xi_{t+1|t}]\}. \quad (2.3.22)$$

Note that  $\odot$  is the element by element product, whereas  $\xi_{t+1|T} \div \xi_{t+1|t}$  symbolizes element by element division.

To summarize the results of the in-sample study, the models without independent spikes provide slightly higher spike probabilities than the models with independent spikes and outperform their independent counterparts in terms of fit, in particular for the logarithm of baseload.

Finally, the quantile-quantile plots in Figure 2.3.2 show that the simulated series generated from the models put forward by Kosater and Mosler (2006) are notably closer to the empirical series than simulated series from the original models of Ethier and Mount (1998) as well as De Jong and Huisman (2003). For the logarithm of baseload, the model without independent spikes of Kosater and Mosler (2006) performs best.

Table 2.3.3: Results on Two- Regime Models with Day-Dependent Spikes, see equations (2.3.17-2.3.21).

	Modified Ethier and Mount (1998)		Modified De Jong and Huisman (2003)	
	log(baseload)	log(peakload)	log(baseload)	log(peakload)
$\beta_1$	-0.260 (0.009)	-0.330 (0.011)	-0.273 (0.009)	-0.338 (0.011)
$\beta_2$	-0.544 (0.009)	-0.638 (0.011)	-0.556 (0.009)	-0.643 (0.011)
$\beta_3$	-0.477 (0.017)	-0.588 (0.019)	-0.482 (0.016)	-0.608 (0.018)
$\beta_4$	0.0003 ( $2.8 \cdot 10^{-5}$ )	0.0003 ( $2.6 \cdot 10^{-5}$ )	0.0003 ( $3.2 \cdot 10^{-5}$ )	0.0003 ( $2.8 \cdot 10^{-5}$ )
$\gamma_1$	0.121 (0.016)	0.105 (0.015)	-0.115 (0.017)	0.110 (0.016)
$\gamma_2$	268.80 (8.247)	-78.839 (8.675)	86.661 (10.100)	-79.033 (9.004)
$\mu_M$	3.018 (0.024)	3.225 (0.022)	3.033 (0.028)	3.230 (0.024)
$\mu_{S,H}$	3.214 (0.066)	3.569 (0.068)	3.496 (0.100)	3.835 (0.083)
$\mu_{S,L}$	2.732 (0.078)	2.887 (0.098)	2.526 (0.115)	2.893 (0.124)
$\rho$	0.322 (0.018)	0.398 (0.019)	0.272 (0.017)	0.338 (0.020)
$\sigma_M$	0.132 (0.003)	0.150 (0.003)	0.137 (0.003)	0.150 (0.003)
$\sigma_{S,H}$	0.468 (0.023)	0.544 (0.028)	0.537 (0.045)	0.530 (0.033)
$\sigma_{S,L}$	0.359 (0.026)	0.570 (0.030)	0.451 (0.061)	0.605 (0.042)
$p$	0.729 (0.054)	0.684 (0.057)	0.681 (0.065)	0.736 (0.049)
$q$	0.970 (0.007)	0.967 (0.007)	0.976 (0.005)	0.972 (0.006)
LL	596.54	372.84	572.30	369.53
AC	-0.7738	-0.4762	-0.7441	-0.4733
SC	-0.7208	-0.4231	-0.6909	-0.4202

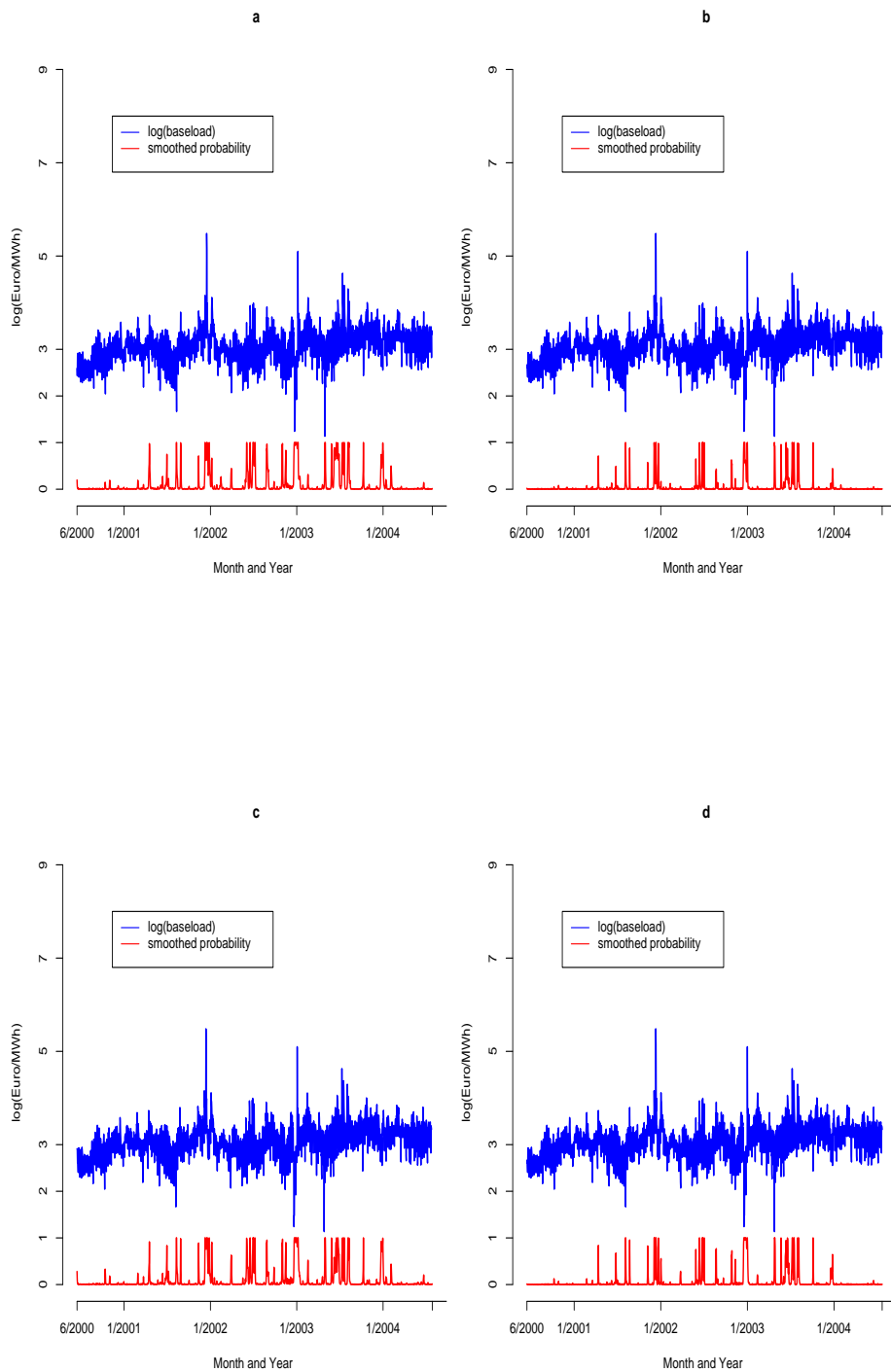


Figure 2.3.1: Plots showing smoothed spike regime probabilities for the following models: (a) Ethier and Mount (1998), (b) De Jong and Huisman (2003), (c) Kosater and Mosler (2006) (*without independent spikes*), (d) Kosater and Mosler (2006) (*with independent spikes*).

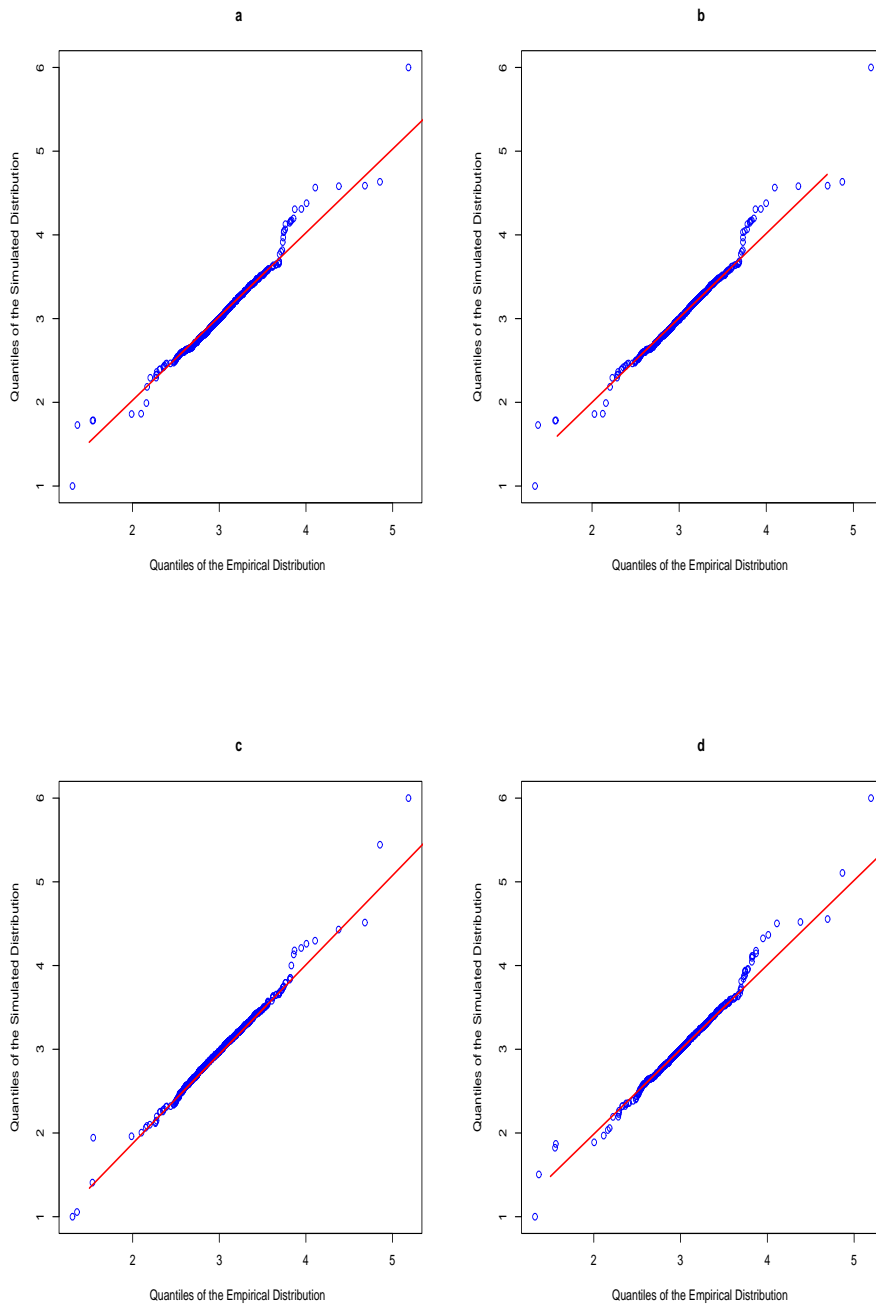


Figure 2.3.2: Quantile-quantile plots for  $\log(\text{baseload})$  from which the deterministic effects have been removed against the estimated models: (a) Ethier and Mount (1998), (b) De Jong and Huisman (2003), (c) Kosater and Mosler (2006) (*without independent spikes*), (d) Kosater and Mosler (2006) (*with independent spikes*), (Note: To guarantee comparability, two elements in each simulated series throughout the four plots are set equal to 1 and 6, respectively).

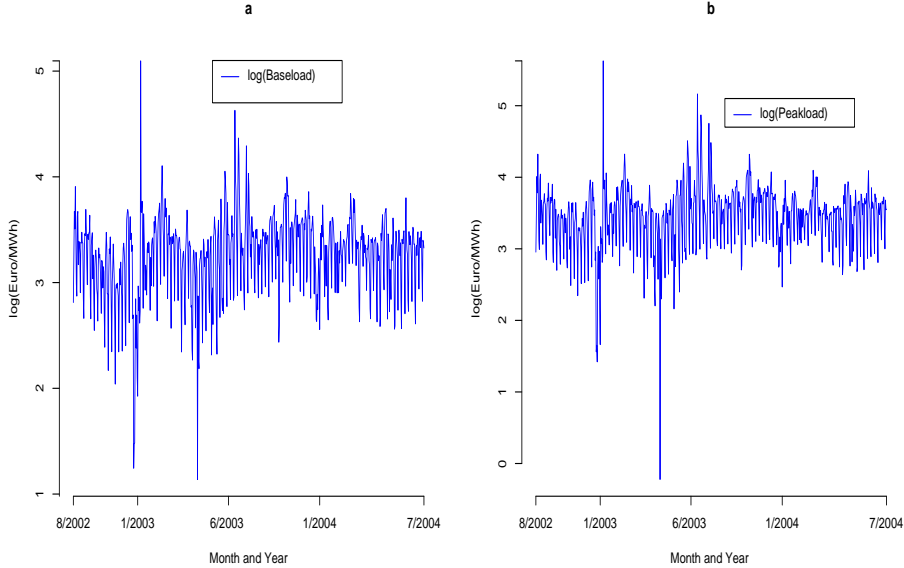


Figure 2.3.3: Forecast horizon : 25<sup>th</sup> August 2002 to 28<sup>th</sup> July 2004.

## 2.4 A Forecast Comparison Study

In this section, we carry out a forecast comparison study to assess the ability of Markov regime-switching models in forecasting.

To list the models considered in the study, we include the AR(1) with drift model as a linear benchmark and denote it Model I. Furthermore, we include the two-regime model with independent spikes of De Jong and Huisman (2003) and its modified version with day-dependent spikes and denote these models Model II, for the first mentioned, and Model IIb for the latter. Finally, we include the model of Ethier and Mount (1998) denoted Model III and its modified version with day-dependent spikes, which we denote Model IIIb.

In our study, we carry out and evaluate ex- ante forecasts in terms of the root mean square error ( RMSE ) and the mean absolute error ( MAE ). All given information available at time  $T$  is exploited and, by this, we use all known electricity prices up to  $T$  to estimate the parameter values. This proceeding is reasonable since electricity prices exhibit strong seasonality and autocorrelation, that are estimated the better the more data is available. The forecasting procedure is close to that of Cuaresma et al. (2004) applied to hourly prices and is described below. The given dataset is divided into an in-sample period which includes observations from 6/16/2000 to 8/24/2002 at the beginning. Moreover, the out-of-sample period ranges from 8/25/2002 to 7/28/2004, see Figure 2.4.1. The forecasting experiment is designed as follows. We use in-sample data to estimate the parameters of the model of interest. We, then, make out-of-sample forecasts up to 100 steps ahead and evaluate them. The in-sample period is then enlarged by one observation and again forecasts for the out-of-sample period are made and evaluated. We repeat this procedure 604 times. This forecasting study has been carried out using the logarithm of baseload and the logarithm of peakload prices, respectively. Fur-

thermore, the used measures have been computed for each  $h$ -step ahead forecast with  $h \in \{1, 2, \dots, 100\}$ .  $P_t$  denotes the actual observed price at time  $t$ , while  $P_t^f$  refers to the predicted price at time  $t$ . The measures used for comparison are

$$RMSE = \sqrt{\frac{1}{k} \cdot \sum_{i=1}^k \left( \log(P_t) - \log(P_t^f) \right)^2}, \quad (2.4.1)$$

$$MAE = \frac{1}{k} \cdot \sum_{i=1}^k \left| \log(P_t) - \log(P_t^f) \right|. \quad (2.4.2)$$

For practical work, we are rather interested in the forecasts of  $P_t^f$  than in forecasts of  $\log(P_t^f)$ . However, we aim to compare the models which are designed for the logarithm of power prices.

### 2.4.1 Theoretical Preliminaries

We carry out the  $h$ -step ahead forecast in the usual way based on conditional expectation  $E[X_{T+h}|\mathcal{F}_T]$ , where  $\mathcal{F}_T$  denotes the information set at time  $T$ . Generally, there are two ways of carrying out forecasts. Both versions ( $\log(P_{T+h,1}^f)$ ,  $\log(P_{T+h,2}^f)$ ) are depicted below. Moreover, it should be noted that these forecast procedures yield different forecasts for the logarithm of power prices  $\log(P_{T+h}^f)$  in the presence of deterministic components. To clarify this, the stochastic part  $X_t$  is substituted by  $\log(P_t) - f_t$  according to equation (2.2.3),

$$\begin{aligned} X_{T+h,1}^f &= \log(P_{T+h,1}^f) - f_{T+h,1}^f \\ &= \rho \cdot \mu_M + (1 - \rho) \cdot X_{T+h-1,1}^f, \\ &= \rho \cdot \mu_M + (1 - \rho) \cdot (\log(P_{T+h-1}) - f_{T+h-1}), \end{aligned} \quad (2.4.3)$$

or

$$\begin{aligned} X_{T+h,2}^f &= \log(P_{T+h,2}^f) - f_{T+h,2}^f \\ &= \mu_M \cdot (1 - (1 - \rho)^h) + (1 - \rho)^h \cdot X_T, \\ &= \mu_M \cdot (1 - (1 - \rho)^h) + (1 - \rho)^h \cdot (\log(P_T) - f_T). \end{aligned} \quad (2.4.4)$$

Preliminary empirical studies suggest that the recursive procedure in equation (2.4.3), provides better forecasts than the second based on the forecast origin.

Although Models II and IIb apparently go beyond the popular Hamilton (1989) methodology, nevertheless, these models still fit into the theoretical Hamilton (1989) framework. Consequently, the forecasting methodology, we use, is based on Hamilton (1989). How to apply this methodology is described below.

Let  $\xi_{(T|\mathcal{F}_T)}$  be the vector of posterior densities at time  $T$ ,

$$\xi_{(T|\mathcal{F}_T)} = \begin{pmatrix} \frac{f(X_T, S_T = M|\mathcal{F}_{T-1})}{f(X_T|\mathcal{F}_{T-1})} \\ \frac{f(X_T, S_T = S|\mathcal{F}_{T-1})}{f(X_T|\mathcal{F}_{T-1})} \end{pmatrix}. \quad (2.4.5)$$

Moreover let  $P$  be the transition matrix,

$$P = \begin{pmatrix} q & 1-p \\ 1-q & p \end{pmatrix}. \quad (2.4.6)$$

The  $h$ -step ahead forecasts for the posterior probabilities are computed as follows,

$$\xi_{T+h}^f = P \cdot \xi_{(T+h-1|\mathcal{F}_T)}. \quad (2.4.7)$$

$V_{T+h}$  is defined as the vector containing the conditional expectations  $E[X_{T+h}|S_{T+h} = j, \mathcal{F}_T]$   $j \in \{M, S\}$  for each regime,

$$V_{T+h} = \begin{pmatrix} E[X_{T+h}|S_{T+h} = M, \mathcal{F}_T] \\ E[X_{T+h}|S_{T+h} = S, \mathcal{F}_T] \end{pmatrix}. \quad (2.4.8)$$

Finally the forecast results as

$$X_{T+h}^f = V_{T+h}^T \cdot \xi_{T+h}^f. \quad (2.4.9)$$

In De Jong and Huisman (2003) the two regimes are assumed to be independent. We aim to avoid spikes in forecasting the stable regime. Therefore, we compute the conditional expectation  $E[X_{T+h}|S_{T+h} = M, \mathcal{F}_T]$  as follows,

$$E[X_{T+h}|S_{T+h} = M, \mathcal{F}_T] = \mu_M \cdot (1 - (1 - \rho)^h) + (1 - \rho)^h \cdot E[X_T|S_T = M, \mathcal{F}_T]. \quad (2.4.10)$$

Furthermore, we should note that in the framework of De Jong and Huisman (2003) the problem remains to determine the last spot price originating from the stable regime. Therefore, an approximation for  $E[X_T|S_T = M, \mathcal{F}_T]$  should be used for forecasting. However, we found that the bias is small when we use the actual value of  $X_T$  as forecast origin instead. This kind of error is of minor importance because spikes rarely occur in the given data. Spot price series which exhibit more spikes might require an approximation as outlined above.

As opposed to the de framework of De Jong and Huisman (2003), forecasting with Models III and IIIb is straightforward in spirit to Hamilton (1989).

Let  $\xi_{(T|\mathcal{F}_T)}$  be the vector of posterior densities at time T,

$$\xi_{(T|\mathcal{F}_T)} = \begin{pmatrix} \frac{f(X_T, S_T = M, S_{T-1} = M|\mathcal{F}_{T-1})}{f(X_T|\mathcal{F}_{T-1})} \\ \frac{f(X_T, S_T = M, S_{T-1} = S|\mathcal{F}_{T-1})}{f(X_T|\mathcal{F}_{T-1})} \\ \frac{f(X_T, S_T = S, S_{T-1} = M|\mathcal{F}_{T-1})}{f(X_T|\mathcal{F}_{T-1})} \\ \frac{f(X_T, S_T = S, S_{T-1} = S|\mathcal{F}_{T-1})}{f(X_T|\mathcal{F}_{T-1})} \end{pmatrix}. \quad (2.4.11)$$

Moreover let  $Q$  be the transition matrix,

$$Q = \begin{pmatrix} q & q & 0 & 0 \\ 0 & 0 & 1-p & 1-p \\ 1-q & 1-q & 0 & 0 \\ 0 & 0 & p & p \end{pmatrix}. \quad (2.4.12)$$

We compute the  $h$ -step ahead forecasts for the posterior densities as follows,

$$\xi_{T+h}^f = Q \cdot \xi_{(T+h-1|\mathcal{F}_T)}. \quad (2.4.13)$$

Let  $V_{T+h}$  again be the vector that contains the conditional expectations  $E[X_{T+h}|S_{T+h} = i, S_{T+h-1} = j, \mathcal{F}_T]$ ,  $i, j \in \{M, S\}$  for each regime.

$$V_{T+h} = \begin{pmatrix} E[X_{T+h}|S_{T+h} = M, S_{T+h-1} = M, \mathcal{F}_T] \\ E[X_{T+h}|S_{T+h} = M, S_{T+h-1} = S, \mathcal{F}_T] \\ E[X_{T+h}|S_{T+h} = S, S_{T+h-1} = M, \mathcal{F}_T] \\ E[X_{T+h}|S_{T+h} = S, S_{T+h-1} = S, \mathcal{F}_T] \end{pmatrix} \quad (2.4.14)$$

Then, according to Krolzig and Clements (1998) the following recursion holds,

$$X_{T+h}^f = V_{T+h}^T \cdot \xi_{T+h}^f, \quad (2.4.15)$$

As  $h \rightarrow \infty$  the posterior probability to be in regime  $j$ ,  $Prob(S_{T+h} = j|X_T)$ , converges to the unconditional probability to be in regime  $j$  since the Markov chain is assumed to be ergodic. This also holds in the framework of De Jong and Huisman (2003),

$$\lim_{h \rightarrow \infty} Prob(S_{T+h} = M|\mathcal{F}_T) = \frac{1-p}{2-p-q}, \quad (2.4.16)$$

$$\lim_{h \rightarrow \infty} Prob(S_{T+h} = S|\mathcal{F}_T) = \frac{1-q}{2-p-q}. \quad (2.4.17)$$

## 2.4.2 Results of the Study

In order to scrutinize the outcome of the study, the linear autoregressive model performs well in terms of very short-run forecasts, in particular, one up to two steps ahead. The results are presented in Figure 2.4.2 and Figure 2.4.3, respectively. For both measures, we cannot observe any clear difference from the remaining models. With respect to the long- run ability, however, non-linear models outperform the linear model which is partly due to the position of spikes in the time series. Another reason is the improved estimation compared to the linear model. Estimation of important parameters for forecasting like deterministic components and  $\mu_M$  is less influenced by spikes. For short- run forecasting better estimates of  $\rho$  are of interest, too. Moreover, modified Models IIb and IIIb outperform their basic counterparts II and III with respect to the RMSE. This is a consequence of the modification of the spike regime, since the direction of spikes is better predicted by the modified models. Finally, Model IIIb provides better long- run forecasts than model IIb, while in terms of short- run forecasting, the opposite is true.

Forecasts for the stable regime have to be based on the forecast origin  $X_T$  in Models II and IIb. A recursive procedure, like in the pure Hamilton (1989) framework, is prohibited due to the assumption of independent regimes. However, there is empirical evidence that in the presence of deterministic components, a recursive procedure provides better forecasts. Another problem arises if  $X_T$  is indeed a spike but treated as originating from the stable regime. Obviously, forecasts for the stable regime based on a spike are biased. Short run forecasts of Model IIb

are better than those of Model IIIb. Therefore, the arising prediction bias when the forecast for the stable regime in Model I Ib is based on  $X_T$ , when  $X_T$  is indeed a spike, seems to be of minor importance.

The recursive procedure in forecasting is the advantage of Model IIIb compared to Model I Ib. Additionally, we have only used the stable regime of Models II and I Ib to make forecasts. These forecasts are denoted by II-stable and I Ib-stable in Figures 2.4.2 and 2.4.3. For Model II, we obtain better forecasts if we renounce to exploit the whole non-linear methodology. However, this holds unless the modification proposed by Kosater and Mosler (2006) is implemented.

Furthermore, outcomes with respect to the two proposed measures are different. In terms of MAE, models which perform best with respect to the RMSE are often nearly or indeed outperformed by their unmodified counterparts. Moreover, the performance of forecasts if we only use the stable regime is remarkably good and sometimes even best with respect to the MAE. To understand these results, it is necessary to bear in mind that deviations due to outliers have much more impact and are more penalized by the RMSE than by the MAE. Therefore, the advantage of modified models compared to the unmodified models is of minor importance with respect to the MAE.

However, we have to stress that prices at the edge of the forecasting sample do not have the same weight on the outcome of the study as prices which lie rather in the middle. This aspect must be taken into consideration when the results of the empirical study are gauged. One consequence is that in our study non-linear models clearly outperform the linear model in terms of long-run forecasting ( 30-80 steps ahead ). Note that in our study, periods with larger sized spikes are settled rather in the middle while stable periods prevail at the beginning and at the end of the whole forecasting sample 8/25/2002 to 7/28/2004.

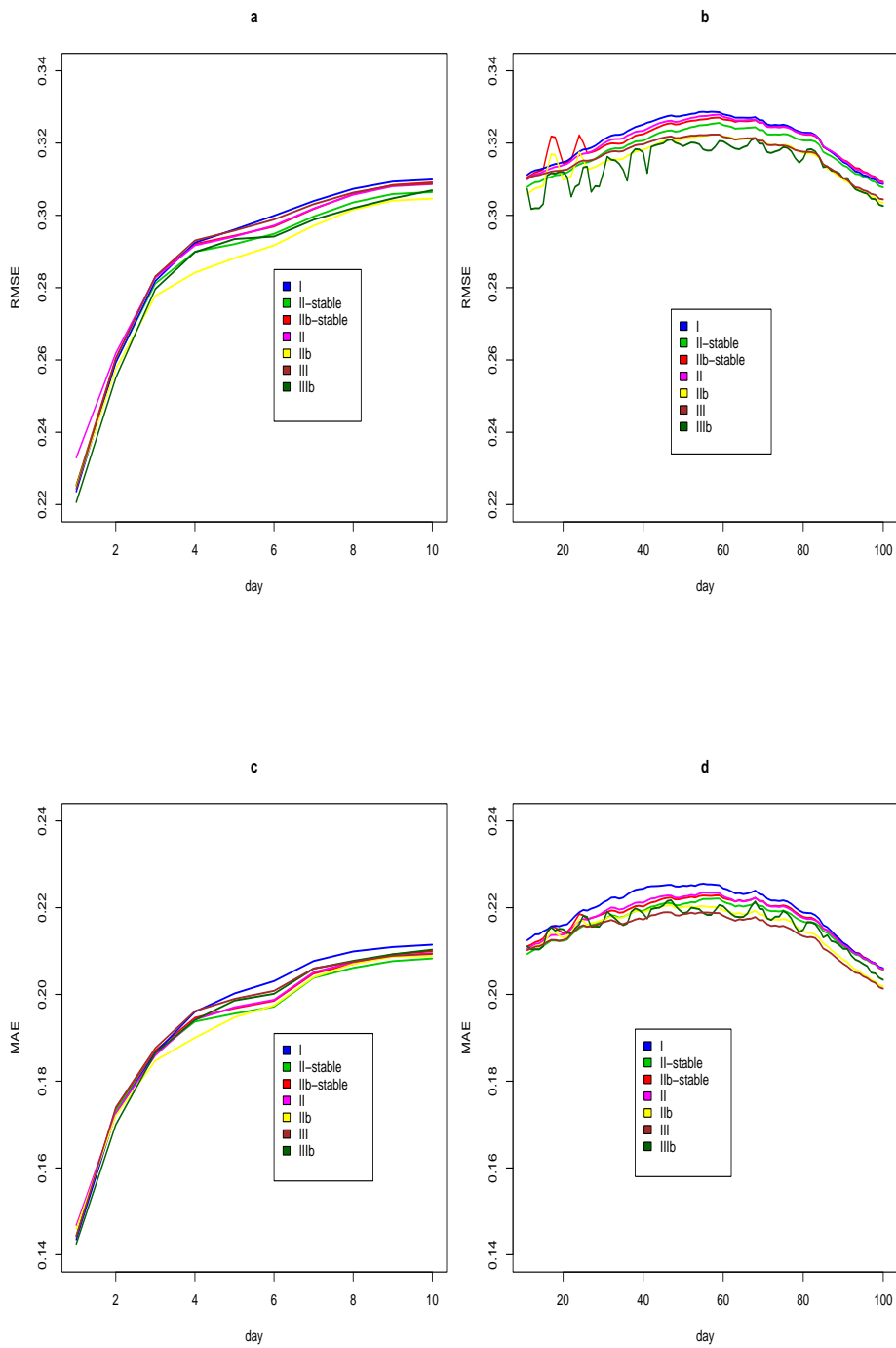


Figure 2.4.1: Results of all models for the log(baseload) time series ( RMSE means root mean square error and MAE means mean absolute error).

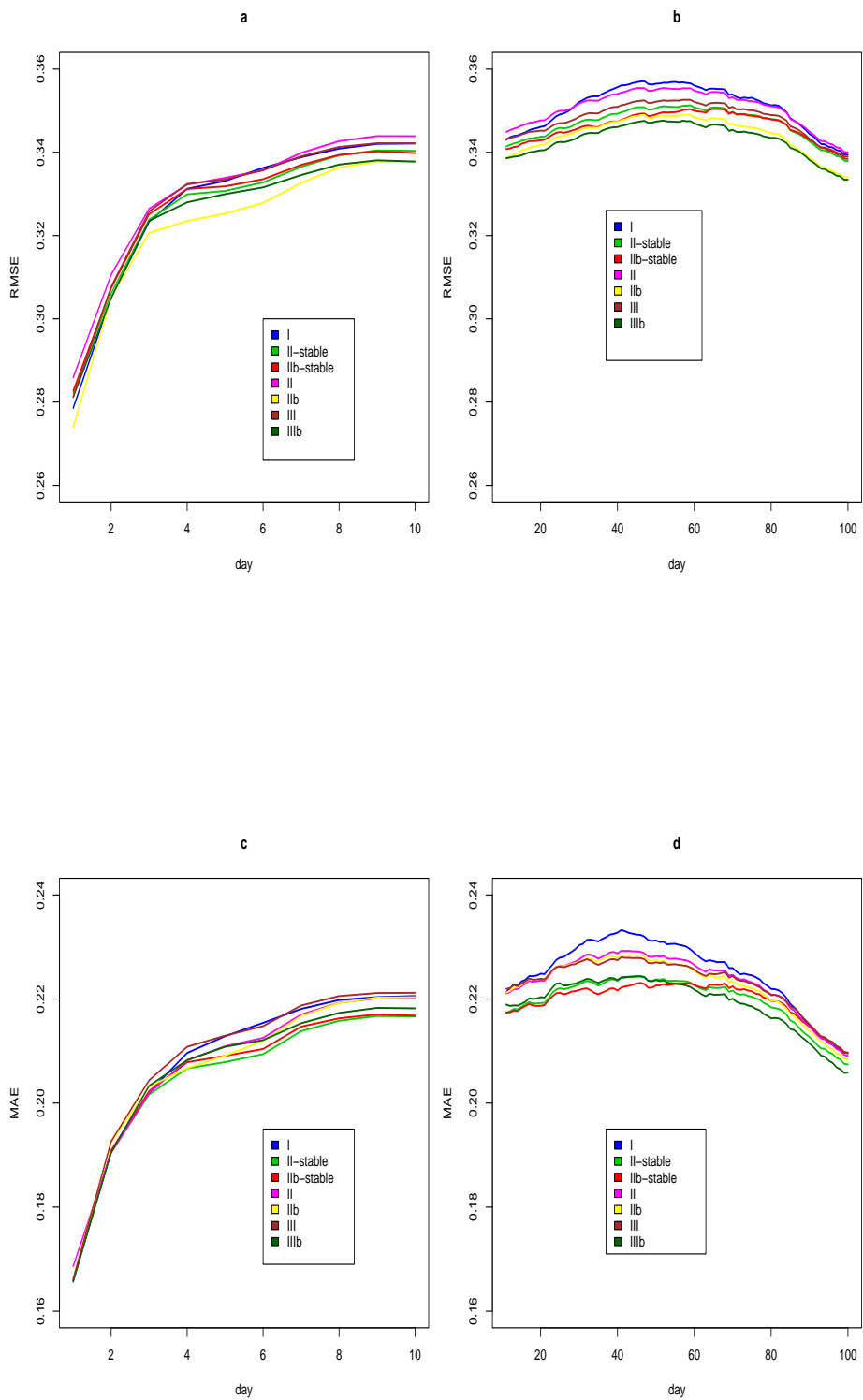


Figure 2.4.2: Results of all models for the  $\log(\text{peakload})$  time series ( RMSE means root mean square error and MAE means mean absolute error).

## 2.5 Regime-Switching Models and GARCH

Extensions of the three basic models Ethier and Mount (1998), the three-regime model of Mahieu and Huisman (2003) and the two-regime model with independent spikes have been restrained to the modification of the spike regime, so far.

Besides the introduction of day-dependent spikes put forward by Kosater and Mosler (2006), Bierbrauer et al. (2004) suggest to draw spikes from a Pareto distribution instead of a normal distribution. By contrast, De Jong (2006) implements a Poisson-normal mixture distribution for the spike regime.

Although Escribano et al. (2002) show that autoregressive conditional heteroscedasticity is an important feature of electricity prices, this feature has so far been neglected.

To start with, we present a jump model, which incorporates GARCH(1,1) dynamics in spirit to Escribano et al. (2002), in the following equations (2.5.1) and (2.5.2). Here, we denote the conditional variance at time  $t$  by  $h_t$ , whereas  $\lambda, \mu_S$  and  $\sigma_S$  have the same meaning as in subsection 2.3.2.

$$X_t = \begin{cases} (1 - \rho)X_{t-1} + h_t^{\frac{1}{2}} \epsilon_{1t} & : \text{ with Probability } 1 - \lambda \\ (1 - \rho)X_{t-1} + h_t^{\frac{1}{2}} \epsilon_{1t} + \mu_S + \sigma_S \epsilon_{2t} & : \text{ with Probability } \lambda \end{cases} \quad (2.5.1)$$

$h_t$  is assumed to follow a GARCH(1,1) process.

$$h_t = \omega + \alpha \epsilon_{t-1}^2 + \beta h_{t-1} \quad (2.5.2)$$

An explanation why this feature has been neglected may become evident when we take into account Figure 2.5.1., where histograms for the logarithm of baseload from which the deterministic effects have been removed are plotted together with the estimated normal probability densities for all considered models in the forecasting study.

As opposed to econometric models applied to financial time series, the regime-switching models seem to fairly well capture the leptokurtic behavior displayed by the logarithm of spot prices. By this, omission of autoregressive conditional heteroscedasticity seems justified. Another reason for the omission is that pricing of derivatives can be carried out more easily if conditional variances are not time-varying.

Recent work of Misiorek et al. (2006) however, highlights the importance of interval forecasting for risk management in the power sector. It is common knowledge that interval forecasts crucially depend on the specification of the conditional variance dynamics. Consequently, omission of potential ARCH or GARCH dynamics may lead to wrong management decisions. Therefore, we investigate how GARCH models can be integrated into the aforementioned Markov regime-switching framework. Secondly, we examine if this model extension is worthwhile compared with the basic models in terms of in-sample fit. A comparison of the out-of-sample interval forecasting performance in spirit to Misiorek et al. (2006) is left for further research.

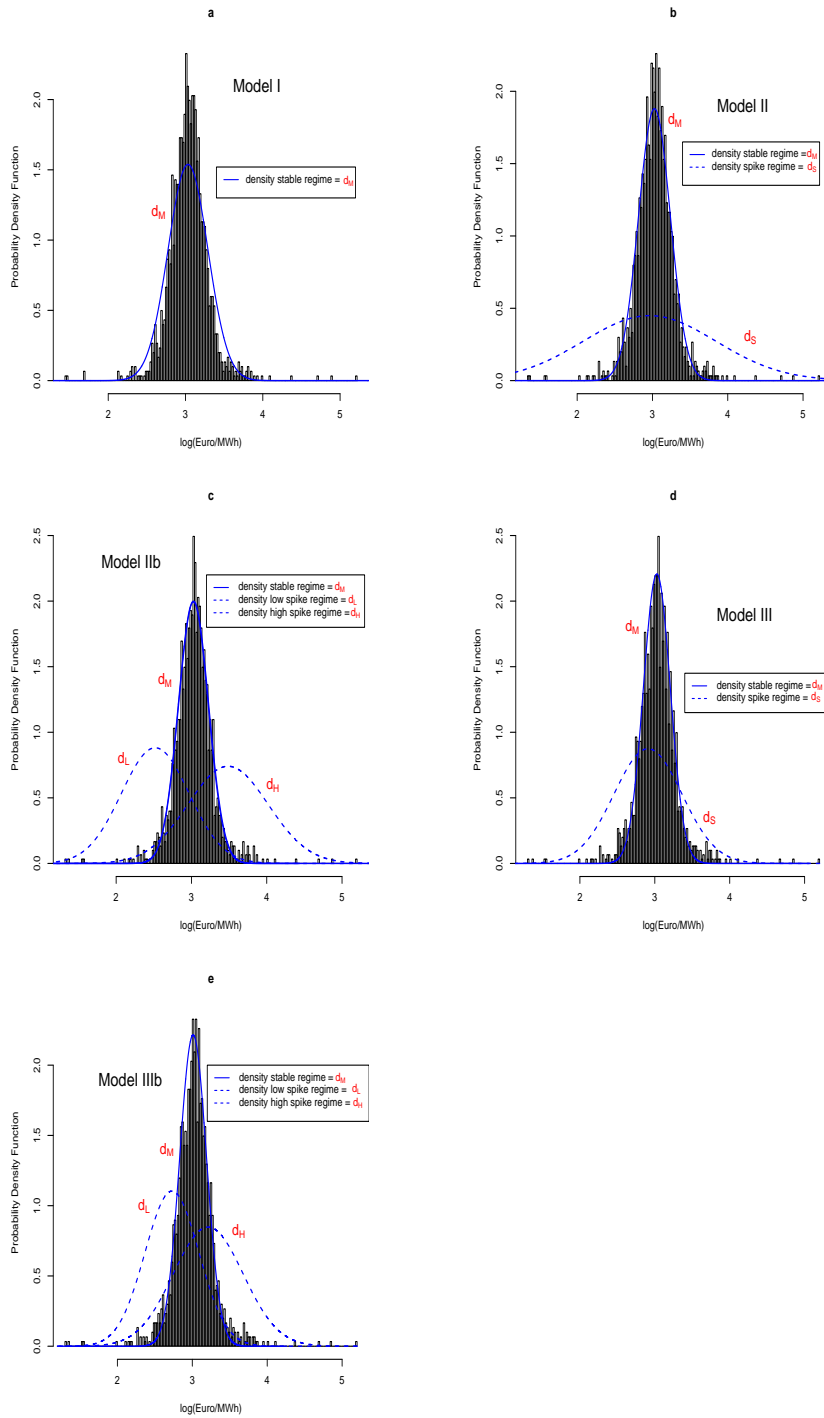


Figure 2.5.1: Histograms for log(baseload) from which the deterministic effects have been removed are plotted together with the estimated normal probability densities for the models I to IIIb, according to section 2.4.

### 2.5.1 Two-Regime Switching Model with GARCH(1,1) Errors

Hamilton and Susmel (1994) as well as Cai (1994) extend the Markov regime-switching framework to ARCH models originally proposed by Engle (1982). However, most popular with modelling of financial and macroeconomic time series is the GARCH(1,1) model suggested by Bollerslev (1986). Whereas the extension of the Markov regime-switching framework to ARCH models is straightforward, the extension to a GARCH(1,1) Markov regime-switching model is more problematic due to a phenomenon known as path dependence. The notion of path dependence describes that the conditional variance  $h_t$  as given in equation (2.5.2) depends on the full history  $\{X_{t-1}, X_{t-2}, \dots, X_1, X_0, S_{t-1}, S_{t-2}, \dots, S_1, S_0\}$ . Let  $h_{M,t}$  be the conditional variance at time  $t$ , given the information set  $\mathcal{F}_{t-1}$  and  $S_t = M$ . Moreover, let  $h_{S,t}$  be similarly defined then

$$\begin{aligned} h_t &= E[X_t^2 | \mathcal{F}_{t-1}] - (E[X_t | \mathcal{F}_{t-1}])^2 & (2.5.3) \\ &= P(S_t = M | \mathcal{F}_{t-1}) \cdot (E[X_t | S_t = M, \mathcal{F}_{t-1}]^2 + h_{M,t}) \\ &\quad + P(S_t = S | \mathcal{F}_{t-1}) \cdot (E[X_t | S_t = S, \mathcal{F}_{t-1}]^2 + h_{S,t}) \\ &\quad - (P(S_t = M | \mathcal{F}_{t-1}) \cdot E[X_t | S_t = M, \mathcal{F}_{t-1}] \\ &\quad + P(S_t = S | \mathcal{F}_{t-1}) \cdot E[X_t | S_t = S, \mathcal{F}_{t-1}])^2. \end{aligned}$$

To circumvent the path dependence problem, we follow Gray (1996) and assume that

$$h_{i,t} = \omega_{\{S_t=i\}} + \alpha_{\{S_t=i\}} \epsilon_{t-1}^2 + \beta_{\{S_t=i\}} h_{t-1} \quad \text{with } i \in \{M, S\}. \quad (2.5.4)$$

Moreover according to Gray (1996), we assume,

$$\begin{aligned} \epsilon_{t-1} &= X_{t-1} - E[X_{t-1} | \mathcal{F}_{t-2}] & (2.5.5) \\ &= X_{t-1} - (P(S_{t-1} = M | \mathcal{F}_{t-2}) \cdot E[X_{M,t-1} | \mathcal{F}_{t-2}] \\ &\quad + P(S_{t-1} = S | \mathcal{F}_{t-2}) \cdot E[X_{S,t-1} | \mathcal{F}_{t-2}]) \quad . \end{aligned}$$

To model the conditional mean, we assume the Markov regime-switching model with day-dependent and without independent spikes according to equations (2.3.4), (2.3.5) and (2.3.19) to (2.3.21).

$$X_{M,t} = \mu_M + (1 - \rho) \cdot (X_{\{S_{t-1}=i\}, t-1} - \mu_{\{S_{t-1}=i\}}) + \epsilon_{M,t}, \quad (2.5.6)$$

$$X_{S,t} = \mu_S + (1 - \rho) \cdot (X_{\{S_{t-1}=i\}, t-1} - \mu_{\{S_{t-1}=i\}}) + \epsilon_{S,t}, \quad (2.5.7)$$

$$\mu_S = \mathbf{1}_H \cdot (\mu_{S,H}) + (\mathbf{1} - \mathbf{1}_H) \cdot (\mu_{S,L}), \quad (2.5.8)$$

$$\epsilon_{S,t} = \mathbf{1}_H \cdot (\epsilon_{S,H,t}) + (\mathbf{1} - \mathbf{1}_H) \cdot (\epsilon_{S,L,t}), \quad (2.5.9)$$

with  $i \in \{M, S\}$ ,  $\epsilon_{M,t} \sim \mathcal{N}(0, h_{M,t})$ ,  $\epsilon_{S,H,t} \sim \mathcal{N}(0, h_{S,H,t})$ ,  $\epsilon_{S,L,t} \sim \mathcal{N}(0, h_{S,L,t})$ .

This model approach seems to work well in the context of financial time series, see Gray (1996) and Haas et. al (2004). Unfortunately, it seems not adequate for German electricity spot prices. We have set  $\alpha_S = \alpha_M = \alpha$  and  $\beta_S = \beta_M = \beta$  to assure convergence. The results indicate as well for the logarithm of baseload as for the logarithm of peakload, respectively, that the Markov regime-switching approach does not fit to the given data. More precisely, parameter estimation

does not yield significant transition parameters  $p$ , for the logarithm of peakload even  $p < 0$  is obtained. The nonsignificant transition parameters indicate, that the regime-switching model should be rejected in favor of a simple mixture model or even a linear model. In addition, the parameters for the low spike regime are not significant. The results for the jump model outlined above and the discussed Markov regime-switching model are collected in table 2.5.1.

Ongoing research puts forward to estimate Markov regime-switching ARMA-GARCH models exploiting Monte Carlo Markov Chain methods. These methods are computationally burdensome. In addition, simultaneous estimation of deterministic effects and the stochastic part may be hardly feasible. A more comprehensive investigation into Markov regime-switching ARMA-GARCH models and Monte Carlo Markov Chain methods in the field of spot electricity prices is left for further research.

Table 2.5.1: Results on the Jump Model and the Two-Regime Switching Model with GARCH(1,1) Errors, see equations(2.5.1-2.5.7).

	Jump Model		Two- Regime Switching Model	
	log(baseload)	log(peakload)	log(baseload)	log(peakload)
$\beta_1$	-0.272 (0.009)	-0.343 (0.011)	-0.268 (0.009)	-0.340 (0.010)
$\beta_2$	-0.550 (0.009)	-0.640 (0.011)	-0.550 (0.010)	-0.636 (0.012)
$\beta_3$	-0.484 (0.016)	-0.636 (0.019)	-0.486 (0.018)	-0.623 (0.022)
$\beta_4$	0.0003 ( $2.9 \cdot 10^{-5}$ )	0.0003 ( $2.6 \cdot 10^{-5}$ )	0.0003 ( $2.8 \cdot 10^{-5}$ )	0.0003 ( $2.5 \cdot 10^{-5}$ )
$\gamma_1$	0.125 (0.017)	0.118 (0.016)	-0.128 (0.017)	0.110 (0.016)
$\gamma_2$	271.27 (8.324)	-78.742 (7.847)	87.657 (7.990)	-82.000 (7.227)
$\mu_M$	3.008 (0.024)	3.211 (0.022)	3.009 (0.024)	3.208 (0.022)
$\mu_S \wedge \mu_{S,H}$	0.109* (0.099)	0.151* (0.087)	4.008 (0.423)	4.267 (0.436)
$\mu_{S,L}$	-	-	1.296* (0.726)	1.852* (0.891)
$\rho$	0.304 (0.020)	0.380 (0.021)	0.312 (0.019)	0.385 (0.021)
$\omega_M$	0.006 (0.001)	0.007 (0.001)	0.003* (0.003)	-0.011 (0.003)
$\sigma_S \wedge \omega_{S,H}$	0.612 (0.064)	0.662 (0.045)	0.238 (0.048)	0.360 (0.096)
$\omega_{S,L}$	-	-	0.195* (0.149)	0.516 (0.236)
$\alpha$	0.167 (0.030)	0.149 (0.026)	0.155 (0.034)	0.130 (0.022)
$\beta$	0.521 (0.065)	0.562 (0.053)	0.404 (0.076)	0.694 (0.034)
$\lambda \wedge p$	0.033 (0.008)	0.049 (0.010)	0.143* (0.083)	-0.016* (0.024)
$q$	-	-	0.967 (0.009)	0.965 (0.009)
LL	600.56	377.72	613.01	394.58
AC	-0.7805	-0.4840	-0.7931	-0.5024
SC	-0.7310	-0.4345	-0.7330	-0.4423

Note that \* means not significant at the 5 % level. Furthermore, instead of  $\omega_S$ , we denote two distinct parameters  $\omega_{S,H}$  for the high spike regime and  $\omega_{S,L}$  for the low spike regime.

## 2.5.2 Two-Regime- Switching Model with ARCH(1) Errors

In this subsection, we include ARCH(1) errors instead of GARCH(1,1) errors as done in the preceding subsection. The advantage is that we merely have to cope with path dependence with respect to  $\{X_{t-1}, X_{t-2}, S_{t-1}, S_{t-2}\}$ . We only assume an ARCH(1) process for the conditional variance of the stable regime.

Here, we furthermore assume equations (2.5.6) to (2.5.9) for the conditional mean. The conditional variance  $h_{M,t}$  is now assumed to be,

$$h_{M,t} = \omega_M + \alpha_M \epsilon_{\{S_{t-1}=j\},t-1}^2 \quad \text{with } i, j \in \{M, S\}. \quad (2.5.10)$$

whereas the conditional variance  $h_{S,t}$  is now

$$h_{S,t} = \mathbf{1}_H \cdot \sigma_{S,H}^2 + (1 - \mathbf{1}_H) \cdot \sigma_{S,L}^2. \quad (2.5.11)$$

Moreover, we compute  $\epsilon_{\{S_{t-1}=j\},t-1}$  as follows,

$$\epsilon_{\{S_{t-1}=j\},t-1} = X_{\{S_{t-1}=j\},t-1} - E[X_{\{S_{t-1}=j\},t-1} | \mathcal{F}_{t-2}]. \quad (2.5.12)$$

Here, as opposed to the Markov regime-switching Model with GARCH(1,1) errors, we assume the ARCH(1) process to prevail in the stable regime only because our data does not support the assumption of distinct parameters for the stable regime and the spike regime. Estimation yields significant estimates around 3 for  $\alpha_S$ , which in other words means that the spike regime possesses a negative unconditional variance. Therefore, we do not exhibit the estimation results in a table.

Secondly, the assumption of an ARCH(1) process evolving across both regimes respectively provides a slightly better fit, on one hand. On the other hand, simulations show that the model with the ARCH(1) in the stable regime only performs better in terms of the quantile-quantile plot.

## 2.5.3 Two-Regime-Switching Model with Independent Spikes and ARCH(1) Errors

To conclude this section, we present an extension of the two- regime framework with independent spikes suggested by De Jong and Huisman (2003).

In our opinion, this model framework does not allow to overcome the problem of path dependence which emerges if we attempt to incorporate a GARCH(1,1) process for one or both regimes, respectively. Therefore, we are satisfied with an ARCH(1) process which can be added to the model specification. However, we have only the possibility to assume two independent ARCH(1) processes for each regime or to leave one regime specification unchanged and to assume an ARCH(1) for the second in this model framework. Spikes are rare and the duration between two consecutive spikes may be very long. Therefore, we leave the spike regime unchanged and confine ourselves to include ARCH(1) errors in the stable regime, exclusively. Consequently, the conditional variance in the spike regime is specified as in equation (2.5.11). The stable regime can be expressed as follows,

$$X_{M,t} = X_{M,t-1} + \rho \cdot (\mu_M - X_{M,t-1}) + \epsilon_{M,t}, \quad \epsilon_{M,t} \sim \mathcal{N}(0, h_{M,t}) \quad (2.5.13)$$

$$h_{M,t} = \omega_M + \alpha_M \cdot \epsilon_{M,t-1}^2. \quad (2.5.14)$$

Consequently, the change in the specification of the stable regime affects the estimation of model parameters. More precisely, the important conditional variance  $Var[X_{M,t}|\mathcal{F}_{t-i}]$  becomes more sophisticated due to the assumption of ARCH(1) errors.

$$Var[X_{M,t}|\mathcal{F}_{t-i}] = \epsilon_{M,t-i}^2 \cdot \left( \sum_{j=0}^{i-1} \alpha_M^{i-j} \cdot (1-\rho)^{2j} \right) + \frac{\omega_M}{\alpha_M - 1} \cdot \sum_{j=0}^{i-1} (\alpha_M^{i-j} - 1) \cdot (1-\rho)^{2j} . \quad (2.5.15)$$

Equation (2.5.16) can be very easily derived if we bear in mind that

$$Var[X_{M,t}|\mathcal{F}_{t-i}] = \sum_{j=0}^{i-1} (1-\rho)^{2j} \cdot Var[\epsilon_{M,t-j}|\mathcal{F}_{t-i}] , \quad (2.5.16)$$

$$Var[\epsilon_{M,t}|\mathcal{F}_{t-i}] = \omega_M \cdot \frac{\alpha_M^i - 1}{\alpha_M - 1} + \alpha_M^i \cdot \epsilon_{M,t-i}^2 . \quad (2.5.17)$$

If we set  $t = t - j$  and  $i = i - j$ , equation (2.5.18) yields

$$Var[\epsilon_{M,t-j}|\mathcal{F}_{t-i}] = \omega \cdot \frac{\alpha_M^{i-j} - 1}{\alpha_M - 1} + \alpha_M^{i-j} \cdot \epsilon_{M,t-i}^2 . \quad (2.5.18)$$

Consequently, we immediately obtain

$$\begin{aligned} Var[X_{M,t}|\mathcal{F}_{t-i}] &= \sum_{j=0}^{i-1} (1-\rho)^{2j} \cdot (\omega_M \cdot \frac{\alpha_M^{i-j} - 1}{\alpha_M - 1} + \alpha_M^{i-j} \cdot \epsilon_{M,t-i}^2) \quad (2.5.19) \\ &= \epsilon_{M,t-i}^2 \cdot \left( \sum_{j=0}^{i-1} \alpha_M^{i-j} \cdot (1-\rho)^{2j} \right) \\ &\quad + \frac{\omega_M}{\alpha_M - 1} \cdot \sum_{j=0}^{i-1} (\alpha_M^{i-j} - 1) \cdot (1-\rho)^{2j} . \quad (2.5.20) \end{aligned}$$

The remaining problem is the determination of  $\epsilon_{M,t-i}$ . We suggest to approximate  $\epsilon_{M,t-i}$  as follows,

$$\epsilon_{M,t-i} \approx$$

$$\sum_{j=0}^{K-1} Prob[S_{t-i-j} = M \wedge S_{t-i-l} \neq M \text{ for } l < j] \cdot (X_{M,t-i} - E[X_{M,t-i}|\mathcal{F}_{t-i-j}]) , \quad (2.5.21)$$

and again  $K = 5$  is assumed. The results of the two- regime models with ARCH(1) errors are reported in table 2.5.2.

To summarize the in-sample results, we obtain a better fit when the ARCH(1) process is included, in particular for the logarithm of baseload. This is not completely true for the logarithm of peakload, since the Schwartz Criterion favors the model with constant volatility. The quantile-quantile plots in Figure 2.5.2, however, seem to support the specification with constant volatility except for the model with independent spikes and ARCH(1) errors, where the opposite seems to be true.

Table 2.5.2: Results on Two-Regime Models with ARCH(1) errors, see equations (2.5.8-2.5.21).

	Without Independent Spikes		With Independent Spikes	
	log(baseload)	log(peakload)	log(baseload)	log(peakload)
$\beta_1$	-0.265 (0.009)	-0.335 (0.011)	-0.272 (0.009)	-0.342 (0.011)
$\beta_2$	-0.548 (0.009)	-0.642 (0.011)	-0.557 (0.009)	-0.650 (0.011)
$\beta_3$	-0.481 (0.017)	-0.612 (0.019)	-0.482 (0.017)	-0.618 (0.018)
$\beta_4$	0.0003 ( $2.9 \cdot 10^{-5}$ )	0.0003 ( $2.7 \cdot 10^{-5}$ )	0.0003 ( $3.2 \cdot 10^{-5}$ )	0.0003 ( $2.9 \cdot 10^{-5}$ )
$\gamma_1$	-0.120 (0.016)	0.107 (0.016)	0.127 (0.018)	0.108 (0.017)
$\gamma_2$	88.071 (8.533)	-78.071 (8.889)	-91.253 (10.100)	-475307.2 (9.363)
$\mu_M$	3.019 (0.024)	3.224 (0.022)	3.031 (0.028)	3.234 (0.024)
$\mu_{S,H}$	3.186 (0.082)	3.571 (0.079)	3.559 (0.141)	3.886 (0.102)
$\mu_{S,L}$	2.667 (0.092)	2.801 (0.123)	2.680 (0.138)	2.817 (0.158)
$\rho$	0.305 (0.018)	0.373 (0.020)	0.260 (0.018)	0.339 (0.022)
$\omega_M$	0.015 (0.001)	0.020 (0.001)	0.015 (0.001)	0.022 (0.001)
$\sigma_{S,H}$	0.508 (0.030)	0.571 (0.033)	0.556 (0.060)	0.553 (0.041)
$\sigma_{S,L}$	0.370 (0.035)	0.554 (0.038)	0.372 (0.050)	0.631 (0.054)
$\alpha_M$	0.164 (0.045)	0.135 (0.040)	0.266 (0.039)	0.103 (0.044)
$p$	0.694 (0.065)	0.604 (0.072)	0.500 (0.090)	0.671 (0.061)
$q$	0.975 (0.006)	0.969 (0.007)	0.975 (0.006)	0.975 (0.006)
LL	606.84	383.86	585.42	370.22
AC	-0.7867	-0.4898	-0.7623	-0.4742
SC	-0.7301	-0.4332	-0.7054	-0.4173

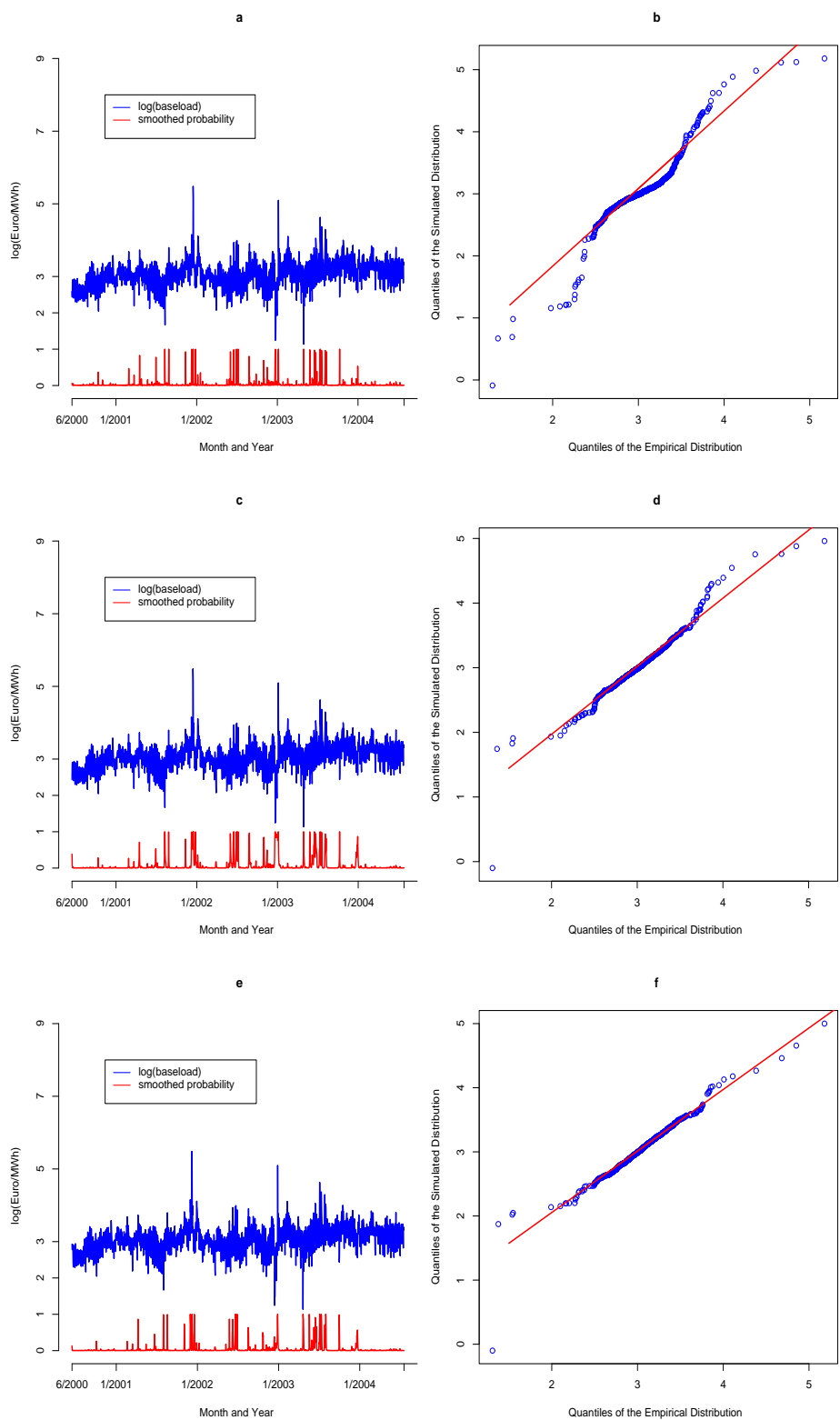


Figure 2.5.2: Smoothed probabilities for the spike regime and quantile-quantile plots for  $\log(\text{baseload})$  from which the deterministic effects have been removed against the estimated models: ((a),(b)) MS Model with GARCH(1,1), ((c),(d)) Two-Regime Model with ARCH(1), ((e),(f)) Two- Regime Model with Independent Spikes and ARCH(1), (*Note: To guarantee comparability, two elements in each simulated series throughout the three quantile-quantile plots (b,d,f) are set equal to -0.1 and 5, respectively*).

## 2.6 Summary

In this chapter, we have started with a discussion of previous Markov regime-switching approaches, put forward in the literature, to modelling the logarithm of daily electricity spot prices. Then we have introduced our own models with day-dependent spikes.

We have assessed the usefulness of the different competing models in terms of in-sample fit on one hand, and in terms of out-of-sample forecasting quality, on the other hand. The study has been carried out using the logarithm of German daily spot prices from the European Energy Exchange in Leipzig.

It turns out that models with day-dependent spikes outperform the previously presented models with respect to in-sample fit as well as out-of-sample prediction quality.

In addition, De Jong (2006) applied different models with day-dependent spikes to daily spot prices from several international electricity exchanges and found this extension to be worthwhile.

Finally in section 2.5, we have addressed the potential autoregressive conditional heteroscedasticity dynamics of electricity spot prices. This is an issue which has so far been neglected in the field of Markov regime-switching models applied to electricity spot prices.

Here, we have presented model extensions of the models with day-dependent spikes which include autoregressive conditional heteroscedasticity in the stable regime.

## Chapter 3

# The Impact of Weather on German Hourly Electricity Prices

### 3.1 Introduction

Besides Rambharat et al. (2005), Knittel and Roberts (2005) and Mount et al.(2006) research has yet been focussed on modelling pure stochastic processes for spot prices and the logarithm of spot prices. In this chapter, we investigate the relation between temperature and wind on one hand and hourly spot prices from the EEX in Leipzig on the other hand.

Lower temperatures cause a higher need for heating and therefore, increase the electricity demand. By contrast, high temperatures can affect demand for electricity due to the need for cooling. Furthermore, also the supply of electricity can be subject to high temperatures. During the extraordinary hot summer in 2003, for example, the operation of thermal power plants in Germany was affected due to poor cooling conditions. German energy policy seeks to promote wind energy by subsidizing the creation and the operation of windmills. The goal is to substitute parts of thermal electricity production and to establish wind energy instead. The trading of emission allowances with the aim to reduce CO<sub>2</sub> emissions is supposed to endorse renewable energy resources and consequently in particular wind energy. Wind energy, however, is exposed to large uncertainty. Hence, we expect that uncertainty and risk due to weather will rise and become of crucial importance in electricity spot markets.

Additionally, short- run forecasting for operational planning will have to explicitly take into account weather, in order to provide sensible results. Therefore, we attempt to specify the general impact of temperature and wind on hourly spot prices, on one hand. On the other hand, we try to quantify the relation between weather and the probability of the occurrence of spikes. Our approach is similar to Mount et al. (2006), whereas we include weather data in the model specification and make the transition probabilities a function of weather. In a further step, load and the reserve margin may be included in the specification, too. However,

there are not yet any time series available for load as well as the reserve margin for Germany, which we could use.

We proceed in the framework of the Kosater and Mosler (2006) model with day-dependent and independent spikes. This model is very well suited to achieve our second goal, which is linking weather and the probability of the occurrence of a spike. We opt for the version with independent spikes because of the results in the forecasting study presented in section 2.4, where this version performed slightly better in terms of short- run forecasting than the model version without independent spikes.

Thereinafter, we work in a multi-model framework consisting of 24 distinct hourly price series. Besides weekly seasonality, hourly prices exhibit a strong intra-day pattern. We do not exploit this intra-day pattern in our study because there is empirical evidence that a multi-model specification should be preferred in forecasting instead ; see Bunn (2000), Cuaresma et al.(2004), Misiolek and Weron (2005) and Misiolek et al. (2006).

We fit our model to each of the 24 hourly price series. Furthermore, we consider two model versions denoted A and B. Version A is the pure stochastic model and is included as a benchmark. In version B, we take into account the general impact, on one hand. Additionally, we attempt to quantify the relation between weather and spike-occurrence probability, on the other hand.

Decisions of market participants are not based on actual measured weather data but its forecasts. Unfortunately, providers of weather data merely archive the actual measured values, whereas weather forecasts are discarded. Therefore, we are forced to take the actually measured weather data as an approximation of their forecasts. In the second part of our study, we carry out a study to examine whether the inclusion of weather data improves forecasting of electricity spot prices.

## 3.2 Data and Descriptive statistics

In this study, we use data including hourly price series in Euro of the EEX and hourly temperature time series measured in  $0.1 \cdot C^\circ$  as well as hourly wind velocity time series measured in  $0.1 \cdot meter/second$  from four measuring stations Hamburg, Holzdorf, Mendig and Ulm in Germany. We have chosen these four measuring stations in order to represent the different parts of Germany. Hamburg is located in the North, Holzdorf near Leipzig represents the East, whereas Mendig can be found in the West of Germany. Finally, Ulm is located in the South of Germany. All data time series range from June 16<sup>th</sup> 2000 to December 31<sup>th</sup> 2004. Additionally, we use temperature forecasts and actually measured values of Ulm from 7 a.m. 05/01/2005 to 6 a.m. 06/01/2005 and wind velocity forecasts as well as actually measured data of Holzdorf for the same period. The data has been provided by the Deutscher Wetterdienst. Subfigure 3.2.1a shows the hourly price series, whereas subfigures 3.2.1b and 3.2.1c present the hourly measured wind velocity of Holzdorf and the hourly measured temperature of Ulm.

We report some descriptive statistics in table 3.2.1 for the 24 hours of the day. At first glimpse, we discover that the hourly price series are characterized by high

standard deviations, high skewness and excess kurtosis. However, this is especially true for the hours 9 until 20 which are referred to as on-peak. During these hours demand is usually very high and due to the hockey stick shape of the supply stack, see Johnson and Bartz (1999), the level of prices can become extremely high. By contrast, price series from 21 to 7 show a different picture with notably smaller standard deviations, only slight skewness and a kurtosis which does not deviate very much from the value 3 which is the value of the kurtosis of a normal distribution. Indeed, hourly series from 1 to 8 are referred to as off-peak I, whereas prices from 21 to 24 are referred to as off-peak II. Although price series at hour 8 and hour 21 already display characteristics which are closer to on-peak prices, nevertheless, they are classified as off-peak prices in trading.

In order to investigate the relation between prices and weather, we have carried out some preliminary least square regressions. As a result, we obtained that the fit and the explanatory power of data depends on the measuring station it is taken from. In our data, we see that among the measuring stations, temperature data of Ulm provides the best fit. The reason for the good performance of temperature of Ulm is its geographical location. In the south, industrial electricity demand is higher than in other parts of Germany. Therefore, electricity demand in this area is more important than in other areas. However in the case of wind, Hamburg and Holzdorf perform best. As opposed to Knittel and Roberts (2005), we do not include the average of the measuring stations, but only include temperature data from Ulm. In the case of wind velocity, it turned out that the average of Holzdorf and Hamburg works best. Hamburg performs well because this town is very near to the North Sea where many off-shore windmills are settled. Holzdorf also offers good conditions for the operation of windmills. Understanding which conditions are appropriate for the operation of windmills requires to take into account some technical facts. A windmill does not start working unless a wind velocity of round about 4 meter/second has been reached, see Federico (2002). Once this velocity is exceeded, produced electricity is proportional to the cube of the present wind velocity. This relation holds unless wind velocity reaches a value of round about 12 meter/second. At this point, we reach the maximal energy output. If wind velocity exceeds the value of 25 meter/second, windmills are switched off, for the sake of safety. We shall come back to the choice of the weather variables in section 3.3.

Subfigures 3.2.2a and 3.2.2b show a scatter plot for temperature of Ulm and the logarithm of power prices as well as a scatter plot for wind velocity of Holzdorf and the logarithm of power prices. In tables 3.2.2 and 3.2.2, we present some descriptive statistics for the measured values of the four stations. Table 3.2.3 and the boxplots presented in subfigure 3.2.1d reveal why Ulm is a bad location for windmills, whereas Hamburg and Holzdorf offer good conditions. More precisely, we can see in subfigure 3.2.1d that more than 75% of the wind velocity measured at Ulm is below the crucial margin of 4 meter/second. To depict this fact, we have added the red line at the value of 4 meter/second for wind velocity in subfigure 3.2.1d.

For a short time period, we have also collected weather forecasts and compare

them with the measured values in order to assess the quality of the approximation of forecasts by measured data. For example, subfigures 3.2.2c and 3.2.2d show the actually measured weather data and its one day-ahead forecasts for the given period from Ulm and Holzdorf, respectively. Additionally, we have examined the relationship between hourly prices and actually measured weather data as well as hourly prices and the one day-ahead forecasts. Subfigures 3.2.2e and 3.2.2f show the results. We see that the one day-ahead forecasts are similarly correlated with the hourly price as the actually measured data, except for some evening hours in the case of wind velocity.

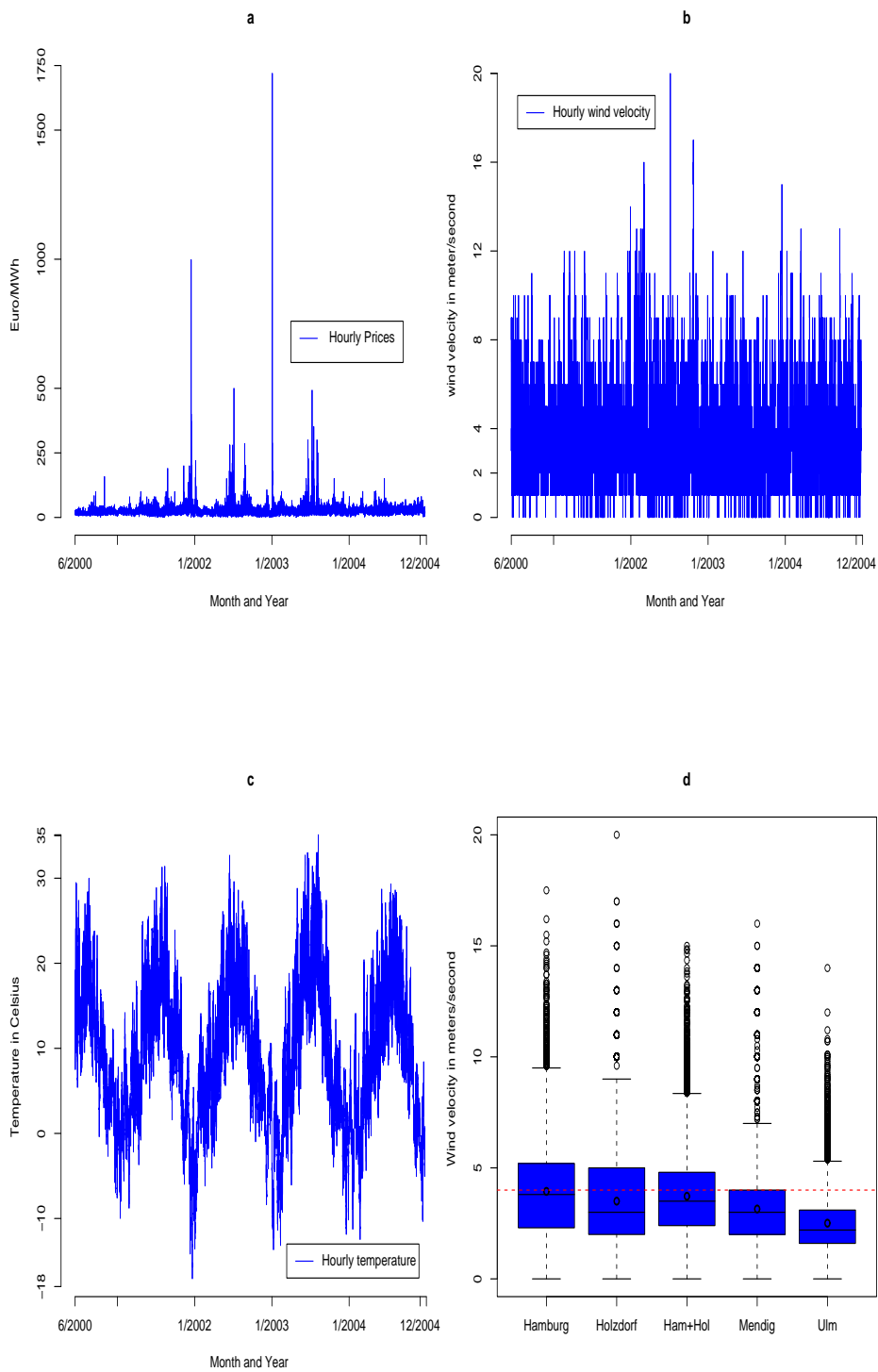


Figure 3.2.1: (a) Hourly power price series of the EEX, (b) Measured hourly wind velocity of Holzdorf, (c) Measured hourly temperature of Ulm, (d) Boxplot for hourly wind velocities, all data ranges from June 16<sup>th</sup> 2000 to December 31<sup>th</sup> 2004.

Table 3.2.1: Descriptive Statistics on Hourly Spot Prices at the EEX in Euro/MWh.

Hour	Mean	Std. Dev.	Skewness	Kurtosis
1	18.33	5.990	0.627	4.081
2	15.49	5.745	0.378	3.044
3	13.99	5.643	0.297	2.809
4	13.16	5.465	0.292	2.772
5	13.47	5.424	0.161	2.694
6	15.80	6.336	0.008	2.703
7	19.30	8.964	-0.006	2.607
8	26.09	14.168	3.137	44.675
9	29.24	17.081	5.952	83.199
10	31.43	16.260	5.164	61.357
11	34.00	19.986	10.266	199.225
12	42.36	35.918	6.992	75.505
13	33.85	18.006	5.807	63.129
14	31.58	17.488	7.329	120.006
15	28.90	15.337	6.280	93.314
16	26.83	13.588	8.132	172.239
17	26.68	21.646	20.359	571.203
18	29.84	24.200	14.125	347.799
19	32.01	52.141	25.317	744.903
20	28.58	16.777	15.154	379.727
21	26.86	10.379	6.438	128.525
22	24.39	7.099	0.507	3.258
23	23.78	6.456	0.691	4.312
24	20.20	5.711	0.282	2.901

Table 3.2.2: Descriptive Statistics on Temperature in  $C^{\circ}$ .

	Ulm	Mendig	Hamburg	Holzdorf
Mean	9.12	10.47	9.82	9.74
Median	9.10	10.3	10.0	9.80
Maximum	35.1	38.6	36.7	36.7
Minimum	-17.1	-15.6	-15.6	-21.1
Std. Dev.	8.27	7.93	8.70	8.70
Skewness	0.092	0.152	0.046	0.098
Kurtosis	2.482	2.799	2.644	2.653

Table 3.2.3: Descriptive Statistics on Wind Velocity in meter/second.

	Ulm	Mendig	Hamburg	Holzdorf
Mean	2.51	3.15	3.94	3.50
Median	2.20	3.00	3.80	3.00
Maximum	14.00	16.00	17.50	20.00
Minimum	0.00	0.00	0.00	0.00
Std. Dev.	1.33	2.03	2.11	1.98
Skewness	1.028	1.142	0.660	1.009
Kurtosis	4.854	4.555	3.420	4.531

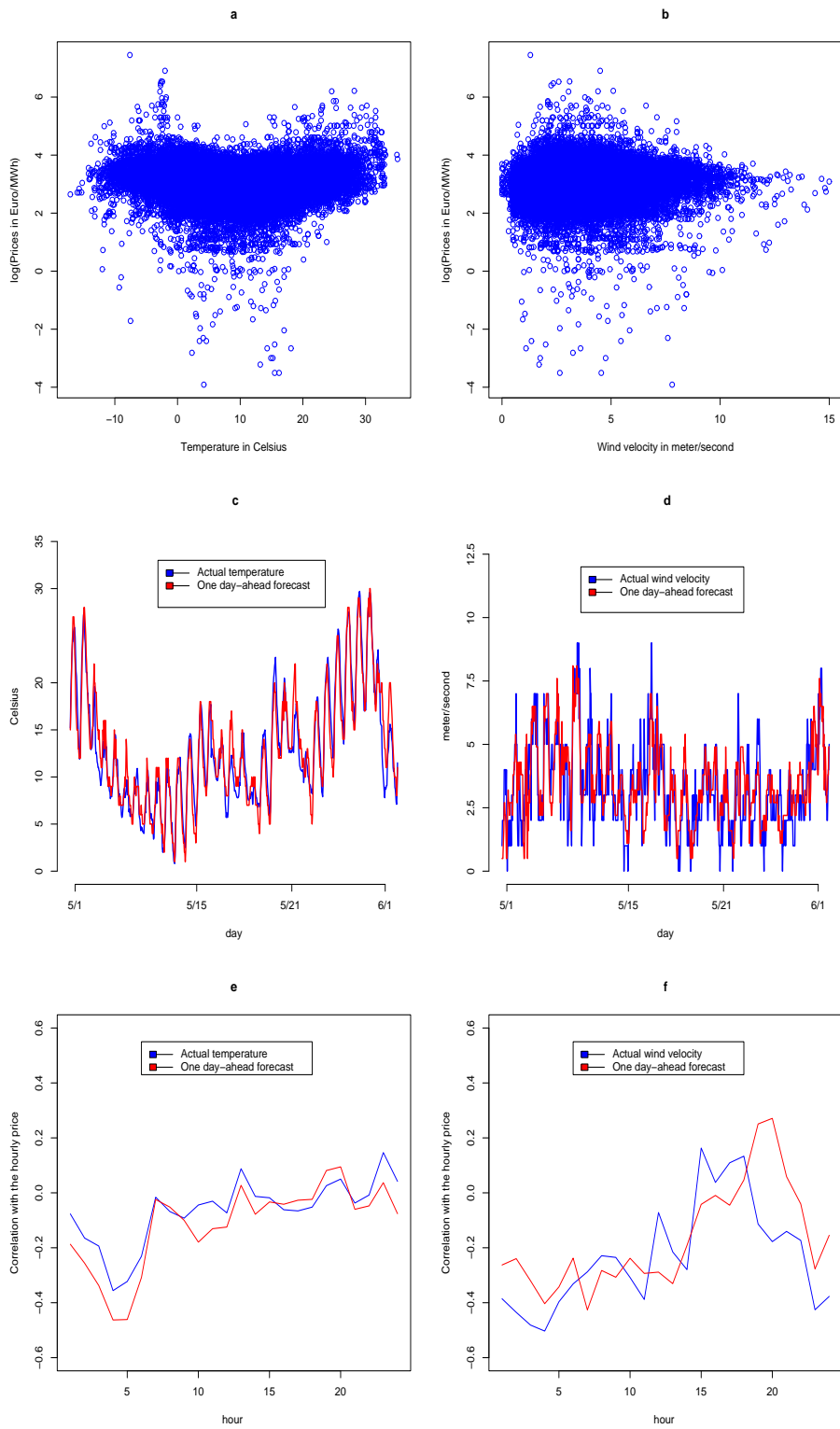


Figure 3.2.2: Scatter plots for hourly temperature from Ulm and the hourly average wind velocity of Holzdorf and Hamburg with the logarithm of the hourly price series (a,b), one day-ahead forecasts for temperature from Ulm and for wind velocity from Holzdorf (c,d), for 7 a.m. 1/05/2005 until 6 a.m. 1/06/2005, Correlation of measured temperature from Ulm and wind velocity from Holzdorf as well as its one day-ahead forecasts with the hourly price for 7 a.m. 1/05/2005 until 6 a.m. 1/06/2005 (e,f).

### 3.3 Choice of the Weather Variables

In this section, we explain the choice of the weather variables for the empirical study. As far as temperature is concerned, we proceed in spirit to Knittel and Roberts (2005). More precisely, we employ only one weather variable for temperature instead of including all data from the four measuring stations as distinct variables. For the sake of consistency, we proceed in the same way with wind velocity. To become more specific, besides temperature, we also add the square and the cube of temperature as explanatory variables in the descriptive regression equations below,

$$P_t = \eta_1^{temp} + \eta_2^{temp} \cdot temp_t + \eta_3^{temp} \cdot temp_t^2 + \eta_4^{temp} \cdot temp_t^3, \quad (3.3.1)$$

$$\log(P_t) = \eta_{1,l}^{temp} + \eta_{2,l}^{temp} \cdot temp_t + \eta_{3,l}^{temp} \cdot temp_t^2 + \eta_{4,l}^{temp} \cdot temp_t^3. \quad (3.3.2)$$

For the temperature variable denoted  $temp_t$ , we employ hourly temperature data for the hours 1 until 24 of Hamburg, Holzdorf, Mendig and Ulm as well as the average of Mendig and Ulm, since Mendig and Ulm perform best across the 24 hours, see subfigures 3.3.1a and 3.3.1b. The average of three or even all four measuring stations yields, especially for the on-peak period, smaller coefficients of determination than the temperature data of Ulm or the average of Ulm and Mendig which is depicted in subfigure 3.3.1e, where the results of equation (3.3.2) are presented. For temperature, the decision on the variable is difficult. While the average of Ulm and Mendig performs better than data of Ulm in the off-peak period, for the on-peak hours the opposite is true.

Finally, we have opted for data of Ulm because it provides a higher coefficient of determination during on-peak hours.

In the case of wind velocity, the specification of the regression equations is not straightforward since we have no hints how wind velocity and power prices interact. Due to this uncertainty, we model this relation as simply as possible in equations (3.3.3) and (3.3.4), respectively.

$$P_t = \eta_1^{wind} + \eta_2^{wind} \cdot wind_t, \quad (3.3.3)$$

$$\log(P_t) = \eta_{1,l}^{wind} + \eta_{2,l}^{wind} \cdot wind_t. \quad (3.3.4)$$

Due to the non-linear relation between wind velocity and the produced energy output, we can expect the relation between power prices and wind velocity to be non-linear, too. Consequently, equation (3.3.4) may provide at least a reasonable approximation of this relation.

Analogously to our procedure with temperature, we employ wind velocity data of the four measuring stations together with the average of Hamburg and Holzdorf in equations (3.3.3) and (3.3.4). The coefficients of determination  $R^2$  are plotted in subfigures 3.3.1c and 3.3.1d, respectively. Here, the results indicate that apart from few hours the average of the data of Hamburg and Holzdorf perform best across the hours of a day. This result is clearly confirmed in subfigure 3.3.1f, where we present the outcome of equation (3.3.4) for the average of three or four of the measuring stations.

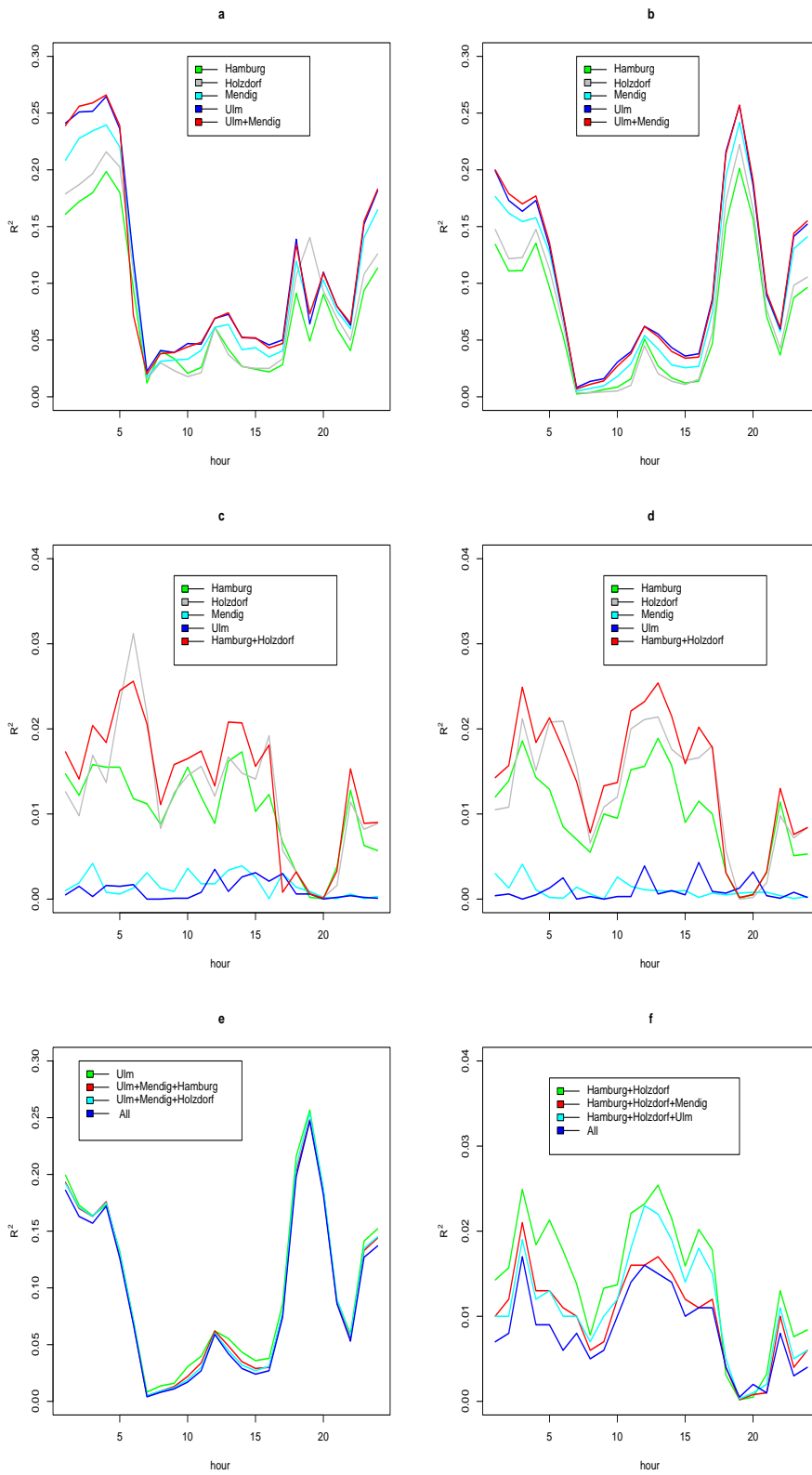


Figure 3.3.1: Coefficients of determination  $R^2$  : (a) equation (3.3.1), (b) equation (3.3.2), (c) equation (3.3.3), (d) equation (3.3.4), (e) equation (3.3.2) for the average of three or four stations, (f) equation (3.3.4) for the average of three or four stations.

### 3.4 The Empirical Study

The empirical study divides into two parts. In the first part, we examine whether the inclusion of weather data into the stochastic model provides a significant improvement in terms of fit compared to the pure stochastic models without weather. In the second part, we carry out a forecasting study to assess the quality of forecasts when weather data is included.

We classify two versions A and B. Version A is the pure approach without weather and with constant transition probabilities.

In version B, we include temperature and wind as explanatory variables to the deterministic components.

$$\log(P_t) = X_t + f_t + w_t. \quad (3.4.1)$$

Analogously to the procedure in the previous chapter, the strong weekly seasonality is taken into account through weekend dummy variables for Saturdays and Sundays as well as a sinusoidal term. Furthermore, we add a dummy variable for public holidays. Moreover, since the range of the data covers more than four years, we include a deterministic trend and a sinusoidal term to consider yearly seasonality. Consequently,  $f_t$  is specified as

$$\begin{aligned} f_t = & \beta_1 \cdot \text{dummy}_{sat} + \beta_2 \cdot \text{dummy}_{sun} + \beta_3 \cdot \text{dummy}_{hol} + \beta_4 \cdot t \quad (3.4.2) \\ & + \gamma_1 \cdot \sin\left((\gamma_2 + t) \cdot \frac{2\pi}{365}\right) + \gamma_3 \cdot \sin\left((\gamma_4 + t) \cdot \frac{2\pi}{7}\right). \end{aligned}$$

Furthermore  $w_t$  is specified as,

$$w_t = \delta_1 \cdot \text{temp}_t + \delta_2 \cdot \text{temp}_t^2 + \delta_3 \cdot \text{wind}_t + \delta_4 \cdot \text{temp}_t^3. \quad (3.4.3)$$

Additionally, we specify time-varying transition probabilities in terms of a logit model. For further valid linking functions, see Filardo (1994) and Filardo (1998). We replace  $q$  with  $\frac{\exp(\mathbf{Z}\phi_M)}{1 + \exp(\mathbf{Z}\phi_M)}$  and  $p$  with  $\frac{\exp(\mathbf{Z}\phi_S)}{1 + \exp(\mathbf{Z}\phi_S)}$  in equation (3.4.4). In addition, we assume for the inner product  $\mathbf{Z}\phi_j$  of the vector of explanatory variables  $\mathbf{Z}$  and the vector of parameters  $\phi_j$ ,  $j \in \{M, S\}$ ,

$$\mathbf{Z}\phi_j = \phi_{j,1} + \phi_{j,2} \cdot \text{temp}_t + \phi_{j,3} \cdot \text{temp}_t^2 + \phi_{j,4} \cdot \text{wind}_t + \phi_{j,5} \cdot \text{temp}_t^3. \quad (3.4.4)$$

In equations (3.4.3) and (3.4.4), we choose the explanatory variables by testing their significance at the 5 %-level. Since one goal is to determine the relation between weather and spikes, we try to be very strict with the inclusion of weather variables and choose this procedure. A likelihood ratio test or the Schwartz criterion could be used to determine which variables should be included instead.

Only the significant explanatory variables are included in the specification as far as the specification of equation (3.4.3) is concerned. The results of equation (3.4.3) are given in table 3.4.8.

However, in the case of time-varying transition probabilities, it happens that none of the estimates of equation (3.4.4) meet the criterion. This occurs for some hours, especially for the transition from the spike to the spike regime. In these cases, we include only the most significant parameter among them. A good example to clarify our procedure with time-varying transition probabilities are the hours from 15

to 17 in tables 3.4.10 and 3.4.11, where the results for the time-varying transition probabilities are reported. For these hours, we employ only the constant  $\phi_{S,1}$  which is actually not significant at the 5 % level.

To conclude, we explain some technical aspects pertinent to the estimation methodology of De Jong and Huisman (2003). As shown in subsection 2.3.5, estimation requires to look for the last logarithm of the spot price originating from the stable regime. For the sake of computational ease, we maximally go  $K = 5$  steps back in time.

### 3.4.1 Results on Model Fit

If spot prices are zero, we replace them by the average of the price at the same day one week before and the price at the same day one week ahead. Another possibility to cope with this problem may be to approximate the prices equal to zero by prices of representative block of hours, such as certain blocks of off-peak hours or certain blocks of on-peak hours.

In tables 3.4.1 to 3.4.3, we report the results for the stochastic component  $X_t$  together with some model selection criteria for all hours. The results for the deterministic component are presented in tables 3.4.4 to 3.4.7. In comparing versions A and B, we see that version B clearly outperforms version A throughout all 24 hours. The Schwartz information criterion indicates that Model B should be preferred.

In order to summarize the results of equation (3.4.3) for  $w_t$  given in table 3.4.8, we see that the linear temperature specification and wind provide significant negative estimates throughout all 24 hours. Negative parameter estimates of temperature indicate that negative temperature causes the demand, and therefore also prices, to rise due to the need for heating in winter, whereas moderate positive temperatures typically are accompanied by lower demand and therefore lower prices. Furthermore, we have to keep in mind that these estimates merely represent an average effect over the year. Therefore, to gain a deeper insight, investigations should be more detailed distinguishing summer and winter time or even take into account the monthly differences. A more detailed modelling of the general impact of weather, however, would increase complexity with regard to our second goal to link weather and spikes. We leave this more detailed examination for further research.

The square of temperature mainly provides small and significant positive estimates in the late afternoon from 16 until the evening hours 24. Moreover, the cube provides small and significant positive estimates in night hours from 1 up to 5 and at hour 8 then partly in the early afternoon hours from 12 to 15. Summarizing the results for the relation between weather and spikes, we can see that there is only evidence for a significant relation in certain hours across the day as shown in tables 3.4.10 and 3.4.11. More precisely, whenever estimation provides significant results for the wind parameter, it turns out that rising wind velocity reduces the transition probability to stay in the stable regime and augments the transition probability to stay in the spike except for hours 10 and 14. We also find a relation between temperature and regime probabilities. The relation is mainly confined to

temperature in its linear specification. The square rarely and the cube very rarely provide significant estimates.

The modelling of the relation between wind velocity and spot prices is not straightforward. Wind velocities below 4 meter/second are not significant for wind energy production but for spot prices. The supply side of electricity is affected when wind energy is not produced. For the main study, we assume that the impact is different for the wind velocities below 4 meter/second. In an additional short forecasting study, we assume that all wind velocities below 4 meter/second have the same impact on spot prices. Moreover, we also examine the case that no wind is added into the specification. The relation between wind velocity and spot prices still remains an interesting problem to tackle for further research.

To conclude the discussion, table 3.4.9 presents the estimates for the constant transition probabilities  $p$  and  $q$ , respectively, together with their standard errors in brackets. In addition, we have computed the average transition probabilities for version B and report them, too. Except for the hours 8, 11, 13, 14 and 18, 19, 24 in which the the average transition probability from spike to spike deviates from the estimated  $p$  for version A, the results for both versions are similar.

Finally, it remains to mention that for the time-varying transition probabilities from spike to spike, the estimates of the constant  $\phi_{S,1}$  are significant for only 5 of the 24 given hours with respect to the 5 % level. This result is due to the approach with independent spikes.

Table 3.4.1: Results on the Stochastic Component and Model Selection Criteria.  
(I)

Hour	Version	$\mu_M$	$\mu_{S,H}$	$\mu_{S,L}$	$\sigma_M$	$\sigma_{S,H}$	$\sigma_{S,L}$	$\rho$
1	A	2.597 (0.025)	2.279 (0.044)	2.128 (0.050)	0.143 (0.003)	0.405 (0.018)	0.314 (0.022)	0.292 (0.020)
	B	2.756 (0.024)	2.477 (0.039)	2.343 (0.046)	0.135 (0.003)	0.351 (0.014)	0.293 (0.018)	0.335 (0.021)
2	A	2.470 (0.028)	1.954 (0.054)	1.769 (0.100)	0.165 (0.004)	0.483 (0.024)	0.633 (0.018)	0.322 (0.022)
	B	2.652 (0.027)	2.171 (0.058)	2.011 (0.100)	0.158 (0.003)	0.456 (0.024)	0.613 (0.018)	0.375 (0.023)
3	A	2.419 (0.029)	1.875 (0.052)	1.659 (0.092)	0.163 (0.004)	0.499 (0.017)	0.679 (0.031)	0.313 (0.023)
	B	2.640 (0.028)	2.143 (0.049)	1.933 (0.086)	0.160 (0.004)	0.460 (0.016)	0.644 (0.028)	0.370 (0.025)
4	A	2.414 (0.029)	1.865 (0.048)	1.678 (0.071)	0.176 (0.004)	0.494 (0.013)	0.626 (0.019)	0.354 (0.025)
	B	2.634 (0.028)	2.142 (0.045)	1.959 (0.071)	0.172 (0.004)	0.469 (0.012)	0.615 (0.018)	0.416 (0.027)
5	A	2.460 (0.027)	1.961 (0.049)	1.568 (0.122)	0.178 (0.004)	0.460 (0.015)	0.893 (0.029)	0.365 (0.023)
	B	2.668 (0.026)	2.234 (0.044)	1.855 (0.113)	0.170 (0.004)	0.422 (0.013)	0.858 (0.026)	0.422 (0.027)
6	A	2.569 (0.024)	2.218 (0.067)	1.533 (0.172)	0.168 (0.004)	0.451 (0.016)	0.971 (0.048)	0.383 (0.023)
	B	2.751 (0.025)	2.415 (0.064)	1.741 (0.166)	0.163 (0.004)	0.420 (0.016)	0.951 (0.046)	0.453 (0.025)
7	A	2.871 (0.021)	2.669 (0.039)	1.925 (0.124)	0.155 (0.004)	0.354 (0.013)	0.980 (0.043)	0.401 (0.025)
	B	3.012 (0.024)	2.806 (0.042)	2.023 (0.127)	0.158 (0.004)	0.344 (0.013)	0.965 (0.044)	0.480 (0.027)
8	A	3.148 (0.020)	3.229 (0.050)	2.339 (0.130)	0.161 (0.004)	0.461 (0.023)	0.806 (0.041)	0.406 (0.024)
	B	3.315 (0.025)	3.402 (0.043)	2.633 (0.107)	0.147 (0.004)	0.390 (0.014)	0.792 (0.033)	0.373 (0.023)
9	A	3.228 (0.022)	3.496 (0.073)	2.555 (0.143)	0.159 (0.004)	0.617 (0.037)	0.708 (0.034)	0.357 (0.020)
	B	3.385 (0.027)	3.616 (0.071)	2.733 (0.143)	0.155 (0.004)	0.599 (0.034)	0.715 (0.033)	0.387 (0.022)
10	A	3.277 (0.023)	3.735 (0.081)	2.703 (0.192)	0.160 (0.003)	0.571 (0.043)	0.851 (0.053)	0.349 (0.020)
	B	3.443 (0.028)	3.874 (0.080)	2.797 (0.205)	0.157 (0.003)	0.559 (0.042)	0.864 (0.058)	0.382 (0.020)
11	A	3.349 (0.023)	3.996 (0.078)	3.090 (0.150)	0.164 (0.003)	0.494 (0.030)	0.690 (0.065)	0.358 (0.020)
	B	3.555 (0.027)	4.128 (0.080)	3.251 (0.165)	0.155 (0.003)	0.500 (0.030)	0.712 (0.078)	0.371 (0.020)
12	A	3.536 (0.025)	4.328 (0.060)	3.421 (0.075)	0.184 (0.004)	0.599 (0.031)	0.486 (0.022)	0.341 (0.019)
	B	3.740 (0.032)	4.473 (0.061)	3.637 (0.072)	0.173 (0.003)	0.589 (0.029)	0.467 (0.020)	0.353 (0.020)

Table 3.4.2: Results on the Stochastic Component and Model Selection Criteria (II).

Hour	Version	$\mu_M$	$\mu_{S,H}$	$\mu_{S,L}$	$\sigma_M$	$\sigma_{S,H}$	$\sigma_{S,L}$	$\rho$
13	A	3.349 (0.023)	3.996 (0.078)	3.090 (0.150)	0.164 (0.003)	0.494 (0.030)	0.690 (0.065)	0.358 (0.020)
	B	3.548 (0.029)	3.994 (0.080)	3.372 (0.146)	0.153 (0.003)	0.512 (0.030)	0.647 (0.054)	0.361 (0.020)
14	A	3.256 (0.020)	3.844 (0.094)	2.904 (0.136)	0.163 (0.003)	0.541 (0.041)	0.647 (0.057)	0.408 (0.022)
	B	3.472 (0.029)	4.054 (0.099)	3.151 (0.147)	0.159 (0.003)	0.526 (0.047)	0.646 (0.058)	0.430 (0.022)
15	A	3.158 (0.019)	3.681 (0.088)	2.514 (0.244)	0.164 (0.003)	0.549 (0.042)	0.955 (0.074)	0.430 (0.022)
	B	3.349 (0.027)	3.840 (0.087)	2.776 (0.228)	0.162 (0.003)	0.545 (0.044)	0.891 (0.064)	0.475 (0.022)
16	A	3.079 (0.020)	3.366 (0.082)	2.641 (0.090)	0.156 (0.004)	0.571 (0.040)	0.594 (0.040)	0.402 (0.022)
	B	3.231 (0.026)	3.506 (0.079)	2.822 (0.092)	0.154 (0.004)	0.546 (0.037)	0.592 (0.039)	0.449 (0.023)
17	A	3.029 (0.024)	3.539 (0.249)	2.527 (0.128)	0.160 (0.003)	0.903 (0.126)	0.669 (0.042)	0.347 (0.018)
	B	3.169 (0.028)	3.687 (0.259)	2.675 (0.132)	0.158 (0.003)	0.901 (0.132)	0.659 (0.042)	0.391 (0.020)
18	A	3.092 (0.032)	3.682 (0.113)	2.877 (0.066)	0.149 (0.003)	0.676 (0.060)	0.501 (0.047)	0.243 (0.014)
	B	3.212 (0.035)	3.717 (0.107)	2.994 (0.073)	0.144 (0.003)	0.650 (0.052)	0.479 (0.050)	0.248 (0.015)
19	A	3.114 (0.027)	3.675 (0.188)	2.829 (0.160)	0.156 (0.003)	0.834 (0.067)	0.809 (0.049)	0.313 (0.017)
	B	3.229 (0.030)	3.763 (0.190)	2.979 (0.202)	0.155 (0.003)	0.808 (0.065)	0.845 (0.059)	0.342 (0.018)
20	A	3.065 (0.024)	3.408 (0.152)	2.367 (0.243)	0.153 (0.003)	0.649 (0.066)	0.791 (0.095)	0.340 (0.018)
	B	3.163 (0.028)	3.450 (0.144)	2.426 (0.271)	0.151 (0.003)	0.638 (0.060)	0.781 (0.106)	0.339 (0.019)
21	A	3.001 (0.026)	3.248 (0.102)	2.493 (0.231)	0.132 (0.002)	0.530 (0.050)	0.654 (0.088)	0.271 (0.017)
	B	3.091 (0.028)	3.320 (0.092)	2.626 (0.213)	0.129 (0.002)	0.496 (0.041)	0.628 (0.079)	0.272 (0.018)
22	A	2.926 (0.027)	2.992 (0.045)	2.412 (0.164)	0.124 (0.003)	0.305 (0.024)	0.490 (0.052)	0.248 (0.016)
	B	3.001 (0.028)	3.062 (0.044)	2.528 (0.147)	0.122 (0.003)	0.291 (0.022)	0.475 (0.047)	0.254 (0.017)
23	A	2.902 (0.030)	2.976 (0.044)	2.651 (0.087)	0.114 (0.002)	0.270 (0.019)	0.358 (0.029)	0.209 (0.014)
	B	2.963 (0.029)	3.031 (0.038)	2.785 (0.073)	0.108 (0.002)	0.241 (0.015)	0.353 (0.026)	0.212 (0.015)
24	A	2.770 (0.026)	2.513 (0.041)	2.215 (0.081)	0.126 (0.003)	0.227 (0.028)	0.413 (0.027)	0.242 (0.016)
	B	2.817 (0.024)	2.912 (0.022)	2.390 (0.080)	0.128 (0.003)	0.069 (0.007)	0.417 (0.030)	0.234 (0.016)

Table 3.4.3: Summary in-sample fit and the Schwartz Criterion (SC) for all 24 hours.

Hour	Version	LL	SC	Hour	Version	LL	SC
1	A	418.74	-0.4299	13	A	316.08	-0.3058
	B	496.12	-0.5100		B	390.76	-0.3737
2	A	27.35	0.0431	14	A	303.87	-0.2911
	B	117.97	-0.0440		B	384.12	-0.3567
3	A	-184.01	0.2985	15	A	276.91	-0.2585
	B	-95.20	0.2225		B	336.14	-0.3122
4	A	-278.74	0.4130	16	A	333.76	-0.3272
	B	-186.30	0.3192		B	373.41	-0.3617
5	A	-301.92	0.4410	17	A	428.59	-0.4418
	B	-227.52	0.3734		B	463.36	-0.4704
6	A	-94.44	0.1903	18	A	391.34	-0.3968
	B	-34.49	0.1357		B	420.04	-0.4180
7	A	-165.64	0.2763	19	A	399.26	-0.4064
	B	-121.30	0.2362		B	429.12	-0.4245
8	A	-59.32	0.1478	20	A	529.34	-0.5636
	B	2.39	0.0912		B	555.48	-0.5817
9	A	68.15	-0.0062	21	A	741.93	-0.8205
	B	120.19	-0.0557		B	772.81	-0.8443
10	A	238.68	-0.2123	22	A	822.35	-0.9176
	B	299.05	-0.2584		B	855.88	-0.9403
11	A	316.08	-0.3058	23	A	922.44	-1.0386
	B	397.48	-0.3818		B	957.24	-1.0627
12	A	2.950	0.0726	24	A	785.17	-0.8727
	B	62.28	0.0143		B	812.88	-0.8928

Table 3.4.4: Results on the Deterministic Component, see equation (3.4.2), (I).

Hour	Version	$\beta_1$	$\beta_2$	$\beta_3$	$\beta_4$
1	A	-0.030 (0.021)	-0.029 (0.012)	-0.030 (0.021)	0.0004 ( $2.5 \cdot 10^{-5}$ )
	B	0.160 (0.011)	-0.031 (0.012)	-0.041 (0.021)	0.0003 ( $2.1 \cdot 10^{-5}$ )
2	A	0.168 (0.015)	-0.085 (0.016)	-0.058 (0.026)	0.0003 ( $2.7 \cdot 10^{-5}$ )
	B	0.166 (0.015)	-0.092 (0.015)	-0.058 (0.025)	0.0003 ( $2.2 \cdot 10^{-5}$ )
3	A	0.168 (0.015)	-0.119 (0.016)	-0.054 (0.027)	0.0003 ( $2.9 \cdot 10^{-5}$ )
	B	0.171 (0.016)	-0.127 (0.015)	-0.065 (0.026)	0.0003 ( $2.4 \cdot 10^{-5}$ )
4	A	0.160 (0.018)	-0.154 (0.018)	-0.110 (0.035)	0.0003 ( $2.7 \cdot 10^{-5}$ )
	B	0.160 (0.018)	-0.164 (0.017)	-0.127 (0.030)	0.0002 ( $2.3 \cdot 10^{-5}$ )
5	A	0.087 (0.018)	-0.249 (0.018)	-0.173 (0.033)	0.0003 ( $2.6 \cdot 10^{-5}$ )
	B	0.087 (0.017)	-0.251 (0.018)	-0.187 (0.030)	0.0002 ( $2.2 \cdot 10^{-5}$ )
6	A	-0.112 (0.016)	-0.523 (0.017)	-0.343 (0.028)	0.0003 ( $2.5 \cdot 10^{-5}$ )
	B	-0.108 (0.016)	-0.529 (0.017)	-0.351 (0.027)	0.0003 ( $2 \cdot 10^{-5}$ )
7	A	-0.403 (0.016)	-1.039 (0.017)	-0.664 (0.033)	0.0003 ( $2.1 \cdot 10^{-5}$ )
	B	-0.405 (0.017)	-1.029 (0.017)	-0.661 (0.031)	0.0003 ( $1.8 \cdot 10^{-5}$ )
8	A	-0.529 (0.016)	-1.162 (0.016)	-0.664 (0.033)	0.0003 ( $2.1 \cdot 10^{-5}$ )
	B	-0.514 (0.015)	-1.151 (0.015)	-0.712 (0.032)	0.0003 ( $2 \cdot 10^{-5}$ )
9	A	-0.443 (0.015)	-0.934 (0.014)	-0.664 (0.025)	0.0003 ( $2.3 \cdot 10^{-5}$ )
	B	-0.443 (0.014)	-0.946 (0.014)	-0.666 (0.027)	0.0003 ( $2.1 \cdot 10^{-5}$ )
10	A	-0.331 (0.014)	-0.740 (0.013)	-0.634 (0.021)	0.0003 ( $2.4 \cdot 10^{-5}$ )
	B	-0.331 (0.014)	-0.749 (0.013)	-0.568 (0.022)	0.0003 ( $2.2 \cdot 10^{-5}$ )
11	A	-0.293 (0.014)	-0.621 (0.014)	-0.625 (0.020)	0.0003 ( $2.5 \cdot 10^{-5}$ )
	B	-0.289 (0.013)	-0.622 (0.013)	-0.608 (0.020)	0.0002 ( $2.2 \cdot 10^{-5}$ )
12	A	-0.331 (0.016)	-0.566 (0.015)	-0.600 (0.026)	0.0002 ( $2.7 \cdot 10^{-5}$ )
	B	-0.324 (0.015)	-0.568 (0.015)	-0.602 (0.026)	0.0002 ( $2.7 \cdot 10^{-5}$ )

Table 3.4.5: Results on the Deterministic Component, see equation (3.4.2), (II).

Hour	Version	$\beta_1$	$\beta_2$	$\beta_3$	$\beta_4$
13	A	-0.293 (0.014)	-0.621 (0.014)	-0.025 (0.017)	0.0003 ( $2.5 \cdot 10^{-5}$ )
	B	-0.288 (0.013)	-0.620 (0.013)	-0.616 (0.021)	0.0003 ( $2.3 \cdot 10^{-5}$ )
14	A	-0.318 (0.014)	-0.623 (0.014)	-0.626 (0.020)	0.0003 ( $2.2 \cdot 10^{-5}$ )
	B	-0.318 (0.014)	-0.652 (0.013)	-0.644 (0.020)	0.0003 ( $2 \cdot 10^{-5}$ )
15	A	-0.318 (0.015)	-0.679 (0.014)	-0.648 (0.021)	0.0003 ( $2.1 \cdot 10^{-5}$ )
	B	-0.317 (0.015)	-0.682 (0.014)	-0.670 (0.020)	0.0003 ( $1.9 \cdot 10^{-5}$ )
16	A	-0.285 (0.014)	-0.661 (0.013)	-0.732 (0.021)	0.0003 ( $2.2 \cdot 10^{-5}$ )
	B	-0.284 (0.014)	-0.664 (0.014)	-0.754 (0.023)	0.0003 ( $1.9 \cdot 10^{-5}$ )
17	A	-0.260 (0.013)	3.539 (0.249)	-0.653 (0.019)	0.0004 ( $2.6 \cdot 10^{-5}$ )
	B	-0.258 (0.013)	-0.601 (0.013)	-0.652 (0.020)	0.0003 ( $2.2 \cdot 10^{-5}$ )
18	A	-0.224 (0.012)	-0.469 (0.012)	-0.572 (0.022)	0.0003 ( $3.2 \cdot 10^{-5}$ )
	B	-0.222 (0.011)	-0.471 (0.011)	-0.593 (0.021)	0.0003 ( $3.1 \cdot 10^{-5}$ )
19	A	-0.171 (0.013)	-0.339 (0.013)	-0.425 (0.021)	0.0003 ( $2.8 \cdot 10^{-5}$ )
	B	-0.172 (0.013)	-0.344 (0.013)	-0.442 (0.021)	0.0003 ( $2.6 \cdot 10^{-5}$ )
20	A	-0.143 (0.012)	-0.241 (0.012)	-0.284 (0.019)	0.0003 ( $2.5 \cdot 10^{-5}$ )
	B	-0.144 (0.012)	-0.242 (0.012)	-0.282 (0.020)	0.0003 ( $2.5 \cdot 10^{-5}$ )
21	A	-0.171 (0.010)	-0.232 (0.010)	-0.257 (0.016)	0.0004 ( $2.7 \cdot 10^{-5}$ )
	B	-0.169 (0.010)	-0.230 (0.010)	-0.264 (0.016)	0.0004 ( $2.7 \cdot 10^{-5}$ )
22	A	-0.149 (0.010)	-0.174 (0.010)	-0.174 (0.016)	0.0003 ( $2.8 \cdot 10^{-5}$ )
	B	-0.146 (0.009)	-0.171 (0.010)	-0.181 (0.016)	0.0003 ( $2.6 \cdot 10^{-5}$ )
23	A	-0.098 (0.009)	-0.088 (0.009)	-0.094 (0.017)	0.0003 ( $3.1 \cdot 10^{-5}$ )
	B	-0.098 (0.009)	-0.086 (0.009)	-0.105 (0.017)	0.0003 ( $2.8 \cdot 10^{-5}$ )
24	A	-0.129 (0.010)	-0.150 (0.010)	-0.116 (0.018)	0.0003 ( $2.7 \cdot 10^{-5}$ )
	B	-0.103 (0.010)	-0.126 (0.011)	-0.115 (0.021)	0.0003 ( $1.8 \cdot 10^{-5}$ )

Table 3.4.6: Results on the Deterministic Component, see equation (3.4.2), (III).

Hour	Version	$\gamma_1$	$\gamma_2$	$\gamma_3$	$\gamma_4$
1	A	-0.128 (0.016)	-33546358 (7.897)	-0.120 (0.008)	-4436609 (0.074)
	B	-0.078 (0.017)	68.74 (11.20)	0.120 (0.008)	1.950 (0.071)
2	A	-0.164 (0.010)	66.28 (6.571)	-0.132 (0.010)	-22.52 (0.080)
	B	0.089 (0.019)	-103.39 (6.23)	0.133 (0.010)	1.968 (0.077)
3	A	-0.169 (0.019)	55.50 (6.253)	0.119 (0.011)	-180.01 (0.092)
	B	-0.021 (0.018)	0.508 (53.12)	-0.123 (0.011)	1.983 (0.091)
4	A	-0.182 (0.018)	54.830 (5.724)	0.120 (0.012)	-82.022 (0.101)
	B	-0.086 (0.022)	62.11 (8.43)	0.122 (0.011)	-5.001 (0.097)
5	A	-0.185 (0.017)	58.56 (5.547)	0.103 (0.012)	8.974 (0.119)
	B	-0.077 (0.022)	56.96 (10.65)	-0.105 (0.012)	-1.501 (0.114)
6	A	-0.164 (0.016)	7435121 (6.023)	-0.072 (0.011)	976925.5 (0.167)
	B	-0.076 (0.011)	-97.87 (11.83)	-0.076 (0.011)	-1.451 (0.156)
7	A	0.088 (0.013)	450310.4 (9.251)	-0.014 (0.012)	1782766 (0.777)
	B	0.035 (0.012)	-37.05 (34.24)	-0.020 (0.012)	-1.174 (0.543)
8	A	0.102 (0.014)	633.84 (8.497)	-0.016 (0.012)	-21.403 (0.642)
	B	0.046 (0.015)	-59.40 (0.948)	-0.026 (0.011)	-0.485 (0.363)
9	A	-0.054 (0.015)	-1604080 (17.72)	-0.015 (0.011)	1371334 (0.609)
	B	0.035 (0.018)	8.49 (31.11)	-0.019 (0.011)	-0.487 (0.483)
10	A	-0.022 (0.016)	492.18 (42.071)	0.011 (0.010)	-304.78 (0.834)
	B	0.057 (0.020)	41.11 (15.50)	-0.015 (0.010)	-0.140 (0.616)
11	A	-0.025 (0.017)	-3846.8 (36.23)	-0.014 (0.010)	-259.33 (0.659)
	B	0.075 (0.020)	45.25 (8.93)	-0.021 (0.009)	-0.343 (0.418)
12	A	0.112 (0.025)	41.63 (9.76)	-0.034 (0.010)	-0.312 (0.335)
	B	0.115 (0.024)	42.64 (9.16)	-0.034 (0.010)	0.331 (0.336)

Table 3.4.7: Results on the Deterministic Component, see equation (3.4.2), (IV).

Hour	Version	$\gamma_1$	$\gamma_2$	$\gamma_3$	$\gamma_4$
13	A	-0.025 (0.017)	-3846.8 (36.23)	-0.014 (0.010)	-259.33 (0.659)
	B	0.071 (0.020)	45.09 (12.75)	-0.021 (0.010)	-0.397 (0.405)
14	A	0.028 (0.014)	2132.69 (29.72)	-0.060 (0.009)	-538.92 (0.166)
	B	0.042 (0.018)	38.41 (19.75)	-0.067 (0.009)	0.041 (0.145)
15	A	-0.041 (0.014)	-605.65 (19.24)	-0.078 (0.009)	-34.93 (0.130)
	B	0.042 (0.016)	22.13 (20.48)	-0.084 (0.009)	0.037 (0.118)
16	A	-0.064 (0.014)	-247.31 (12.57)	-0.087 (0.010)	-112.2 (0.110)
	B	0.046 (0.013)	-13.18 (22.38)	-0.091 (0.010)	-0.004 (0.106)
17	A	-0.141 (0.015)	-263.85 (7.060)	-0.077 (0.010)	-0.097 (0.120)
	B	0.095 (0.016)	-60.79 (11.36)	-0.082 (0.010)	-0.080 (0.114)
18	A	-0.289 (0.019)	-1001.92 (4.33)	-0.067 (0.008)	-0.169 (0.123)
	B	0.250 (0.021)	-84.63 (5.05)	-0.070 (0.008)	-0.135 (0.116)
19	A	-0.307 (0.016)	3371.17 (3.438)	-0.071 (0.009)	-0.200 (0.122)
	B	0.266 (0.019)	-92.53 (3.99)	-0.073 (0.009)	-0.188 (0.122)
20	A	-0.255 (0.016)	-1371.07 (3.610)	-0.067 (0.009)	-0.211 (0.128)
	B	0.230 (0.020)	-89.84 (4.51)	-0.069 (0.008)	-0.207 (0.123)
21	A	-0.148 (0.017)	-1081403 (6.671)	-0.056 (0.007)	-1160257 (0.129)
	B	0.121 (0.019)	-81.45 (8.69)	-0.060 (0.007)	-0.175 (0.119)
22	A	-0.071 (0.016)	-290.436 (13.989)	-0.043 (0.007)	48.96 (0.167)
	B	0.047 (0.018)	-90.09 (21.66)	-0.046 (0.007)	-0.044 (0.153)
23	A	-0.080 (0.017)	-7272566 (13.198)	-0.020 (0.006)	129443.9 (0.332)
	B	-0.064 (0.019)	60.74 (6.05)	-0.022 (0.006)	-0.075 (0.288)
24	A	-0.090 (0.016)	-1900865 (11.714)	-0.018 (0.007)	-268829.4 (0.419)
	B	-0.047 (0.016)	46.19 (16.29)	0.021 (0.007)	-39.79 (0.302)

Table 3.4.8: Results on the Weather Component  $w_t$ , see equation (3.4.3) .

Hour	$\delta_1$	$\delta_2$	$\delta_3$	$\delta_4$
1	-0.002 (0.0002)	-	-0.002 (0.0002)	$3.1 \cdot 10^{-7}$ ( $4 \cdot 10^{-8}$ )
2	-0.002 (0.0002)	-	-0.002 (0.0003)	$5 \cdot 10^{-8}$ ( $7.4 \cdot 10^{-9}$ )
3	-0.003 (0.0002)	-	-0.002 (0.0003)	$4.2 \cdot 10^{-8}$ ( $8.2 \cdot 10^{-9}$ )
4	-0.002 (0.0003)	-	-0.002 (0.0003)	$4.6 \cdot 10^{-8}$ ( $9.0 \cdot 10^{-9}$ )
5	-0.002 (0.0002)	-	-0.003 (0.0004)	$3.2 \cdot 10^{-8}$ ( $8.8 \cdot 10^{-9}$ )
6	-0.001 (0.0002)	-	-0.003 (0.0003)	-
7	-0.001 (0.0003)	-	-0.002 (0.0003)	-
8	-0.001 (0.0002)	-	-0.002 (0.0003)	$1.6 \cdot 10^{-8}$ ( $4 \cdot 10^{-9}$ )
9	-0.001 (0.0002)	$4.7 \cdot 10^{-6}$ ( $9.1 \cdot 10^{-7}$ )	-0.002 (0.0003)	-
10	-0.003 (0.0002)	$1.8 \cdot 10^{-5}$ ( $3.5 \cdot 10^{-6}$ )	-0.002 (0.0003)	-
11	-0.001 (0.0002)	$2.8 \cdot 10^{-6}$ ( $8.1 \cdot 10^{-7}$ )	-0.003 (0.0003)	-
12	-0.001 (0.0002)	-	-0.003 (0.0003)	$7.4 \cdot 10^{-9}$ ( $2.7 \cdot 10^{-9}$ )
13	-0.001 (0.0002)	-	-0.002 (0.0003)	$7.6 \cdot 10^{-9}$ ( $2.1 \cdot 10^{-9}$ )
14	-0.001 (0.0002)	-	-0.002 (0.0003)	$9.1 \cdot 10^{-9}$ ( $1.9 \cdot 10^{-9}$ )
15	-0.001 (0.0002)	-	-0.002 (0.0003)	$9.1 \cdot 10^{-9}$ ( $1.9 \cdot 10^{-9}$ )
16	-0.001 (0.0002)	$3.8 \cdot 10^{-6}$ ( $7 \cdot 10^{-7}$ )	-0.002 (0.0002)	-
17	-0.001 (0.0003)	$4.1 \cdot 10^{-6}$ ( $7.2 \cdot 10^{-7}$ )	-0.001 (0.0003)	-
18	-0.001 (0.0002)	$3.6 \cdot 10^{-6}$ ( $7.4 \cdot 10^{-7}$ )	-0.001 (0.0002)	-
19	-0.001 (0.0002)	$4.1 \cdot 10^{-6}$ ( $8.5 \cdot 10^{-7}$ )	-0.001 (0.0002)	-
20	-0.001 (0.0002)	$2.3 \cdot 10^{-6}$ ( $9 \cdot 10^{-7}$ )	-0.001 (0.0002)	-
21	-0.001 (0.0002)	$2.4 \cdot 10^{-6}$ ( $8 \cdot 10^{-7}$ )	-0.001 (0.0002)	-
22	-0.001 (0.0002)	$2.7 \cdot 10^{-6}$ ( $7.8 \cdot 10^{-7}$ )	-0.001 (0.0002)	-
23	-0.001 (0.0002)	$3.7 \cdot 10^{-6}$ ( $8.1 \cdot 10^{-7}$ )	-0.001 (0.0002)	-
24	-0.001 (0.0002)	$4.9 \cdot 10^{-6}$ ( $7.8 \cdot 10^{-7}$ )	-0.001 (0.0002)	-

Table 3.4.9: Results on Constant Transition Probabilities, see equation(3.4.4) .

Hour	Version	$p$	$q$
1	A	0.766 (0.040)	0.958 (0.007)
	B	0.780	0.956
2	A	0.803 (0.030)	0.957 (0.007)
	B	0.773	0.954
3	A	0.847 (0.022)	0.944 (0.008)
	B	0.849	0.950
4	A	0.879 (0.020)	0.949 (0.008)
	B	0.872	0.959
5	A	0.825 (0.025)	0.941 (0.009)
	B	0.831	0.949
6	A	0.724 (0.039)	0.940 (0.008)
	B	0.764	0.943
7	A	0.668 (0.043)	0.891 (0.013)
	B	0.695	0.903
8	A	0.509 (0.057)	0.893 (0.013)
	B	0.379	0.864
9	A	0.434 (0.057)	0.916 (0.010)
	B	0.418	0.918
10	A	0.440 (0.065)	0.947 (0.008)
	B	0.392	0.947
11	A	0.706 (0.047)	0.974 (0.005)
	B	0.560	0.964
12	A	0.861 (0.025)	0.975 (0.005)
	B	0.856	0.971

Hour	Version	$p$	$q$
13	A	0.706 (0.047)	0.974 (0.005)
	B	0.774	0.972
14	A	0.592 (0.062)	0.965 (0.006)
	B	0.506	0.966
15	A	0.557 (0.064)	0.966 (0.006)
	B	0.587	0.970
16	A	0.500 (0.072)	0.953 (0.008)
	B	0.500	0.955
17	A	0.518 (0.075)	0.977 (0.005)
	B	0.503	0.978
18	A	0.643 (0.058)	0.962 (0.007)
	B	0.368	0.947
19	A	0.661 (0.066)	0.975 (0.005)
	B	0.400	0.973
20	A	0.628 (0.075)	0.981 (0.005)
	B	0.573	0.979
21	A	0.410 (0.101)	0.971 (0.006)
	B	0.420	0.970
22	A	0.562 (0.096)	0.966 (0.008)
	B	0.580	0.963
23	A	0.388 (0.104)	0.942 (0.012)
	B	0.391	0.927
24	A	0.717 (0.059)	0.972 (0.006)
	B	0.568	0.936

Table 3.4.10: Summary of results for the time-varying transition probabilities (I), see equation (3.4.4) .

Hour	$\phi_{M,1}$	$\phi_{M,2}$	$\phi_{M,3}$	$\phi_{M,4}$	$\phi_{M,5}$
1	3.076 (0.182)	-	-	-	-
2	4.852 (0.456)	-0.008 (0.003)	-	-0.034 (0.008)	-
3	4.285 (0.518)	-0.018 (0.006)	-	-0.024 (0.008)	$7.7 \cdot 10^{-7}$ ( $2.9 \cdot 10^{-7}$ )
4	3.128 (0.178)	-	-	-	-
5	3.583 (0.388)	-	-	-0.019 (0.009)	-
6	4.380 (0.457)	-	$-4 \cdot 10^{-5}$ ( $1.5 \cdot 10^{-5}$ )	-0.030 (0.008)	-
7	3.595 (0.395)	-	-	-0.034 (0.008)	-
8	2.674 (0.318)	-	-	-0.022 (0.007)	$1.1 \cdot 10^{-7}$ ( $5.4 \cdot 10^{-8}$ )
9	2.423 (0.133)	-	-	-	-
10	3.329 (0.314)	0.023 (0.005)	-0.0006 ( $2 \cdot 10^{-4}$ )	-	$2.9 \cdot 10^{-6}$ ( $1.2 \cdot 10^{-6}$ )
11	3.403 (0.267)	0.016 (0.004)	$-8.2 \cdot 10^{-5}$ ( $1.8 \cdot 10^{-5}$ )	-	-
12	3.5237 (0.201)	-	-	-	-
13	3.306 (0.298)	0.019 (0.005)	$-8.8 \cdot 10^{-5}$ ( $1.8 \cdot 10^{-5}$ )	-	-
14	4.168 (0.321)	-	$-2.6 \cdot 10^{-5}$ ( $6.8 \cdot 10^{-6}$ )	-	-
15	4.416 (0.064)	-0.006 (0.001)	-	-	-
16	3.040 (0.182)	-	-	-	-
17	3.794 (0.227)	-	-	-	-
18	2.847 (0.165)	-	-	-	-
19	3.588 (0.215)	-	-	-	-
20	3.837 (0.241)	-	-	-	-
21	3.440 (0.219)	-	-	-	-
22	4.179 (0.435)	-	-	-0.024 (0.009)	-
23	3.042 (0.364)	-	-	-0.015 (0.008)	-
24	2.681 (0.188)	-	-	-	-

Table 3.4.11: Summary of results for the time-varying transition probabilities (II), see equation (3.4.4).

Hour	$\phi_{S,1}$	$\phi_{S,2}$	$\phi_{S,3}$	$\phi_{S,4}$	$\phi_{S,5}$
1	-	-	-	0.047 (0.008)	-
2	-	-	-	0.045 (0.007)	-
3	-	0.011 (0.002)	-	0.041 (0.009)	-
4	-	0.011 (0.003)	-	0.052 (0.011)	-
5	-	0.013 (0.0002)	-	0.037 (0.008)	-
6	1.171 (0.190)	-	-	-	-
7	0.825 (0.192)	-	-	-	-
8	-	-0.006 (0.003)	-	-	-
9	-	-0.003 (0.002)	-	-	-
10	-	-	-	-0.010 (0.006)	-
11	-	-	-	-	$6.3 \cdot 10^{-8}$ ( $2.8 \cdot 10^{-8}$ )
12	1.785 (0.206)	-	-	-	-
13	0.573 (0.259)	-	-	-	-
14	-	-	-0.0002 ( $6.7 \cdot 10^{-5}$ )	-0.048 (0.021)	$5.4 \cdot 10^{-7}$ ( $2.4 \cdot 10^{-7}$ )
15	0.399 (0.249)	-	-	-	-
16	0.002 (0.287)	-	-	-	-
17	0.006 (0.315)	-	-	-	-
18	-	-0.006 (0.003)	-	-	-
19	-	-0.014 (0.005)	-	0.025 (0.010)	-
20	-	-	-	0.010 (0.010)	-
21	-0.353 (0.413)	-	-	-	-
22	-	-	-	0.011 (0.010)	-
23	-0.464 (0.439)	-	-	-	-
24	0.274 (0.253)	-	-	-	-

### 3.4.2 A Forecasting Experiment

In the preceding first part of this chapter, we have found that there is a significant relation between weather and spot prices. In the second part of this chapter, we want to examine whether this relation can be exploited for forecasting the one day-ahead spot price.

The forecasting methodology is the same as outlined in section 2.4.1 for the models with independent spikes.

Following Kosater and Mosler (2006), we set  $E[X_T|S_T = M, \mathcal{F}_T] = X_T$  and use the actual value  $X_T$  as forecast origin. In addition, we determine  $E[X_T|S_T = M, \mathcal{F}_T]$  as follows. First, we look for the last logarithm of the spot price which belongs to the stable regime. Starting at  $X_T$ , we look for the last logarithm of the spot price with a smoothed probability smaller than 0.5 to be in the spike regime. Let  $X_{T-i}$  be the stochastic part of such a logarithm of spot price. Then, we replace the actual value  $X_T$  by its forecast based on  $X_{T-i}$  with  $i \in \{0, 1, \dots, T-1\}$  as the forecast origin. By this, we approximate the forecast  $E[X_{T+1}|S_{T+1} = M, \mathcal{F}_T]$  with  $E[X_{T+1}|S_{T+1} = M, \mathcal{F}_{T-i}]$ .

$$\begin{aligned} E[X_{T+1}|S_{T+1} = M, \mathcal{F}_{T-i}] &= \mu_M \cdot \rho + & (3.4.5) \\ & (1 - \rho) \cdot ((1 - \rho)^i \cdot X_{T-i} + \mu_M \cdot (1 - (1 - \rho)^i)) \\ & = (1 - \rho)^{i+1} \cdot X_{T-i} + \mu_M \cdot (1 - (1 - \rho)^{i+1}). & (3.4.6) \end{aligned}$$

The one-step ahead forecast in both cases is thus,

$$P_{T+1}^f = \exp\left(X_{T+1}^f + f_{T+1}^f\right). \quad (3.4.7)$$

The advantage of our alternative approach is that we avoid forecasts for the stable regime based on spikes. However, one drawback is that the prediction error rises. Secondly, we renounce to exploit the forecast of the deterministic component at  $T$ . A possible procedure to avoid the loss in terms of seasonality could be to first remove the deterministic components from the actual time series. The stochastic model could be then fitted to the data from which deterministic components have been removed, as done by Misiorek et al. (2006).

Anticipating the results of the forecasting study, we found that the new approach presented in this paper outperforms the methodology in Kosater and Mosler (2006) for hours from 19 to 6. Spot prices for hours 21 to 6 do not differ much throughout the different types of days because demand is always low. Therefore, for these hours the deterministic component is not as important as for the hours from 9 till 20. We always report the best of all forecasts provided by the two methods. We can proceed this way, because the best performing method performs best for both versions A and B. Additionally, we have also assessed the performance of version B including the constant in equation (3.4.4) whenever the constant turned out to be not significant in the first part of the study. We have only obtained slightly better forecasts for hours 1 and 5.

Here, we have neglected the intra-day correlations of hourly prices. However, for many applications, such as risk management, derivative valuation and asset optimization these correlations are of crucial interest. In addition, Cuaresma et al. (2004) show that the inclusion of intra-day correlations between hours into

the model specification improves the forecasting performance. In the presented stochastic approach, other hourly price series could be included as explanatory variables similar to temperature or wind velocity to capture relations between hours during a day. However, the inclusion of lagged regressors of the same price series in this framework is not possible. In such a case, the original approach of Hamilton (1989) should be used instead.

### 3.4.3 Results of the Forecasting Study

In this forecast comparison study, we carry out and evaluate ex- ante forecasts in terms of the root mean square error ( RMSE ) and the mean absolute error ( MAE ). All given information available at time  $T$  is exploited and, by this, we use all known electricity prices up to  $T$  to estimate the parameter values.

The given dataset is divided into an in-sample period which includes observations from 6/16/2000 to 9/21/2004 at the beginning. The out-of-sample period ranges from 9/22/2004 to 12/30/2004. The forecasting experiment is designed as follows. We use in-sample data to estimate the parameters of the model version of interest. Then, we make out-of-sample one-step ahead forecasts and evaluate them. The in-sample period is then enlarged by one observation and again forecasts for the out-of-sample period are made and evaluated. We repeat this procedure 100 times. This forecasting study is carried out using the logarithm of all hourly 24 price series. As aforementioned, we use the actually measured values at the day the forecast is made for, instead of the forecast which we do not possess.  $P_{T+1}$  denotes the actual observed price at time  $T + 1$ , while  $P_{T+1}^f$  refers to the predicted price at time  $T + 1$ . The measures used for comparison are,

$$RMSE = \sqrt{\frac{1}{100} \cdot \sum_{i=1}^{100} \left( P_{T+1,i} - P_{T+1,i}^f \right)^2}, \quad (3.4.8)$$

$$MAE = \frac{1}{100} \cdot \sum_{i=1}^{100} \left| P_{T+1,i} - P_{T+1,i}^f \right|. \quad (3.4.9)$$

The two- steps ahead hardly and the three -steps ahead forecasts not at all resemble the measured values for both temperature and wind velocity, see Figure 3.4.1.

Therefore, we only carry out one-step ahead forecasts. For practical application, meteorologists provide forecasts up to six days ahead. Table 3.4.12 together with subfigures 3.4.2a and 3.4.2b present the results of the forecasting study. The results of the main study suggest to use weather data for forecasting prices for off-peak hours. For the remaining hours, the incorporation of weather data does not necessarily provide better forecasts. Furthermore, to understand the results of the study, we have carried out the following regressions,

$$P_t = \eta_1 + \eta_2 \cdot temp_t + \eta_3 \cdot temp_t^2 + \eta_4 \cdot temp_t^3 + \eta_5 \cdot wind_t, \quad (3.4.10)$$

$$\log(P_t) = \eta_{1,l} + \eta_{2,l} \cdot temp_t + \eta_{3,l} \cdot temp_t^2 + \eta_{4,l} \cdot temp_t^3 + \eta_{5,l} \cdot wind_t. \quad (3.4.11)$$

In subfigure 3.4.2c, we present the results of equations (3.4.9) and (3.4.10). In a second step, we have extracted some outliers from the electricity spot prices. Then, we regressed the remaining prices according to equations (3.4.9) and (3.4.10). The

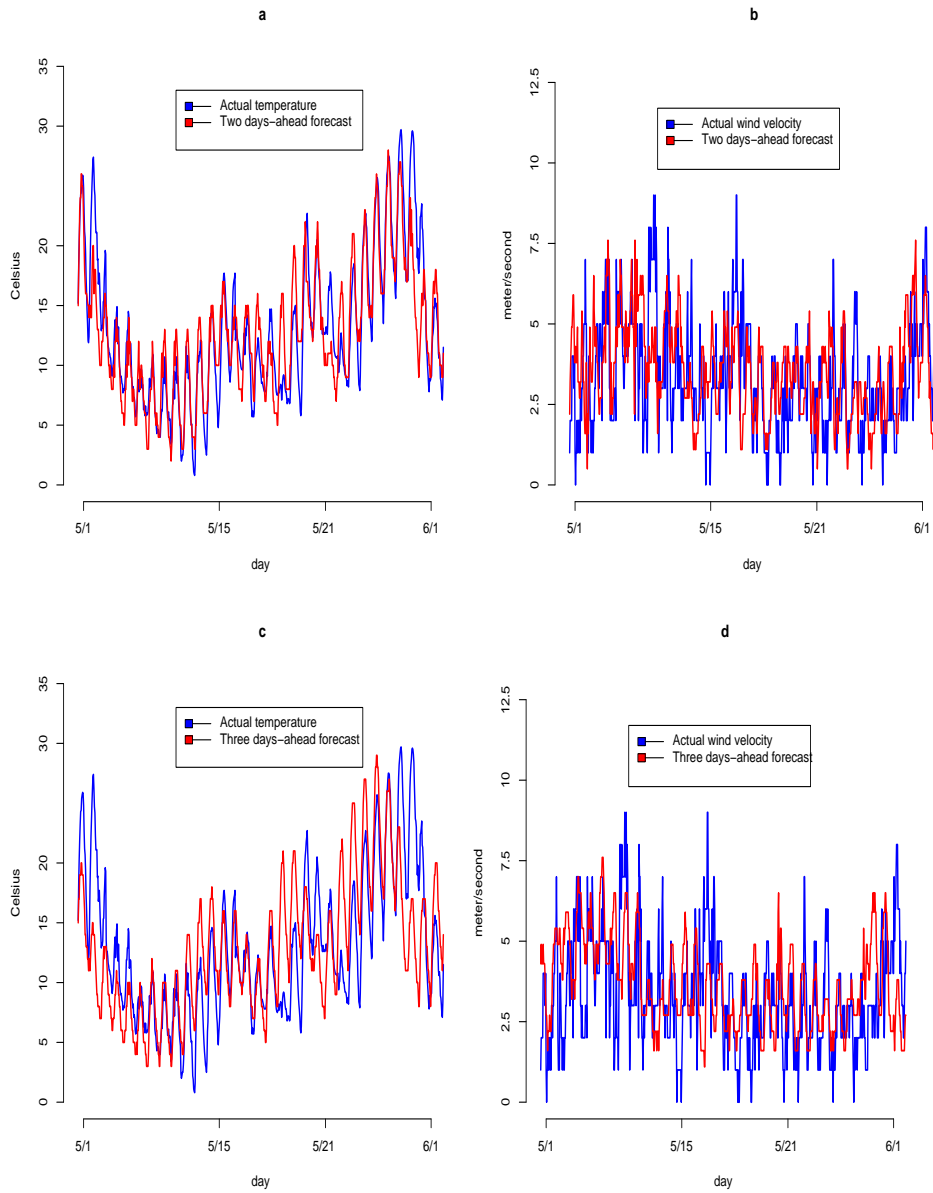


Figure 3.4.1: Measured temperature from Ulm (a),(c) and measured wind velocity (b),(d) together with their two and three days ahead forecasts from hour 7 a.m. 1/05/2005 until hour 6 a.m. 1/06/2005.

results of the confined regressions are plotted in subfigure 3.4.2d. Subfigures 3.4.2c and 3.4.2d show a very low coefficient of determination  $R^2$  for those hours where versions B fails to clearly outperform version A.

Table 3.4.12: Summary Out-Of-Sample Forecasting Study. (Best results are emphasized in bold.)

	RMSE		MAE	
Hour	A	B	A	B
1	4.957	<b>4.559</b>	3.709	<b>3.518</b>
2	5.179	<b>4.864</b>	4.244	<b>3.983</b>
3	5.014	<b>4.737</b>	3.885	<b>3.748</b>
4	4.815	<b>4.511</b>	3.656	<b>3.390</b>
5	5.000	<b>4.687</b>	3.911	<b>3.586</b>
6	4.550	<b>4.458</b>	<b>3.263</b>	3.328
7	5.574	<b>5.374</b>	3.997	<b>3.986</b>
8	6.449	<b>6.264</b>	<b>4.664</b>	4.712
9	6.317	<b>6.136</b>	4.436	<b>4.353</b>
10	<b>5.844</b>	5.930	<b>4.160</b>	4.191
11	6.023	<b>6.006</b>	4.428	<b>4.231</b>
12	8.218	<b>7.991</b>	5.642	<b>5.499</b>
13	5.653	<b>5.344</b>	4.036	<b>3.809</b>
14	<b>6.008</b>	6.369	<b>4.487</b>	4.492
15	5.411	<b>5.324</b>	4.060	<b>3.953</b>
16	<b>5.079</b>	5.111	<b>3.649</b>	3.677
17	5.396	<b>5.393</b>	3.973	<b>3.857</b>
18	9.252	<b>9.049</b>	6.825	<b>6.608</b>
19	8.540	<b>8.255</b>	6.122	<b>5.884</b>
20	6.611	<b>6.500</b>	4.786	<b>4.524</b>
21	4.664	<b>4.405</b>	3.066	<b>2.880</b>
22	3.940	<b>3.699</b>	2.886	<b>2.747</b>
23	3.154	<b>3.019</b>	2.257	<b>2.117</b>
24	3.499	<b>3.305</b>	2.659	<b>2.577</b>

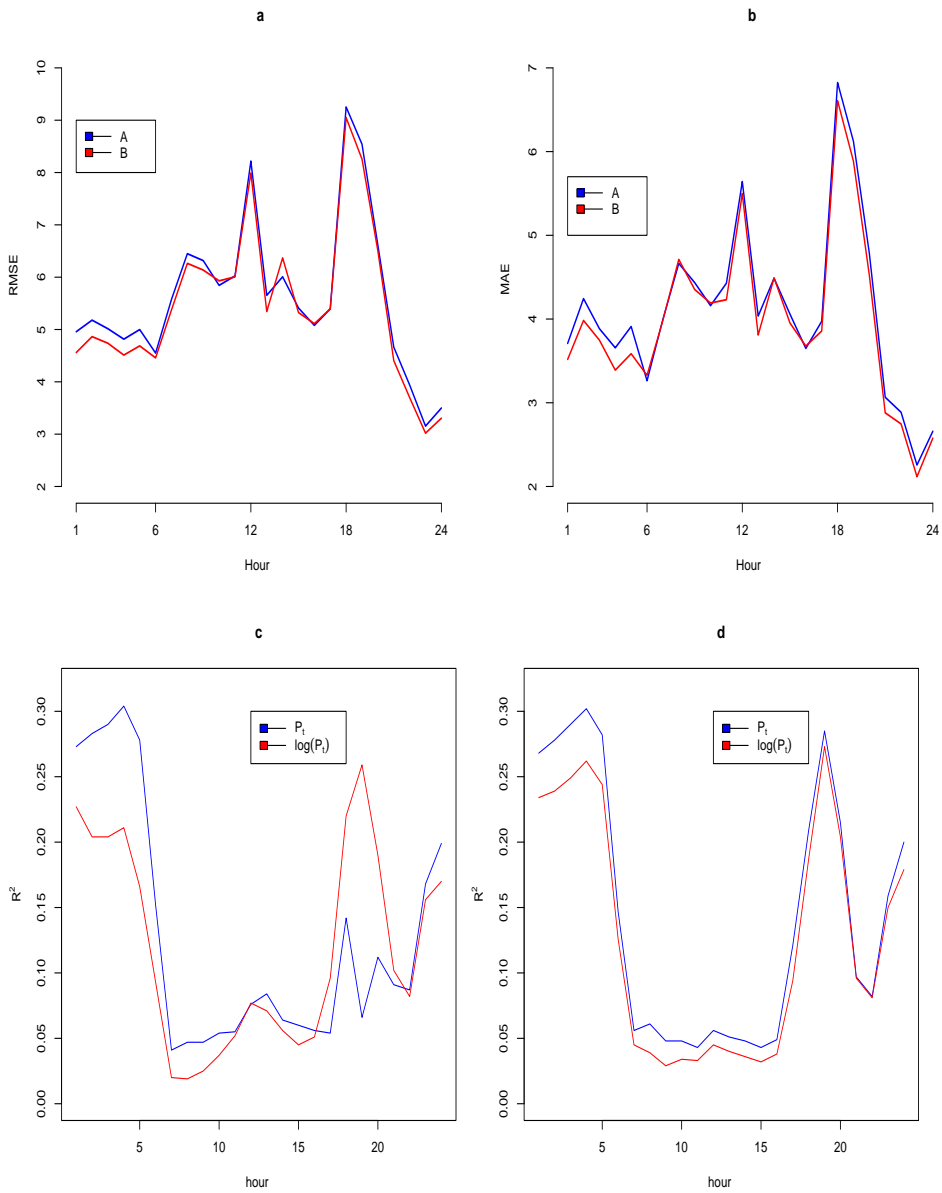


Figure 3.4.2: Results of the forecasting study (a,b), (c,d)  $R^2$  of equations (3.4.9) and (3.4.10).

### 3.4.4 An Additional Small Forecasting Study

To analyze the relevance of wind velocity for forecasting, we also carry out a small forecasting study for hours 4,12 and 22. We have chosen hour 4 and hour 22 to represent the off-peak I and II periods, respectively, whereas hour 12 is thought to be representative for on-peak hours.

We carry out the study without wind velocity. Secondly, we transform wind velocity in order to take into account that wind velocities below the margin of 4 meter/second are not significant for production. The transformation is implemented as follows,

$$wind_{trans} = \begin{cases} 0 & : & \text{wind velocity} < 4, \\ \text{wind velocity} - 4 & : & 4 \leq \text{wind velocity} \leq 12, \\ 8 & : & \text{wind velocity} > 12. \end{cases} \quad (3.4.12)$$

Furthermore, we also assess the performance of the unrestricted models incorporating all possible regressors for  $w_t$  as well as for the time-varying transition probabilities according to equations (3.4.3) and (3.4.4). Wind velocity and temperature are left unchanged compared with the main study. The results of the additional study are summarized in tables 3.4.13 and 3.4.14. They suggest that wind velocity is relevant for forecasting.

Additionally, we see that instead of actual wind velocity, we should implement a transformation which takes into account the technical conditions of the operation of windmills. Finally, incorporating all regressors may be an asset for forecasting, on one hand. On the other hand, we run risk of heavy losses due to overfitting.

In a second step, we want to compare the results with results of some linear models. Therefore, we also carry out one- step ahead forecasts with three further linear models denoted Models I to III. Model I is an autoregressive model of order one for the stochastic part of the logarithm of the spot price  $X_t$ . In Model II compared to Model I, we additionally include an autoregressive term of order seven to take into account the strong weekly seasonality. Finally in Model III, we specify the most sophisticated among the considered linear models, namely a seasonal autoregressive integrated moving average process  $ARIMA(1,0,1) \times SARIMA(1,0,1)_7$  to capture mean reversion and weekly seasonality. Additionally, we also examine the impact of weather on hourly spot prices in the framework of these models I to III. By this, we again denote two model versions A and B. For the linear models I to III, we specify version B according to equation (3.4.3).

**Model I:**

$$X_t = \rho \cdot \mu_M + (1 - \rho) \cdot X_{t-1} + \epsilon_t, \quad \epsilon_t \sim \mathcal{N}(0, \sigma_M^2). \quad (3.4.13)$$

**Model II:**

$$X_t = (\rho_1 - \rho_2) \cdot \mu_M + (1 - \rho_1) \cdot X_{t-1} + \rho_2 \cdot X_{t-7} + \epsilon_t, \quad \epsilon_t \sim \mathcal{N}(0, \sigma_M^2). \quad (3.4.14)$$

**Model III:**

$$\begin{aligned}
X_t = & \rho_1 \cdot (1 - \rho_2) \cdot \mu_M + (1 - \rho_1) \cdot X_{t-1} + \epsilon_t - \theta \cdot \epsilon_{t-1} - \omega \cdot (\epsilon_{t-7} - \theta \cdot \epsilon_{t-8}) \\
& + \rho_2 \cdot (X_{t-7} - (1 - \rho_1) \cdot X_{t-8}) , \quad \epsilon_t \sim \mathcal{N}(0, \sigma_M^2). \quad (3.4.15)
\end{aligned}$$

The logarithm of the spot price for hour 12 is characterized by alternating periods of very high volatility due to spiky and calm periods. Therefore, we carry out forecasting not only in the very calm period from 9/22/2004 to 12/30/2004 but additionally for the period from 5/30/2003 to 9/8/2003. Estimation of parameters for the second spiky period is based on the sub-sample from 6/16/2000 to 5/29/2003, at the beginning. Tables 3.4.15 and 3.4.16 present the results of the comparison of the out-of-sample prediction performance of the model with day-dependent and independent spikes with Models I to III. Results for the first calm period are denoted I and for the spiky period II.

In order to summarize the outcome of the study, Model III performs very well across the three hours 4,12 and 22. For the calm period I of hour 12, Model III even clearly outperforms the non-linear model applied in the main study. For the spiky period, however, the opposite is true. Furthermore, the study proves that non-linear models are valuable competing methods to sophisticated linear models with still hidden potential. This hidden potential lies in linking non-linear Markov regime-switching models to economic explanatory variables such as load and the reserve margin as pointed out in Mount et al. (2006).

Table 3.4.13: RMSE for The Three Selected Hours.( Best results are emphasized in bold.)

Hour	without wind	modified wind	all regressors	main study
4	4.759	<b>4.366</b>	4.729	4.511
12	8.319	7.910	<b>7.412</b>	7.991
22	3.835	3.713	<b>3.682</b>	3.699

Table 3.4.14: MAE for The Three Selected Hours.( Best results are emphasized in bold.)

Hour	without wind	modified wind	all regressors	main study
4	3.581	<b>3.304</b>	3.518	3.390
12	5.694	5.397	<b>5.114</b>	5.499
22	2.812	<b>2.719</b>	2.729	2.747

Table 3.4.15: RMSE for The Three Selected Hours.( Best results are emphasized in bold.)

Hour	Version	Model I	Model II	Model III	main study
4	A	5.028	5.264	4.702	4.815
4	B	5.114	4.802	<b>4.354</b>	4.511
12 (I)	A	9.168	7.549	6.510	8.218
12 (I)	B	8.892	7.324	<b>6.432</b>	7.991
12(II)	A	<b>58.501</b>	63.316	59.782	58.759
12 (II)	B	59.474	60.428	59.012	59.456
22	A	4.260	4.363	4.195	3.940
22	B	4.188	4.199	3.941	<b>3.699</b>

### 3.5 Summary

In this chapter, we have examined the relation between hourly prices from the EEX and weather represented by temperature and wind velocity. On one hand, we have explored whether a relation can be detected in the given data. On the other hand, we have examined if this relation can be exploited for forecasting of future spot prices.

The study has been carried out with the Markov regime-switching model with day-dependent and independent spikes put forward in section 2.3.6. We try to capture the general impact of weather on hourly spot prices, on one hand. Additionally, we model time-varying transition probabilities as functions of temperature and wind velocity to link weather and spikes.

As a result, we have found that including weather data yields better results in terms of fit than the pure stochastic models. However, the forecasting experiment reveals only that weather data should be used for forecasting prices in the hours from 19 until 6. During the remaining hours, including weather into the model does not necessarily provide better forecasts.

Due to emission allowances and the tendency towards renewable energy in elec-

Table 3.4.16: MAE for The Three Selected Hours. ( Best results are emphasized in bold.)

Hour	Version	Model I	Model II	Model III	main study
4	A	3.901	4.186	3.631	3.656
4	B	4.047	3.822	3.408	<b>3.390</b>
12 (I)	A	6.067	4.870	4.346	5.642
12 (I)	B	6.127	4.990	<b>4.179</b>	5.499
12 (II)	A	29.407	30.744	32.022	29.810
12 (II)	B	30.032	30.921	30.877	<b>29.121</b>
22	A	3.033	3.247	2.963	2.886
22	B	2.893	3.081	2.781	<b>2.747</b>

tricity production however, inclusion of weather will presumably become an asset for forecasting hourly prices throughout the whole day in the future. Some earlier results on the topic discussed in this chapter have been published in Kosater (2006).

For further research, load and the reserve margin should be incorporated in a good model specification. The general impact of weather on prices should be specified more precisely taking into account the four seasons or even the different months of the year. Finally, research should also focus on modelling the relation between spot prices and wind velocity.

## Chapter 4

# Cross-City Hedging with Weather Derivatives using Bivariate GARCH Models with Dynamic Conditional Correlations

### 4.1 Introduction and Literature Review

Many sectors of the economy such as energy, agriculture, retail and tourism are exposed to weather risk. The earnings of producers of ice cream and energy companies, for example, are very much depending on the weather conditions, they are faced with. To cope with the volumetric risk due to uncertain weather conditions, weather derivatives have become a common instrument. These instruments allow electricity suppliers to protect their earnings from warm winters or ice cream producers from cold summers. Especially in the USA, the market for weather derivatives, as well over the counter as exchange-based, is fast growing.

As of September 1999, the Chicago Mercantile Exchange, also referred to as CME, began listing futures and options on temperature indices of ten cities across the USA. Today, indices for eighteen U.S. cities are available. Besides, contracts on indices for nine European and two Japanese cities can be struck. These cities have been chosen based on population, the variability in their seasonal temperatures and the activities in over-the-counter markets. The total number of contracts traded was 4165 in 2002 and 14234 in 2003. Through September 2005, there were 630 000 weather contracts traded with a notional value of 22 billion dollars.

Weather derivative instruments include weather swaps, options, option collars and short straddles, to mention a few among them. The payoffs of these instruments may be linked to various underlying meteorological variables such as average temperature, minimum temperature, maximum temperature, heating degree days and cooling degree days, as well as wind speed, rainfall and sunshine.

Here, we concentrate on temperature derivatives, since about 90 % of the traded derivatives are based on temperature. To be more specific, we focus on contracts written on heating degree day (HDD) and cooling degree day indices (CDD), respectively. HDD indices can be used to protect from a bland winter, whereas CDD indices are designed to hedge against a cold summer.

A degree day measures how much a day's average deviates from 65° F ( or 18.33° C ) a level of outdoor temperature considered to be utmost comfortable by the utility industry. The idea behind this choice is that, for each degree below 65° F, more energy is needed for heating. By contrast, for each degree above 65° F, more energy is needed to power air conditioners. Most contracts are written on the accumulation of HDDs or CDDs over a calendar month or a season so that one contract can hedge against revenue fluctuations over the concerned period. Moreover, so-called energy degree day indices (EDD) are additionally offered by the CME. These contracts allow for more flexibility. For example, a different level than 65° F can be specified. More precisely, we denote the daily

$HDD = \max[0, 65^\circ \text{ F} - \text{daily average temperature}]$ , whereas for the daily CDD, we denote,  $CDD = \max[0, \text{daily average temperature} - 65^\circ \text{ F}]$ . Note that daily average temperature is computed as the average of the maximum and minimum temperatures on a certain day. Further basic elements of contracts with HDDs or CDDs as underlyings are the accumulation period and the station which records temperatures used to construct the underlying variable. Finally, the so-called tick size has to be determined. The tick size indicates the amount of money attached to each HDD or CDD, respectively.

However outside the USA, trading develops slowly or does not develop at all. For example, the Deutsche Börse Group had offered heating degree days (HDD) and cooling degree days (CDD) indices since December 2000 for thirty European cities. Among these cities were the German cities Berlin, Essen, Frankfurt and Hamburg. In the meantime, the Deutsche Börse Group has withdrawn from this market due to the lack of demand for standardized contracts and liquidity. Moreover, reliable and comprehensive weather data is not as easily available as in the USA. Additionally, the relevance of air conditioning in the summertime is not as pronounced as in the USA. Consequently, the demand for CDDs is much lower than in the USA. Attempts to establish an exchange-based trading of weather derivatives have failed in other European countries either. Therefore in Europe, trading of weather derivatives mainly takes place over the counter.

When we talk about valuation of temperature derivatives, we have to bear in mind that temperature as underlying has some salient characteristics. Since it is a meteorological variable rather than a traded asset, the conventional risk-neutral, arbitrage-free valuation methodology does not apply. By contrast, theoretically adequate valuation can only be based on an equilibrium model which takes into account the stochastic dynamics of the underlying as well as the risk aversion of the investors.

Another open question is whether the HDDs, CDDs should be directly modelled for each contract. Cao and Wei (2000) argue that direct modelling of the HDDs, CDDs has certain shortcomings. Instead, modelling the daily temperature enables

us to handle temperature contracts of any maturity and for any season. Moreover, estimation of model parameters has to be carried out only once. By contrast, direct modelling of HDDs and CDDs requires a separate estimation procedure for each contract taking into account the season and the maturity of the contract due to the nature of temperature behavior. As a result, modelling temperature rather than the HDDs and CDDs seems more adequate.

Literature on weather derivatives is rather scanty. In the following paragraphs, we report some important contributions, at least in our opinion, on temperature derivatives.

To start with, Dischel (1998) and Brody et al. (2002), propose to simulate future behavior of temperature as a continuous time or discrete time stochastic process which takes into account the salient features of temperature such as mean reversion and seasonality. These processes can be then fitted to data and used to value any contingent claim by taking expectation of the discounted future payoff.

Davis (2001) puts forward to value temperature derivatives based on HDDs and CDDs in an equilibrium framework. Besides the stochastic dynamics of temperature, the author takes into account optimal consumption and investment rules when he derives explicit pricing formulas for the valuation of swap rates and option values. Torro et al. (2003) model air temperature behavior in Spain combining techniques for the modelling of short-term interest rates with a generalized autoregressive conditional heteroscedastic (GARCH) time series approach. They suggest to create a population-weighted index of daily temperatures from four different measuring stations to compute HDDs or CDDs. Furthermore, Cao and Wei (2004) propose an equilibrium framework linking the temperature uncertainty and the economy's aggregate output therein. They suggest a serially correlated bivariate-process for the temperature and the aggregate output. Finally, their framework allows to address the market price of weather risk. They apply their framework to temperature from five CME-traded cities in the USA. Campbell and Diebold (2005) take a simple but systematic time series approach to modelling and forecasting daily average temperature in 10 U.S. cities. They find strong evidence that point and density forecasts from their approach prove useful for participants in the weather derivatives market.

In addition, Taylor and Buizza (2004) and Taylor and Buizza (2005) compare temperature density forecasts from time series models with atmospheric models in terms of short-run predictions one up to ten days ahead. They find evidence that so-called weather ensemble density forecasts of daily midday temperature data recorded at five locations in the UK outperform forecasts provided by time series models. Weather ensemble forecasts consist of multiple future scenarios for a weather variable generated from atmospheric models. In a second step, Taylor and Buizza (2005) assess forecasts of the conditional mean and quantiles of the density of the payoff of a 10 day-ahead put option provided by univariate time series models, on one hand, and from atmospheric models, on the other hand. Again, the obtained results suggest to use weather ensemble forecasts.

In this chapter, we intend to particularly address aspects of multivariate analysis and cross-city hedging as put forward by Campbell and Diebold (2005). Trading of

temperature derivatives requires to fix the station which records the temperature data that is used to compute the payoff of the derivative. At the CME, contracts are struck on data from few selected measuring stations to ensure liquidity. Campbell and Diebold (2005) argue that hedging of weather risk in remote locations is only possible if the risk of the remote location is highly correlated with the risk of a location for which a liquid market exists. Since HDDs and CDDs are computed at a daily basis, a multivariate model which captures daily correlation dynamics between locations may provide a very rich picture of reality and be therefore a very useful tool for risk management. In previous work of Torro et al (2003), Cao and Wei (2004) and Campbell and Diebold (2005) on univariate modelling, the authors have revealed that temperature displays rich dynamics such as yearly seasonality as well in the conditional mean as in the conditional variance. Consequently, it is probably naive to assume that the conditional correlation between two locations is the same in winter as in summer. We may rather expect the opposite to be true. At the CME, temperature derivatives based on data from nine European cities, among them Berlin and Essen, can be traded. Henceforth, if EnBW an important electricity supplier in the south-west of Germany plans to hedge his volume risk in the area of Stuttgart at the CME, for example, he must be aware of the correlation dynamics of daily average temperature at Stuttgart and the traded cities. Consequently, the correlation dynamics between the series from Stuttgart-Echterdingen and Berlin may be of special interest for EnBW. However, the modelling of correlation dynamics between temperature time series has not been paid much attention to, so far. Maybe this is one possible reason why many investors prefer to negotiate customized contracts over the counter on data from the region of their interest rather than to engage in standardized contracts on data from traded cities.

A rather neglected aspect of temperature derivatives is its usefulness in terms of portfolio management. Cao, Wei and Li (2004) stress that in incomplete markets a new asset class, such as weather derivatives, will always improve the risk-return trade-off in the perspective of the Markowitz mean-variance efficiency. Moreover, the relatively lower correlation between weather derivatives and conventional financial assets suggests that weather derivatives can be an excellent diversification vehicle.

Following and extending the previous work of Torro et al (2003) and Campbell and Diebold (2005) on univariate GARCH models, we choose a bivariate GARCH framework. In more detail, our focus in this chapter is twofold. On one hand, we want to assess the ability of bivariate GARCH models with dynamic conditional correlations in modelling time-varying correlation dynamics between temperature time series. On the other hand, we aim to apply the elaborated methodology to help an investor to correlate his own exposure with tradeable cities. As we mentioned before, knowledge of these correlation dynamics is the key to constructing a sensible hedge.

Previous contributions of Campbell and Diebold (2005), Franses et al.(2001), Torro et al. (2003), Taylor and Buizza (2004) and Tol (1996) show that generalized autoregressive conditional heteroscedastic (GARCH) models are useful in modelling and forecasting of univariate temperature time series.

Besides two benchmark models, we fit and gauge two univariate GARCH approaches to our temperature time series. Moreover in a second step, we move on to a bivariate GARCH framework to examine the correlation dynamics between different locations. Recently, several multivariate GARCH models have been designed to allow for parsimony or to guarantee a positive definite covariance matrix, or often both. We should keep in mind, that these models have originally been conceived to model dynamics of financial time series. Temperature time series display yearly seasonality in the conditional variance, which is a salient feature compared with financial time series. Consequently, the incorporation of seasonality dynamics in the existing multivariate GARCH framework is the main task that we are faced with the modelling of temperature series.

A thorough analysis of different multivariate GARCH approaches has revealed that dynamic conditional correlation models, abbreviated DCC, are well suited for modelling correlations between temperature time series.

DCC models offer a high degree of flexibility in modelling the conditional variance and conditional correlation dynamics. A further advantage of DCC models is the numerical stability, also for higher dimensions, due to a two-step estimation procedure that can be applied.

## 4.2 Data

The data comprises actually measured daily average temperature ( measured in  $C^\circ$  ) from three measuring stations ranging from January 1<sup>st</sup> 1991 to April 29<sup>th</sup> 2005.

One of the measuring stations is located at Stuttgart, namely Echterdingen. Moreover, we have decided to take data from Berlin (-Tempelhof) and Hamburg (-Fuhlsbüttel). The data from Berlin is used to compute European CDDs and HDDs at the CME. Therefore, this choice is quite natural. Hamburg and Echterdingen, however, are located in the north and south of Germany. We expect temperature at other locations to exhibit correlation dynamics in between these two. Daily average temperature have been computed as the arithmetic mean of daily maximum and daily minimum temperature series. Finally, according to Campbell and Diebold (2005) and Taylor and Buizza (2004), we have discarded the 29<sup>th</sup> February in leap years.

In the original series of Echterdingen, we have found three extremal observations larger than  $43 C^\circ$ . In our opinion, these values must be wrong. Therefore, we have replaced these aberrant observations by the average of temperatures observed one year before and one year after.

In table 4.2.1, we present some descriptive statistics for the three daily average temperature time series, whereas table 4.2.2 shows the correlations between the different temperature series. The estimated Kurtosis ranges between 2.27 and 2.44 and is far below 3 the value for the normal distribution. This is due to the different levels of temperature in winter and summer. By this, the distribution of these temperature series rather resembles a two-component mixture of normals than a normal distribution. In order to motivate our modelling approach in Section 4.3,

we analyze the data from Echterdingen. The remaining temperature series exhibit similar time series characteristics. Consequently, we treat them analogously. Hence, subfigure 4.2.1a shows the series of the station at Echterdingen, while subfigure 4.2.1b presents the histogram of this series together with the superimposed estimated normal density. As aforementioned, the empirical distribution seems slightly bimodal. The correlations between the temperature time series are positive and exceed 0.9.

Subfigure 4.2.1c shows the autocorrelation function which resembles a cosine function. This shape of the autocorrelation function indicates a strong yearly seasonality in the data. Finally, subfigure 4.2.1d suggests that the conditional mean of the considered time series should be modelled by a low- ordered autoregressive moving average process (ARMA).

Table 4.2.1: Descriptive Statistics on Temperature Series in  $C^\circ$  from The Three Selected Stations.

	S-Echterdingen	Berlin	Hamburg
Mean	9.58	9.85	9.32
Median	9.70	9.85	9.20
Maximum	27.55	29.55	29.60
Minimum	-13.90	-14.50	-15.05
Std. Dev.	7.52	7.87	7.02
Skewness	-0.14	-0.09	-0.07
Kurtosis	2.33	2.27	2.44
Jarque-Bera	113.59	122.55	72.88

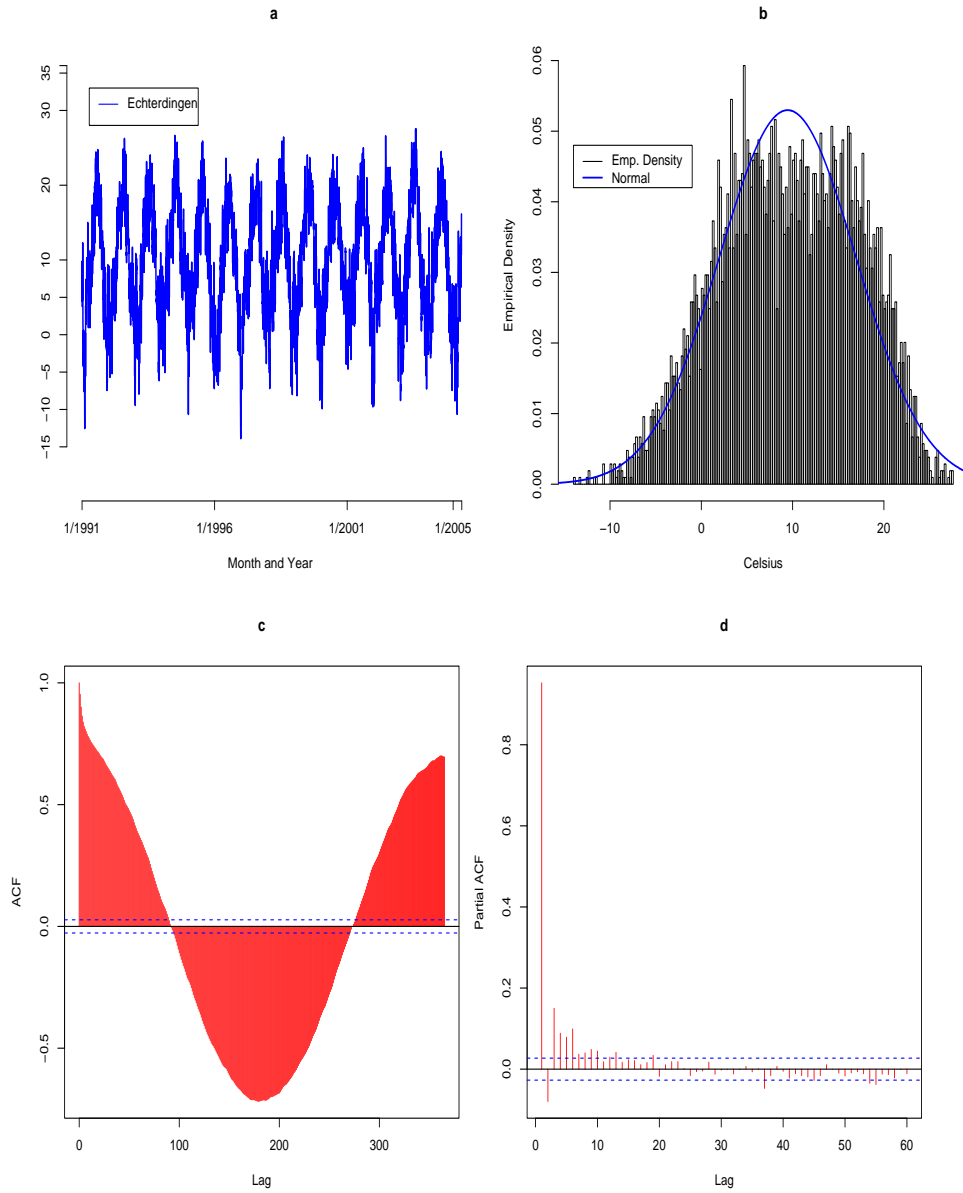


Figure 4.2.1: Daily average temperature from Echterdingen( 01/01/1991 until 04/29/2005 (a), Histogram for Echterdingen (b), Autocorrelation function ( ACF ) for Echterdingen (c), Partial autocorrelation function ( PACF )for Echterdingen (d).

Table 4.2.2: Correlations of Temperature Series in  $C^\circ$  from The Three Selected Stations.

	S-Echterdingen	Berlin	Hamburg
S-Echterdingen	1.000		
Berlin	0.942	1.000	
Hamburg	0.927	0.975	1.000

### 4.3 Univariate Modelling

Our modelling approach of the average daily temperature time series is substantially inspired by the work of Franses et al.(2001) and Campbell and Diebold (2005). At the beginning, we outline the previous two contributions.

Franses et al. (2001) examine weekly Dutch temperature data. They observe a yearly seasonal pattern in the mean and in the variance, respectively. Furthermore, they detect conditional heteroscedasticity in the data. Finally, they argue that the impact on the conditional variance of temperatures higher than expected is different from the impact of temperatures lower than expected. In order to capture these important features, they suggest a modified version of the following so-called Quadratic (Q)GARCH(1,1) model, originally put forward by Sentana (1995),

$$\begin{aligned}
 T_t &= s(\mu_0, \mu_1, \mu_2, t) + \rho_1 \cdot T_{t-1} + \epsilon_t \\
 \epsilon_t &= \sqrt{h_t} u_t \\
 h_t &= s(\omega_0, \omega_1, \omega_2, t) + \alpha \cdot (\epsilon_{t-1} - s(\gamma_1, \gamma_2, \gamma_3, t))^2 + \beta h_{t-1} \quad .
 \end{aligned}
 \tag{4.3.1}$$

Here,  $T_t$  denotes daily average temperature, whereas  $u_t$  is an i.i.d. error term. The terms of the form  $s(\xi_0, \xi_1, \xi_2, t)$  are employed to model seasonality and the asymmetric impact of lower and higher temperatures on the conditional variances. More precisely,  $s(\xi_0, \xi_1, \xi_2, t)$  is designed as follows,

$$s(\xi_0, \xi_1, \xi_2, t) = \xi_0 + \xi_1 w_t + \xi_2 w_t^2 \quad .
 \tag{4.3.2}$$

In this context,  $w_t$  is a repeating step function that numbers the weeks from 1 to 52 within each year.

Campbell and Diebold (2005) choose a structural approach combined with GARCH to take into account the conditional variance dynamics. The equations from (4.3.3)

to (4.3.8) highlight their modelling approach.

$$T_t = Trend_t + Season_t + \sum_{l=1}^L \rho_{t-l} T_{t-l} + \epsilon_t \quad (4.3.3)$$

$$\epsilon_t = \sqrt{h_t} u_t \quad (4.3.4)$$

$$Trend_t = \sum_{m=0}^M \beta_m t^m \quad (4.3.5)$$

$$Season_t = \sum_{p=1}^P \left( \lambda_{c,p} \cos(2\pi p \frac{d_t}{365}) + \lambda_{s,p} \sin(2\pi p \frac{d_t}{365}) \right) \quad (4.3.6)$$

$$h_t = \sum_{q=1}^Q \left( \lambda_{c,q} \cos(2\pi q \frac{d_t}{365}) + \lambda_{s,q} \sin(2\pi q \frac{d_t}{365}) \right) + \omega + \alpha \epsilon_{t-1}^2 + \beta h_{t-1} \quad (4.3.7)$$

$$u_t \sim \mathcal{N}(0, 1) \quad (4.3.8)$$

$d_t$  is a repeating step function that numbers the days from 1 to 365 within each year. Campbell and Diebold (2005) set  $P = Q = 3$ ,  $L = 25$  and  $M = 1$ .

In the first step, we model the conditional mean of the three daily average temperature time series of interest. Thereby, we take into account the descriptive time series characteristics depicted in figure 4.2.1. Similar to the work of Taylor and Buizza (2004) modelling seasonality with a low-ordered Fourier series, equation (4.3.6), turns out to be better suited for modelling the conditional mean than the quadratic function in equation (4.3.2). As opposed to Campbell and Diebold (2005) and Cao and Wei (2004), we do not find any evidence for a linear trend in any of the examined series. One reason is that we consider shorter time series. Secondly, the areas that we examine, are not as urbanized as Atlanta or Chicago where local temperatures have dramatically increased due to air pollution over the last decades. Furthermore, we do not fit an autoregressive model of order  $L = 25$  as suggested by Campbell and Diebold (2005). On the contrary, we prefer an autoregressive moving average process ARMA(1,1) for the two temperature series except for Hamburg. In the case of Hamburg, we opt for an ARMA(2,1). Finally, we specify the yearly seasonality according to equation (4.3.6) with  $P = 1$ . Our approach for the two locations, except for Hamburg, is summarized in equation (4.3.9). The specification for Hamburg is presented in equation (4.3.10) and denoted Model I\*.

#### Model I

$$T_t = \lambda_{c,1} \cos(2\pi \frac{d_t}{365}) + \lambda_{s,1} \sin(2\pi \frac{d_t}{365}) + \rho_1 \mu_m + (1 - \rho_1) T_{t-1} + \epsilon_t + \theta \epsilon_{t-1}, \quad (4.3.9)$$

#### Model I\*

$$T_t = \lambda_{c,1} \cos(2\pi \frac{d_t}{365}) + \lambda_{s,1} \sin(2\pi \frac{d_t}{365}) + (\rho_1 - \rho_2) \mu_m + (1 - \rho_1) T_{t-1} + \rho_2 T_{t-2} + \epsilon_t + \theta \epsilon_{t-1}, \quad (4.3.10)$$

where  $\epsilon_t \sim \mathcal{N}(0, \sigma^2)$ . Figure 4.3.1 presents some results on model fit for Model I for data from Echterdingen. Subfigures 4.3.1a and 4.3.1b show that the residuals do not exhibit any notable pattern of autocorrelation. However, the subfigures 4.3.1c and 4.3.1d suggest that the squared residuals are slightly autocorrelated.

Furthermore, subfigure 4.3.1e shows that the residuals are leptokurtic. Hence, the results put forward to model the conditional variance. Since the introduction of the (generalized) autoregressive conditional heteroscedasticity model (G)ARCH by Engle (1982) and Bollerslev (1986), a plethora of GARCH models has been proposed to take into account volatility clustering and the asymmetric effect of news on volatility.

For our purposes, we have chosen two among these models which potentially are capable of modelling the characteristics of temperature time series.

Following Campbell and Diebold (2005), we divide the conditional variance  $h_t$  into a seasonal and a GARCH part denoted  $\sigma_t^2$ .

$$h_t = \text{Seasonal}_t + \sigma_t^2 \quad (4.3.11)$$

$$\text{Seasonal}_t = \sum_{q=1}^Q \left( \lambda_{c,q+1} \cos(2\pi q \frac{d_t}{365}) + \lambda_{s,q+1} \sin(2\pi q \frac{d_t}{365}) \right) \quad (4.3.12)$$

In equation (4.3.12), we set  $Q = 2$  for all three stations. Besides Model I (Model I\*), we specify three further models which only differ in terms of the specification of  $\sigma_t^2$ . The conditional mean is specified according to equation (4.3.9)(equation (4.3.10)), while the seasonal part of the conditional variance follows from equation (4.3.12). Therefore, we confine ourselves, thereafter, to report the specification of  $\sigma_t^2$  for each model.

#### Model II

$$\sigma_t^2 = \sigma^2 \quad (4.3.13)$$

In Model II, which is similar to the specification of the conditional variance in Cao and Wei (2004), we assume no GARCH-dynamics in the conditional variance.

#### Model III

$$\sigma_t^2 = \omega + \alpha \epsilon_{t-1}^2 + \beta \sigma_{t-1}^2 \quad (4.3.14)$$

Model III is the basic symmetric specification of the GARCH(1,1) model proposed by Bollerslev (1986) and suggested by Campbell and Diebold (2005).

#### Model IV

$$\sigma_t^2 = \omega + \alpha (\epsilon_{t-1} - \gamma_1 - \gamma_2 d_t - \gamma_3 d_t^2)^2 + \beta \sigma_{t-1}^2 \quad (4.3.15)$$

In Model IV, we follow Franses et al. (2001) and link the potential asymmetry to a daily repeating step function  $d_t$ . At first glimpse, this approach seems most appealing, since potential asymmetry is directly linked to its seasonal source. Obviously, Model IV nests Model III if we set  $\gamma_1 = \gamma_2 = \gamma_3 = 0$ .

We have also examined other asymmetric GARCH models such as the GJR proposed by Glosten, Jagannathan and Runkle (1993) and the EGARCH proposed by Nelson (1991). However, it turned out that Model IV is best suited for our subject among the alternative univariate asymmetric GARCH specifications.

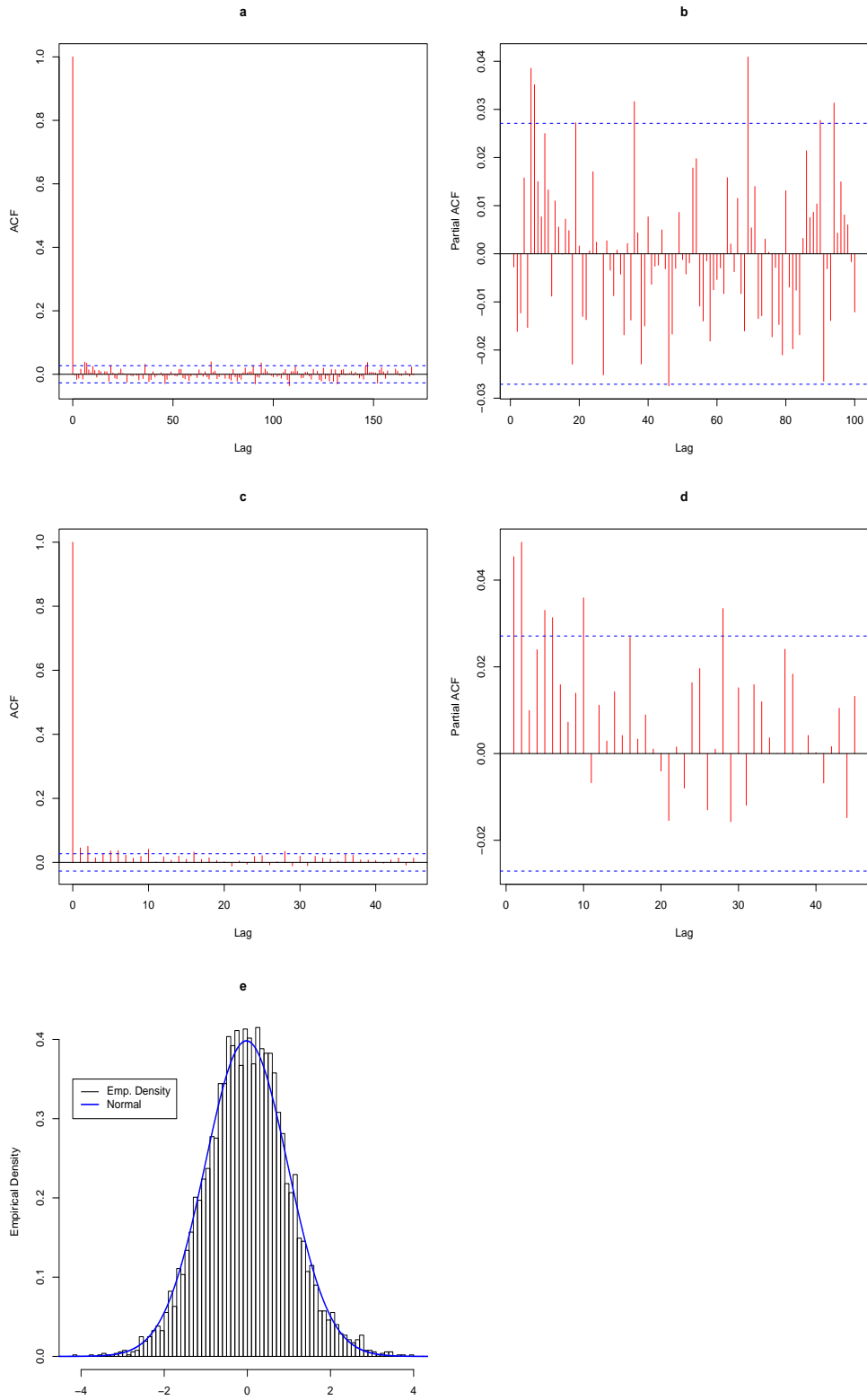


Figure 4.3.1: ACF of the residuals from equation(4.3.9) (a), PACF of the residuals from equation(4.3.9) (b), ACF of the squared residuals from equation(4.3.9) (c), PACF of the squared residuals from equation(4.3.9)(d), plot of the standardised squared residuals from equation (4.3.9)(e), histogram of the residuals from equation(4.3.9)(f).

### 4.3.1 Results on Model Fit

The aim of the modelling procedure is to capture as much as possible of the structure in the data. Therefore, we gauge the outcome not only in terms fit, but additionally consider the deviation of the standardized residuals from normality. Therefore, we also report skewness, kurtosis and the value of the Jarque-Bera (1987) statistic. In tables from 4.3.1 to 4.3.3, we report some descriptive statistics of the standardized residuals for all four models and each time series, whereas parameter estimates of the four models fitted to each of the three time series are collected in tables 4.3.4 and 4.3.5. The results indicate that Model II, which is almost the time series specification proposed by Cao and Wei (2004) already provides a sufficiently good fit. Model IV outperforms the remaining models in terms of fit but not with respect to the Jarque-Bera statistic. Especially, for Berlin and Hamburg the standardized residuals obtained for Models III and IV are more skewed than those of the benchmark model II. However, the kurtosis is closer to 3, which is the value of the kurtosis in the case that standardized residuals are normally distributed. Furthermore, we report the value of the Ljung-Box statistics for the standardized residuals  $u_t$  and the squared standardized residuals  $u_t^2$ . The standardized residuals pass the test only at a level between 1% and 2% for Echterdingen and Berlin. We renounced to add an additional AR(2) term due to the lack of significance. The squared standardized residuals do not exhibit any notable autocorrelation. Finally, figure 4.3.2 shows the estimated conditional variance series generated from Models III and IV for the temperature time series from Echterdingen.

Table 4.3.1: Summary In-Sample Fit : Echterdingen.

	Model			
	I	II	III	IV
Skewness	0.0633	-0.0101	-0.0093	0.0546
Kurtosis	3.3737	3.3046	3.2935	3.2585
Jarque-Bera	33.9040	20.3035	18.8381	17.1549
LL	-11450.09	-11400.05	-11394.80	-11372.32
LB Q(7) for $u_t$	18.762	17.054	16.990	16.184
LB Q(7) for $u_t^2$	45.775	12.262	2.6556	2.1367
SC	4.3901	4.3775	4.3788	<b>4.3751</b>

Table 4.3.2: Summary In-Sample Fit : Berlin.

	Model			
	I	II	III	IV
Skewness	0.1155	0.1077	0.1238	0.1755
Kurtosis	3.2948	3.1855	3.1676	3.1384
Jarque-Bera	30.5579	17.6077	19.4618	31.0090
LL	-11452.39	-11418.15	-11407.73	-11384.98
LB Q(7) for $u_t$	16.511	16.263	14.907	13.941
LB Q(7) for $u_t^2$	36.943	23.816	0.8667	1.3347
SC	4.3910	4.3845	4.3837	<b>4.3800</b>

Table 4.3.3: Summary In-Sample Fit : Hamburg.

	Model			
	I	II	III	IV
Skewness	0.1460	0.1507	0.1979	0.2538
Kurtosis	3.2431	3.1942	3.1034	3.1134
Jarque-Bera	31.4344	27.9987	36.4407	58.9014
LL	-11424.78	-11391.89	-11366.80	-11325.05
LB Q(7) for $u_t$	11.992	12.093	11.649	12.710
LB Q(7) for $u_t^2$	87.048	59.554	2.1903	2.8629
SC	4.3829	4.3769	4.3706	<b>4.3595</b>

Table 4.3.4: Estimates of Models I and II (equations (4.3.9),(4.3.10) and (4.3.13)).

	Model I			Model II		
	Echterdingen	Berlin	Hamburg	Echterdingen	Berlin	Hamburg
$\lambda_{s,1}$	-2.5206 (0.2020)	-2.6495 (0.2120)	-2.6329 (0.2048)	-2.6084 (0.1876)	-2.6902 (0.1942)	-2.6696 (0.1865)
$\lambda_{c,1}$	-8.8638 (0.2002)	-9.3603 (0.2019)	-8.0895 (0.1948)	-8.8804 (0.2014)	-9.4387 (0.2109)	-8.1662 (0.2065)
$\mu$	9.7103 (0.1424)	9.9798 (0.1471)	9.4409 (0.1420)	9.7215 (0.1385)	9.9973 (0.1436)	9.4515 (0.1384)
$\rho_1$	0.2618 (0.0106)	0.2536 (0.0106)	0.5122 (0.0959)	0.2687 (0.0113)	0.2552 (0.0110)	0.5198 (0.1062)
$\rho_2$	-	-	0.2119 (0.0787)	-	-	0.2166 (0.0865)
$\theta$	0.2183 (0.0154)	0.2257 (0.0152)	0.4024 (0.0927)	0.2217 (0.0159)	0.2178 (0.0155)	0.3992 (0.1028)
$\sigma$	4.6759 (0.0870)	4.6800 (0.0872)	4.6347 (0.0871)	4.6633 (0.0914)	4.6705 (0.0900)	4.6280 (0.0900)
$\lambda_{s,2}$	-	-	-	0.2934 (0.1138)	0.6498 (0.1185)	0.4717 (0.1130)
$\lambda_{c,2}$	-	-	-	1.2007 (0.1360)	0.5106 (0.1320)	0.5585 (0.1347)
$\lambda_{s,3}$	-	-	-	-0.0669* (0.1251)	-0.2795 (0.1241)	-0.2441 (0.1221)
$\lambda_{c,3}$	-	-	-	0.4673 (0.1157)	0.5632 (0.1222)	0.6787 (0.1216)

Note that \* means not significant at the 5 % level.

Table 4.3.5: Estimates of Models III and IV, (equations (4.3.14) and (4.3.15)).

	Model III			Model IV		
	Echterdingen	Berlin	Hamburg	Echterdingen	Berlin	Hamburg
$\lambda_{s,1}$	-2.6142 (0.1860)	-2.7204 (0.1942)	-2.7065 (0.1853)	-2.6569 (0.1882)	-2.7211 (0.1972)	-2.7071 (0.1878)
$\lambda_{c,1}$	-8.8058 (0.2004)	-9.3269 (0.2111)	-7.9083 (0.2039)	-8.8657 (0.2033)	-9.4561 (0.2124)	-8.1187 (0.2007)
$\mu$	9.7240 (0.1377)	10.0003 (0.1438)	9.4898 (0.1377)	9.7903 (0.1424)	10.0809 (0.1478)	9.5875 (0.1403)
$\rho_1$	0.2679 (0.0115)	0.2510 (0.0112)	0.4965 (0.1164)	0.2649 (0.0115)	0.2502 (0.0113)	0.4817 (0.1146)
$\rho_2$	-	-	0.2016 (0.0947)	-	-	0.1888 (0.0932)
$\theta$	0.2248 (0.0171)	0.2170 (0.0167)	0.3799 (0.1129)	0.2233 (0.0168)	0.2133 (0.0164)	0.3659 (0.1111)
$\omega$	1.6460 (0.8037)	1.1994 (0.5066)	1.2209 (0.3194)	1.1120 (0.3375)	0.8829 (0.2691)	1.2091 (0.2228)
$\alpha$	0.0348 (0.0135)	0.0434 (0.0137)	0.0714 (0.0133)	0.0370 (0.0110)	0.0342 (0.0106)	0.0682 (0.0133)
$\gamma_1$	-	-	-	2.9282 (1.1958)	2.0431* (1.2375)	3.6364 (0.8753)
$\gamma_2$	-	-	-	-0.0753 (0.0201)	-0.0762 (0.0234)	-0.0751 (0.0139)
$\gamma_3$	-	-	-	$2 \cdot 10^{-4}$ ( $5.4 \cdot 10^{-5}$ )	$2 \cdot 10^{-4}$ ( $6.4 \cdot 10^{-5}$ )	$2 \cdot 10^{-4}$ ( $3.8 \cdot 10^{-5}$ )
$\beta$	0.6121 (0.1800)	0.7001 (0.1171)	0.6650 (0.0756)	0.6665 (0.0796)	0.7083 (0.0649)	0.5994 (0.0580)
$\lambda_{s,2}$	0.2708 (0.1137)	0.5890 (0.1186)	0.4359 (0.1152)	0.3804 (0.1665)	0.4893 (0.1931)	0.5166 (0.1158)
$\lambda_{c,2}$	1.0846 (0.1434)	0.4458 (0.1313)	0.4865 (0.1365)	1.9234 (0.3679)	1.6577 (0.5304)	0.9674 (0.2817)
$\lambda_{s,3}$	-0.0832* (0.1260)	-0.3044 (0.1238)	-0.1973* (0.1201)	-0.2037* (0.1337)	-0.3073 (0.1766)	-0.2640* (0.1403)
$\lambda_{c,3}$	0.4208 (0.1165)	0.4493 (0.1233)	0.4657 (0.1257)	0.1863* (0.1661)	0.1319* (0.1766)	-0.1751* (0.1803)

Note that \* means not significant at the 5 % level.

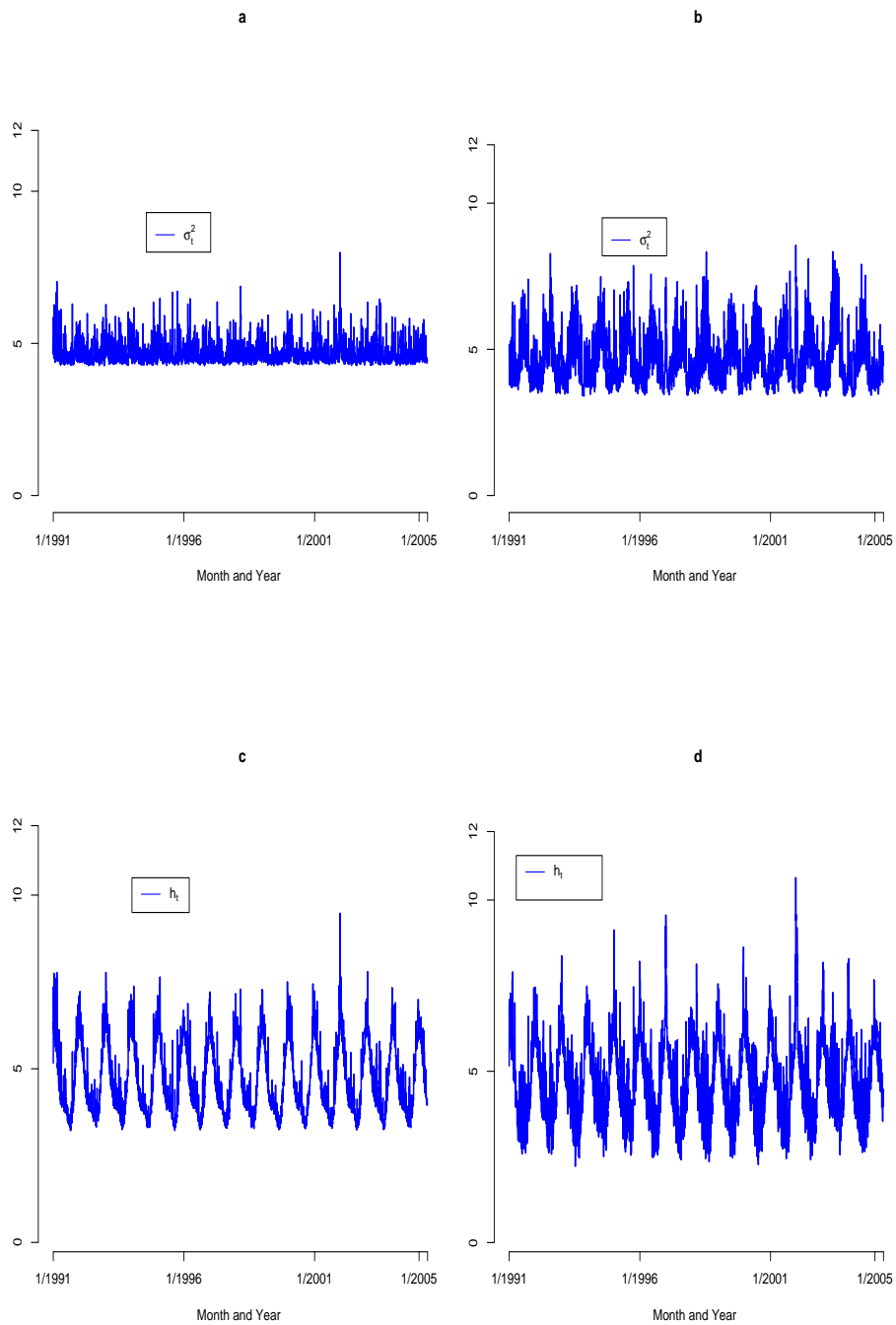


Figure 4.3.2:  $\sigma_t^2$ : Model III (a),  $\sigma_t^2$ : Model IV (b),  $h_t$ : Model III (c),  $h_t$ : Model IV (d), all series for Echtingen.

### 4.3.2 Examining the Departure from Normality

The Jarque-Bera statistic rejects the null hypothesis of normality for all models and all of the three temperature time series. Therefore, we try to inquire the source of departure from normality exhibited by the standardized residuals. First, we have presumed that the standardized residuals follow a student t-distribution and in the second step a the generalized error distribution instead of the normal distribution. As opposed to our expectation, the results became even worse.

Finally, we have additionally applied intervention analysis to the three series of interest and for Models III and IV, as last resort. Thereby, we have modelled so-called additive outliers in the conditional mean equation to mitigate the impact of potential aberrant observations. Here, we have included the additive outliers as follows,

$$T_t = E[T_t|\mathcal{F}_{t-1}] + \sum_{j=1}^J d_j \mathbf{I}_{t=t_{out}} + \epsilon_t \quad (4.3.16)$$

$E[T_t|\mathcal{F}_{t-1}]$  denotes the conditional mean, conditioned on the information set at time  $t - 1$   $\mathcal{F}_{t-1}$ . The dummy variable  $\mathbf{I}_{t=t_{out}}$  takes value 1 if at  $t$  an aberrant observation occurs. In this case, we denote  $t = t_{out}$ . Furthermore, we assume  $J$  additive outliers. The identification of outliers in the context of autoregressive moving average models can be done in several ways. For example Chen and Liu (1993), propose a procedure to identify outliers and to jointly estimate parameters and outlier effects.

Identification procedures for outliers are in general cumbersome to implement and slowly proceeding. Moreover, they rely on a test for which critical values are not known. In more detail, the searching procedure proposed by Chen and Liu (1993) leads to sequences of decision rules which cause that test-statistics are typically not distributed as  $\chi^2$  or standard normal. Henceforth, if we choose a critical value which is too low, we may detect too many outliers. Vice versa, if we set the critical value too high, we may not identify any outliers. In empirical work, it is often not easy to distinguish between extreme observations and outliers.

Since we do not focus on outliers, we have identified the most eye catching outliers using a heuristic method.

Generally speaking, we simply look for extreme values with respect to the quantiles of a standard normal distribution among the standardized residuals.

Finally, we jointly estimate the parameters together with dummy variables for the additive outliers. The results for skewness, kurtosis, the Jarque-Bera statistic and the value of the logarithmic likelihood together with the number  $J$  of included outlier-related dummy variables are summarized in tables 4.3.6 and 4.3.7. The results suggest that the departure from normality can be at least to some extent explained by extreme daily average temperatures on certain days. This seems especially true for the series from Echterdingen. For the remaining two series, we observe an improvement in terms of fit and the value of the Jarque-Bera statistic but this improvement is not sufficient to arrive at normality.

We denote the model versions with outlier-related dummy variables Model IIIb and Model IVb, respectively.

In Figure 4.3.3, we present the estimated conditional variance series  $h_t$  for Models

III, IIIb, IV and IVb for Echterdingen.

Table 4.3.6: Summary In-Sample Fit: Model IIIb.

	Model IIIb		
	Echterdingen	Berlin	Hamburg
Skewness	0.0199	0.1231	0.1930
Kurtosis	3.1568	3.0412	2.9702
Jarque-Bera	5.7012	13.5691	32.6384
LL	-11360.66	-11376.36	-11336.79
LB Q(7) for $u_t$	17.259	15.285	10.632
LB Q(7) for $u_t^2$	4.9785	2.6652	1.9411
SC	4.3756	4.3848	4.3755
$J$	6	8	10

Table 4.3.7: Summary In-Sample Fit: Model IVb.

	Model IVb		
	Echterdingen	Berlin	Hamburg
Skewness	0.0610	0.1613	0.2227
Kurtosis	3.1146	3.0246	2.9693
Jarque-Bera	6.0994	22.8101	43.4210
LL	-11334.30	-11349.49	-11290.72
LB Q(7) for $u_t$	17.611	13.664	11.797
LB Q(7) for $u_t^2$	3.3824	2.2804	2.8132
SC	4.3737	4.3795	4.3611
$J$	8	8	9

### 4.3.3 Out-of-sample Forecasting Study

For bivariate modelling, we have to choose a univariate specification to model the conditional variance, first. Model fit and the distribution of the standardized residuals are two important criteria when choosing a model. Another important feature, if not even the most important, is the out-of-sample forecasting quality of a model.

To start with, the forecasts for the conditional mean can be obtained as follows,

$$T_{t+1}^f = \lambda_{c,1} \cos(2\pi \frac{d_{t+1}}{365}) + \lambda_{s,1} \sin(2\pi \frac{d_{t+1}}{365}) + (\rho_1 - \rho_2)\mu_m + (1 - \rho_1)T_t + \rho_2 T_{t-1} + \theta \epsilon_t, \quad (4.3.17)$$

$$T_{t+h}^f = \lambda_{c,1} \cos(2\pi \frac{d_{t+h}}{365}) + \lambda_{s,1} \sin(2\pi \frac{d_{t+h}}{365}) + (\rho_1 - \rho_2)\mu_m + (1 - \rho_1)T_{t+h-1} + \rho_2 T_{t+h-2}. \quad (4.3.18)$$

We present the prediction procedure for the more elaborate ARMA(2,1) model fitted to data from Hamburg. Furthermore, we compute forecasts of the conditional variance,

$$(\sigma_{ii,t+h}^2)^f = E[\omega + \alpha(\epsilon_{t+h-1} - \gamma_1 - \gamma_2 d_{t+h} - \gamma_3 d_{t+h}^2)^2 + \beta \sigma_{t+h-1}^2 | \mathcal{F}_t] \quad (4.3.19)$$

$$= \omega + (\alpha + \beta) \sigma_{ii,t+h-1}^2 + \alpha(\gamma_1 + \gamma_2 d_{t+h} + \gamma_3 d_{t+h}^2)^2$$

$$(h_{ii,t+h})^f = (\sigma_{ii,t+h}^2)^f + Seasonal_{ii,t+h}^f. \quad (4.3.20)$$

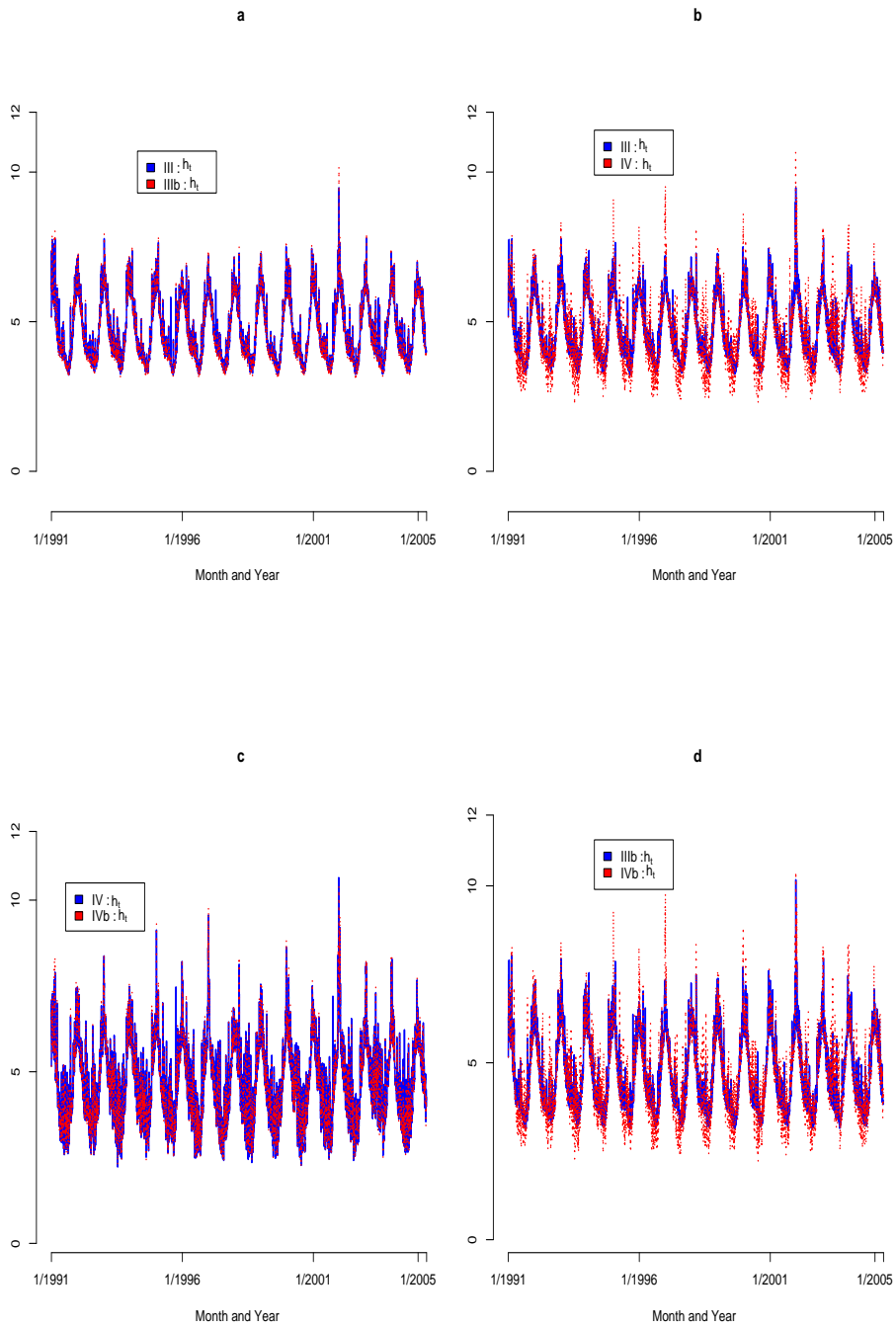


Figure 4.3.3:  $h_t$ : Model III and IIIb (a),  $h_t$ : Model III and Model IV (b),  $h_t$ : Model IV and IVb (c),  $h_t$ : Model IIIb and Model IVb (d), all series for Echterdingen.

Here, we assess the forecasting ability of Models III and IV. Furthermore, we also examine the performance of these model specifications taking into account the outlier effects. Outliers can lead to biased estimates, model misspecification and inaccurate forecasts. Therefore, we want to examine if the inclusion of dummy variables for additive outliers, in fact, improves out-of-sample forecasts.

The number of actually included additive outliers also depends on numerical stability. Too many dummy variables slow up likelihood maximization or can, even, turn it impossible.

In our forecast experiment, we follow Franses et al. (2001) and assess the one-step ahead forecasts of the conditional variance  $h_t$  for 150 observations from 08/21/2004 to 01/18/2005. We estimate model parameters beginning with the in-sample from 08/20/2004 to 01/17/2005. For every forecast, we re-estimate the parameters for the models of interest, using all observations prior to the forecast origin. As a measure of the true variance, we use the squared residuals  $\hat{\epsilon}_t^2$  from Model I obtained in each estimation round on the in-sample augmented by one observation. The results are summarized in table 4.3.8.

We gauge the results by means of the measures RMSE and MAE, see equations (4.3.21) and (4.3.22).

$k$  denotes the number of results which we take into consideration to compute the measures RMSE and MAE, respectively. We have obtained  $k = 150$  for Hamburg, Berlin  $k = 141$  and Echterdingen  $k = 150$ . Only results where all of the four models achieved convergence were taken into consideration. If at least one did not successfully converge, we discarded the results from all models for this observation from computation of RMSE and MAE.

Unfortunately in the case of Echterdingen, optimization of the logarithmic likelihood of Model IV often yielded negative parameter estimates for GARCH parameters which should be positive. However, this shortcoming did not emerge with Model IVb. Consequently, we only report the results for Model IVb.

Summarizing the results for Berlin and Hamburg, we see no clear difference between the QGARCH and the symmetric GARCH model with respect to both measures RMSE and MAE, except for Echterdingen where the RMSE for Model IVb is notably larger than for Models III and IIIb, respectively.

Secondly, the inclusion of dummy variables to mitigate the effect of additive outliers does not notably improve the point forecast performance. However, we should bear in mind that the inclusion of dummy variables to mitigate outliers may improve the interval forecasting performance.

$$RMSE = \sqrt{\frac{1}{k} \cdot \sum_{i=1}^k \left( P_{T+1,i} - P_{T+1,i}^f \right)^2}, \quad (4.3.21)$$

$$MAE = \frac{1}{k} \cdot \sum_{i=1}^k \left| P_{T+1,i} - P_{T+1,i}^f \right|. \quad (4.3.22)$$

As a result of the univariate study, we employ Model IV to model the conditional variance dynamics. Especially, due to the in-sample fit and the fact that the QGARCH nests Model III as a special case, we think that this is the right choice. Furthermore, we renounce to include the additive outliers because the inclusion

Table 4.3.8: Results on The Out-Of-Sample Forecasting Study.( Best results are emphasized in bold.)

	Echterdingen		Berlin		Hamburg	
	RMSE	MAE	RMSE	MAE	RMSE	MAE
III	6.1091	4.3914	7.1809	4.6736	6.2768	4.2391
IIIb	<b>6.1058</b>	4.3792	7.1930	4.6697	6.2834	4.2276
IV	-	-	<b>7.1114</b>	<b>4.6383</b>	<b>6.1760</b>	<b>4.1344</b>
IVb	7.4592	<b>4.3601</b>	7.1122	4.6591	6.1985	4.1508

of these outliers may unnecessarily complicate optimization. This may become an even more severe problem when we turn to bivariate modelling.

However, the role of outliers, especially for interval forecasting, in the present context may be an interesting issue for further research.

## 4.4 Bivariate Modelling

Research on multivariate GARCH models is very active due to their relevance for many financial applications such as asset pricing, portfolio selection, hedging and risk management. Quite alike the development in univariate GARCH modelling, we can observe several different more or less sophisticated approaches to multivariate GARCH models. For a comprehensive survey on multivariate GARCH models, we refer to Bauwens et al. (2006).

We continue with our approach from univariate modelling and assume the conditional covariance matrix  $H_t$  to consist of a seasonal part and a GARCH(1,1) part denoted  $\Sigma_t$ .

$$H_t = Seasonal_t + \Sigma_t \quad \text{with } \Sigma_t = \begin{pmatrix} \sigma_{11,t}^2 & \sigma_{12,t} \\ \sigma_{21,t} & \sigma_{22,t}^2 \end{pmatrix}. \quad (4.4.1)$$

The seasonal term of  $h_{ii,t}$ , with  $i \in \{1, 2\}$ , is specified as in the univariate case with  $Q = 2$ ,

$$Seasonal_{ii,t} = \sum_{q=1}^Q \left( \lambda_{i,c,q+1} \cos(2\pi q \frac{d_t}{365}) + \lambda_{i,s,q+1} \sin(2\pi q \frac{d_t}{365}) \right). \quad (4.4.2)$$

Here, we work in the framework of so-called dynamic conditional correlation models. Dynamic conditional correlation models have certain advantages. They allow to include seasonality in the conditional variance specification without running risk of numerical problems which is neither guaranteed by any version of VEC models proposed by Bollerslev et al. (1988) nor by any version of BEKK models advocated by Baba et al.(1991), respectively. Secondly, the specification of the conditional variance is not confined to be a standard GARCH(1,1) according to Bollerslev (1986). Therefore, we can take into account the asymmetry displayed by

the temperature series due to the different impact of temperature higher than expected and lower than expected on the conditional variance. Orthogonal GARCH models, see van der Weide (2002), are also flexible with the specification of the conditional variance. However, orthogonal GARCH models are a special case of BEKK models. Consequently, these models do not possess distinct parameters, which exclusively govern the correlation dynamics. However, we opt for utmost flexibility in modelling. This is especially true with respect to correlation dynamics, the main subject of our study. Dynamic conditional correlation models warrant an utmost flexible modelling compared with the remaining approaches such as VEC and BEKK models.

#### 4.4.1 The DCC Model Class

Dynamic conditional correlation models allow to separately specify the individual conditional variances, on one hand, and the conditional correlation matrix or another measure of dependence between the individual series, like a copula of the conditional joint density, on the other hand.

First attempts to design dynamic conditional correlation models have been undertaken by Engle (2002), Tse and Tsui (2002), Christodoulakis and Satchell (2002). The dynamic conditional correlation model class nests the popular constant correlation coefficient model introduced by Bollerslev (1990). The main advantage of DCC models over VEC or BEKK models is parsimony in parametrization which alleviates estimation and allows to overcome the curse of dimensionality for higher than the bivariate case. A disadvantage is that theoretical results on stationarity, ergodicity and moments cannot be easily derived as for VEC and henceforth also BEKK models.

The center piece of this model class is the fact that  $H_t$  can be decomposed as follows,

$$H_t = D_t R_t D_t, \quad (4.4.3)$$

where  $D_t$  is the diagonal matrix of time-varying standard deviations from univariate GARCH models with  $\sqrt{h_{ii,t}}$  on the  $i^{th}$  diagonal and  $R_t$  is the (possibly) time-varying correlation matrix. This class of models was originally designed to allow for two-step estimation of the typically high dimensional matrix  $H_t$  in the context of portfolio optimization, where very many assets are involved.

In the first step univariate volatility models are fitted for each of the assets or temperature series and estimates of  $h_{ii,t}$  are obtained. In the second step, parameters of the conditional correlation are estimated given the estimated parameters and conditional variances from the first step.

Unfortunately, model parameters are not simultaneously estimated by means of quasi maximum likelihood and therefore inefficient. However, Engle and Sheppard (2001) show that consistency and asymptotic normality of the parameter estimates of the two-step DCC estimator closely follow the results for GMM.

For the bivariate DCC model,  $H_t$  can be expressed as,

$$H_t = \begin{pmatrix} \sqrt{h_{11,t}} & 0 \\ 0 & \sqrt{h_{22,t}} \end{pmatrix} \begin{pmatrix} 1 & r_{12,t} \\ r_{21,t} & 1 \end{pmatrix} \begin{pmatrix} \sqrt{h_{11,t}} & 0 \\ 0 & \sqrt{h_{22,t}} \end{pmatrix}. \quad (4.4.4)$$

Since correlations lie between -1 and 1, these models must include a rescaling procedure. The models of Engle (2002), Tse and Tsui (2002) are very similar. Therefore, we work only with the model of Engle (2002) for some reasons. This model is easier to handle in terms of specification and forecasting. In addition, Capiello et al. (2003) present an asymmetric extension to the model put forward by Engle (2002). Asymmetry in correlation dynamics between temperature time series may potentially be a very important feature.

More precisely, the evolution of the correlation in the model of Engle (2002) is given by,

$$Q_t = \begin{pmatrix} q_{11,t} & q_{12,t} \\ q_{21,t} & q_{22,t} \end{pmatrix} \quad (4.4.5)$$

$$Q_t^* = \begin{pmatrix} \sqrt{q_{11,t}} & 0 \\ 0 & \sqrt{q_{22,t}} \end{pmatrix} \quad (4.4.6)$$

$$R_t = (Q_t^*)^{-1} Q_t (Q_t^*)^{-1} \quad (4.4.7)$$

$$Q_t = (1 - \phi - \psi) \bar{Q} + \phi \mathbf{u}_{t-1} \mathbf{u}_{t-1}' + \psi Q_{t-1}, \quad (4.4.8)$$

where  $\phi$  and  $\psi$  are scalars, whereas  $\bar{Q} = E[\mathbf{u}_t \mathbf{u}_t']$  is the unconditional correlation matrix of the  $u_{i,t} = \frac{\epsilon_{i,t}}{\sqrt{h_{ii,t}}}$ . Obviously, the matrix  $(Q_t^*)^{-1}$  is used for rescaling.

As aforementioned, Capiello et al. (2003) propose an asymmetric extension to the model of Engle (2002). The evolution of  $Q_t$  is now supposed to be,

$$Q_t = \left( \bar{Q} - \Phi' \bar{Q} \Phi - \Psi' \bar{Q} \Psi - \Upsilon' E[\eta_t \eta_t'] \Upsilon \right) + \Phi' \mathbf{u}_{t-1} \mathbf{u}_{t-1}' \Phi + \Psi' Q_{t-1} \Psi + \Upsilon' \eta_{t-1} \eta_{t-1}' \Upsilon. \quad (4.4.9)$$

Here, we denote  $\eta_{i,t} = \min(\mathbf{u}_{i,t}, \mathbf{0})$ . Additionally, we substitute the expectations  $\bar{Q} = E[\mathbf{u}_t \mathbf{u}_t']$  and  $E[\eta_t \eta_t']$  with their sample analogues  $\frac{1}{T} \sum_{t=1}^T \mathbf{u}_t \mathbf{u}_t'$  and  $\frac{1}{T} \sum_{t=1}^T \eta_t \eta_t'$ , respectively.

Here, we only consider the bivariate scalar asymmetric model version, where  $\phi$ ,  $\psi$  and  $v$  are scalars. In our opinion, this is no shortcoming, since our data does not support a more elaborate parametrization. The interesting specification is expressed in equation (4.4.10),

$$Q_t = \left( \bar{Q} - \phi \bar{Q} - \psi \bar{Q} - v E[\eta_t \eta_t'] \right) + \phi \mathbf{u}_{t-1} \mathbf{u}_{t-1}' + \psi Q_{t-1} + v \eta_{t-1} \eta_{t-1}'. \quad (4.4.10)$$

Dynamic conditional correlation models are still the subject of very active ongoing research. Here, we only present and exploit very fundamental models and methodology.

To name some of the recent contributions in this field, Hafner and Franses (2006) suggest semi-parametric modelling of conditional correlations. Pelletier (2006) puts forward to extend the dynamic conditional correlation framework to regime switching dynamic conditional correlation models. Teräsvirta (2005) considers a smooth transition conditional correlation model that allows the conditional correlations to vary between two extremes. Other authors pursue the modelling of the dependence between financial time series rather than the correlation, see Patton (2000), and Jondeau and Rockinger (2001). The investigation of the more sophisticated approaches and model extensions is left as a challenging task for further research.

#### 4.4.2 Flexible Dynamic Correlations models

Due to the rescaling procedure which ensures that conditional correlations lie between -1 and 1, it is not possible to include a Fourier series to capture potential yearly seasonality in the conditional correlation series in the framework of Engle (2002). This is also true for the framework of Tse and Tsui (2002).

Christodoulakis and Satchell (2002) put forward a potential remedy which warrants full flexibility in modelling conditional correlation dynamics. The authors use the Fisher transformation of the correlation coefficient to ensure that  $-1 \leq r_{12,t} \leq 1$ . More precisely, Christodoulakis and Satchell (2002) suggest

$$r_{12,t} = \frac{\exp(2r_{12,t}^*) - 1}{\exp(2r_{12,t}^*) + 1}. \quad (4.4.11)$$

Moreover, Baur (2006) proposes a transformation which is described in equation (4.4.12),

$$r_{12,t} = \frac{r_{12,t-1}^*}{\sqrt{1 + (r_{12,t-1}^*)^2}}, \quad (4.4.12)$$

Additionally, we have found that the following transformation works well for the considered temperature time series in terms of fit.

$$r_{12,t} = \frac{r_{12,t-1}^*}{1 + |r_{12,t-1}^*|} \quad (4.4.13)$$

Finally, we compute the covariance  $h_{12,t}$  according to equations (4.4.14) and (4.4.15). We determine the correlation  $r_{12,t}$  using one of the transformations presented in equations (4.4.11) to (4.4.13).

$$\begin{aligned} r_{12,t}^* &= \omega_{12} + \phi u_{1,t-1} u_{2,t-1} + \psi r_{12,t-1}^* + \nu \eta_{1,t-1} \eta_{2,t-1} \\ &\quad + \lambda_{c,1}^* \cos(2\pi \frac{d_t}{365}) + \lambda_{s,1}^* \sin(2\pi \frac{d_t}{365}) \end{aligned} \quad (4.4.14)$$

$$h_{12,t} = r_{12,t} \sqrt{h_{11,t} h_{22,t}} \quad (4.4.15)$$

#### 4.4.3 Two-Step Estimation Procedure

The DCC models as well as the FDC models are estimated by means of the two-step estimation procedure suggested in Engle (2002) and quasi maximum likelihood, respectively. Here, we outline the two-step procedure referring to the original contribution in Engle (2002). The results of the univariate study put forward that assuming  $\epsilon_t | \mathcal{F}_{t-1} \sim \mathcal{N}(0, H_t)$ , where  $\mathcal{F}_{t-1}$  is the information set at time  $t-1$ , is a possible choice. The logarithmic likelihood  $L(\varphi, \theta)$  for this estimator can be expressed as,

$$\begin{aligned} L(\varphi, \theta) &= -\frac{1}{2} \sum_{t=1}^T \left( n \log(2\pi) + \log |H_t| + \epsilon_t' H_t^{-1} \epsilon_t \right) \\ L(\varphi, \theta) &= -\frac{1}{2} \sum_{t=1}^T \left( n \log(2\pi) + \log |D_t R_t D_t| + \epsilon_t' D_t^{-1} R_t^{-1} D_t^{-1} \epsilon_t \right) \\ L(\varphi, \theta) &= -\frac{1}{2} \sum_{t=1}^T \left( n \log(2\pi) + 2 \log |D_t| + \log |R_t| + \mathbf{u}_t' R_t^{-1} \mathbf{u}_t \right) \end{aligned} \quad (4.4.16)$$

The parameters in  $D_t$  are denoted  $\varphi$ , whereas the additional parameters in  $R_t$  are denoted  $\theta$ . Furthermore  $n$  is the number of assets or in our case temperature

series. Henceforth, in our study  $n$  equals 2 ( $n = 2$ ). To implement the two step estimation strategy, Engle (2002) suggests to replace  $R_t$  by the identity matrix to obtain a consistent estimator in the first step of the estimation procedure. In such a case, the univariate quasi logarithmic likelihood function  $QL_1(\varphi)$  becomes

$$QL_1(\varphi) = -\frac{1}{2} \sum_{t=1}^T \left( n \log(2\pi) + \sum_{i=1}^n \left( \log(h_{ii,t}) + \frac{\epsilon_{i,t}^2}{h_{ii,t}} \right) \right). \quad (4.4.17)$$

The first step provides estimates  $\hat{\varphi}$ . In the second step of the estimation procedure, we estimate the remaining parameters  $\theta$  conditioned on the estimates from the first step. Since parameters  $\varphi$  are determined, the relevant part for estimation in the second step is the quasi logarithmic likelihood denoted  $QL_2(\theta|\hat{\varphi})$ .

$$QL_2(\theta|\hat{\varphi}) = -\frac{1}{2} \sum_{t=1}^T \left( \log |R_t| + \mathbf{u}_t' R_t^{-1} \mathbf{u}_t \right) \quad (4.4.18)$$

In the bivariate case,  $L_C(\theta)$  can be quite simply written as,

$$QL_2(\theta|\hat{\varphi}) = -\frac{1}{2} \sum_{t=1}^T \left( \log(1 - r_{12,t}^2) + \frac{(u_{1,t}^2 + u_{2,t}^2 - 2r_{12,t}u_{1,t}u_{2,t})}{(1 - r_{12,t}^2)} \right). \quad (4.4.19)$$

To compare this two step likelihood with the logarithmic likelihood of other models, we can compute its value as follows,

$$L(\varphi, \theta) = QL_1(\varphi) + QL_2(\theta|\hat{\varphi}) + \frac{1}{2} \sum_{t=1}^T \mathbf{u}_t' \mathbf{u}_t. \quad (4.4.20)$$

#### 4.4.4 Results on Model fit

We estimate the logarithmic likelihood given in equation (4.4.21). For simplicity, standardized residuals are assumed to be normally distributed,

$$\log L(\theta, \varphi) = -\frac{T}{2} \log(2\pi) - \frac{1}{2} \log(|H_t|) - \frac{1}{2} \epsilon_t' H_t \epsilon_t. \quad (4.4.21)$$

Temperature derivatives based on temperature from Berlin are traded at the CME. Therefore, we have designed two pairs, Echterdingen-Berlin and Hamburg-Berlin, for the empirical study. We estimate all five models with the two- step method put forward by Engle (2002) and described in subsection 4.3.3. Additionally, we take the estimates of the two-step procedure as starting values and carry out a simultaneous quasi maximum likelihood estimation of the likelihood in equation (4.4.21). Estimates of parameters which enter the correlation equations are collected in tables 4.4.1 to 4.4.10. Here, the remaining parameters are of minor interest, therefore we do not explicitly address them, but they can be obtained upon request. However for the two- step method, the remaining parameters are given in table 4.3.5 . In addition, figure 4.4.1 shows the estimated conditional correlations for the pairs Echterdingen-Berlin and Hamburg-Berlin provided by the five considered versions of dynamic conditional correlation models.

The estimates of the quasi maximum likelihood estimation provide higher values of the logarithmic likelihood throughout all models compared with the two- step method. The in-sample results of the five DCC models do not indicate, that any model version clearly performs best.

For the pair Echterdingen-Berlin, the symmetric DCC model provides the highest in-sample fit. Conditional correlations between the temperature series from Echterdingen and Berlin only display weak yearly seasonality. Consequently, the inclusion of seasonality in the flexible dynamic conditional correlation models is of minor importance. By contrast, conditional correlations between Hamburg and Berlin seem to display a very pronounced yearly seasonality. As a result, the flexible dynamic correlation models outperform the dynamic conditional correlation models for the pair Hamburg-Berlin in terms of fit. In our study, we see no evidence that an asymmetric component as suggested by Capiello et al. (2003) is necessary to model conditional correlation dynamics.

Furthermore, the flexible dynamic correlation models provide very similar results. The parameter estimates of  $\psi$  are very small throughout all five dynamic conditional correlation models. For the three flexible dynamic correlation models, the parameter estimates of  $\phi$  are large and significant for the pair Echterdingen-Berlin. By contrast, they are not significant for the pair Hamburg-Berlin. For the pair Hamburg-Berlin, it seems, that it is only the yearly seasonality that really counts throughout the flexible dynamic correlations models.

In practice, an energy supplier may often wish to isolate his volumetric risk to more than one location. In such a case, the analysis can become trivariate and even higher dimensional which disqualifies the flexible dynamic correlation models because they only work in the bivariate case, whereas DCC models in spirit to Engle (2002) are designed for high dimensional multivariate GARCH, too.

In the bivariate case, conditional correlations can strongly differ across the different model versions. This seems to be particularly true if conditional correlations display strong seasonality patterns as in the case of Hamburg and Berlin.

In such a case, one may wish to base model selection not only on in-sample fit. In addition, the density of bivariate temperature time series generated by the different DCC model versions could be estimated by means of a Monte Carlo simulation. These estimated densities could be then compared to the empirical density of the actually measured temperature data.

Diebold, Hahn and Tay (1999) advocate a more sophisticated approach which entails to evaluate multivariate density forecasts using an integral transform dating back to Rosenblatt (1952).

Table 4.4.1: Summary In-Sample Fit : DCC Models by Engle (2002) and Capiello et al. (2003), ( Two- step estimation ).

	Symmetric DCC	
	Echterdingen-Berlin	Hamburg- Berlin
$\phi$	0.084 (0.013)	0.091 (0.010)
$\psi$	0.421 (0.110)	0.398 (0.092)
LL	-22189.25	-21078.05
SC	8.5410	8.1190

*Note that \* means not significant at the 5 % level.*

Table 4.4.2: Summary In-Sample Fit : DCC Models by Engle (2002) and Capiello et al. (2003), ( Two- step estimation ).

	Asymmetric DCC	
	Echterdingen-Berlin	Hamburg- Berlin
$\phi$	0.083 (0.014)	0.085 (0.011)
$\psi$	0.408 (0.110)	0.321 (0.094)
$\nu$	0.011* (0.024)	0.041* (0.021)
LL	-22189.15	-21076.53
SC	8.5426	8.1201

*Note that \* means not significant at the 5 % level.*

Table 4.4.3: Summary In-Sample Fit: DCC Models by Engle (2002) and Capiello et al. (2003), ( QML ).

	Symmetric DCC	
	Echterdingen-Berlin	Hamburg- Berlin
$\phi$	0.068 (0.013)	0.059 (0.018)
$\psi$	0.473 (0.120)	0.652 (0.078)
LL	-22122.79	-20836.03
SC	8.5189	8.0280

*Note that \* means not significant at the 5 % level.*

Table 4.4.4: Summary In-Sample Fit: DCC Models by Engle (2002) and Capiello et al. (2003), ( QML ).

	Asymmetric DCC	
	Echterdingen-Berlin	Hamburg- Berlin
$\phi$	0.068 (0.014)	0.063 (0.011)
$\psi$	0.473 (0.120)	0.674 (0.071)
$\nu$	-0.002* (0.026)	-0.021* (0.014)
LL	-22122.85	-20835.81
SC	8.5205	8.0296

Note that \* means not significant at the 5 % level.

Table 4.4.5: Summary In-Sample Fit : Satchell and Christodoulakis (2002), equation(4.4.11).

	Two- step estimation	
	Echterdingen-Berlin	Hamburg- Berlin
$\omega_{12}$	0.140 (0.048)	0.950 (0.191)
$\phi$	0.042 (0.009)	0.019 (0.007)
$\psi$	0.662 (0.108)	-0.196* (0.228)
$\nu$	-0.007* (0.019)	0.070 (0.022)
$\lambda_{s,1}^*$	0.013* (0.007)	0.024* (0.018)
$\lambda_{c,1}^*$	0.009* (0.006)	0.175 (0.040)
LL	-22202.82	-21074.280
SC	8.5528	8.1241

Note that \* means not significant at the 5 % level.

Table 4.4.6: Summary In-Sample Fit : Satchell and Christodoulakis (2002), equation(4.4.11).

	QML	
	Echterdingen-Berlin	Hamburg- Berlin
$\omega_{12}$	0.152 (0.061)	1.334 (0.349)
$\phi$	0.033 (0.009)	0.010* (0.008)
$\psi$	0.675 (0.122)	-0.411* (0.358)
$\nu$	0.004* (0.019)	0.040* (0.023)
$\lambda_{s,1}^*$	0.013* (0.008)	0.054* (0.030)
$\lambda_{c,1}^*$	0.009* (0.007)	0.214 (0.062)
LL	-22131.05	-20827.10
SC	8.5286	8.0311

Note that \* means not significant at the 5 % level.

Table 4.4.7: Summary In-Sample Fit : Baur (2006), equation(4.4.12).

	Two- step estimation	
	Echterdingen-Berlin	Hamburg-Berlin
$\omega_{12}$	0.155 (0.052)	1.040 (0.211)
$\phi$	0.049 (0.011)	0.029 (0.010)
$\psi$	0.636 (0.111)	-0.177* (0.223)
$\nu$	-0.004* (0.022)	0.095 (0.030)
$\lambda_{s,1}^*$	0.010* (0.007)	0.034* (0.025)
$\lambda_{c,1}^*$	-0.004* (0.022)	0.230 (0.053)
LL	-22202.50	-21074.72
SC	8.5526	8.1243

Note that \* means not significant at the 5 % level.

Table 4.4.8: Summary In-Sample Fit : Baur (2006), equation(4.4.12).

	QML	
	Echterdingen-Berlin	Hamburg- Berlin
$\omega_{12}$	0.158 (0.063)	1.479 (0.420)
$\phi$	0.039 (0.011)	0.017* (0.012)
$\psi$	0.674 (0.120)	-0.349* (0.368)
$\nu$	0.003* (0.021)	0.062 (0.036)
$\lambda_{s,1}^*$	0.010* (0.008)	0.077* (0.044)
$\lambda_{c,1}^*$	0.003* (0.021)	0.299 (0.093)
LL	-22130.92	-20827.83
SC	8.5285	8.0315

Note that \* means not significant at the 5 % level.

Table 4.4.9: Summary In-Sample Fit : Kosater (2006), equation(4.4.13).

	Two- step estimation	
	Echterdingen-Berlin	Hamburg- Berlin
$\omega_{12}$	0.299 (0.089)	2.265 (0.456)
$\phi$	0.135 (0.028)	0.139 (0.043)
$\psi$	0.532 (0.120)	-0.143* (0.203)
$\nu$	0.017* (0.056)	0.349 (0.118)
$\lambda_{s,1}^*$	0.104 (0.041)	0.109* (0.077)
$\lambda_{c,1}^*$	0.045* (0.042)	0.709 (0.081)
LL	-22201.09	-21075.55
SC	8.5521	8.1246

Note that \* means not significant at the 5 % level.

Table 4.4.10: Summary In-Sample Fit : Kosater (2006), equation(4.4.13).

	QML	
	Echterdingen-Berlin	Hamburg- Berlin
$\omega_{12}$	0.299 (0.114)	3.853 (1.139)
$\phi$	0.109 (0.030)	0.081* (0.057)
$\psi$	0.614 (0.130)	-0.340* (0.369)
$\nu$	0.023* (0.058)	0.263* (0.159)
$\lambda_{s,1}^*$	0.122 (0.053)	0.264 (0.131)
$\lambda_{c,1}^*$	0.057* (0.053)	0.967 (0.131)
LL	-22130.49	-20828.99
SC	8.5284	8.0319

*Note that \* means not significant at the 5 % level.*

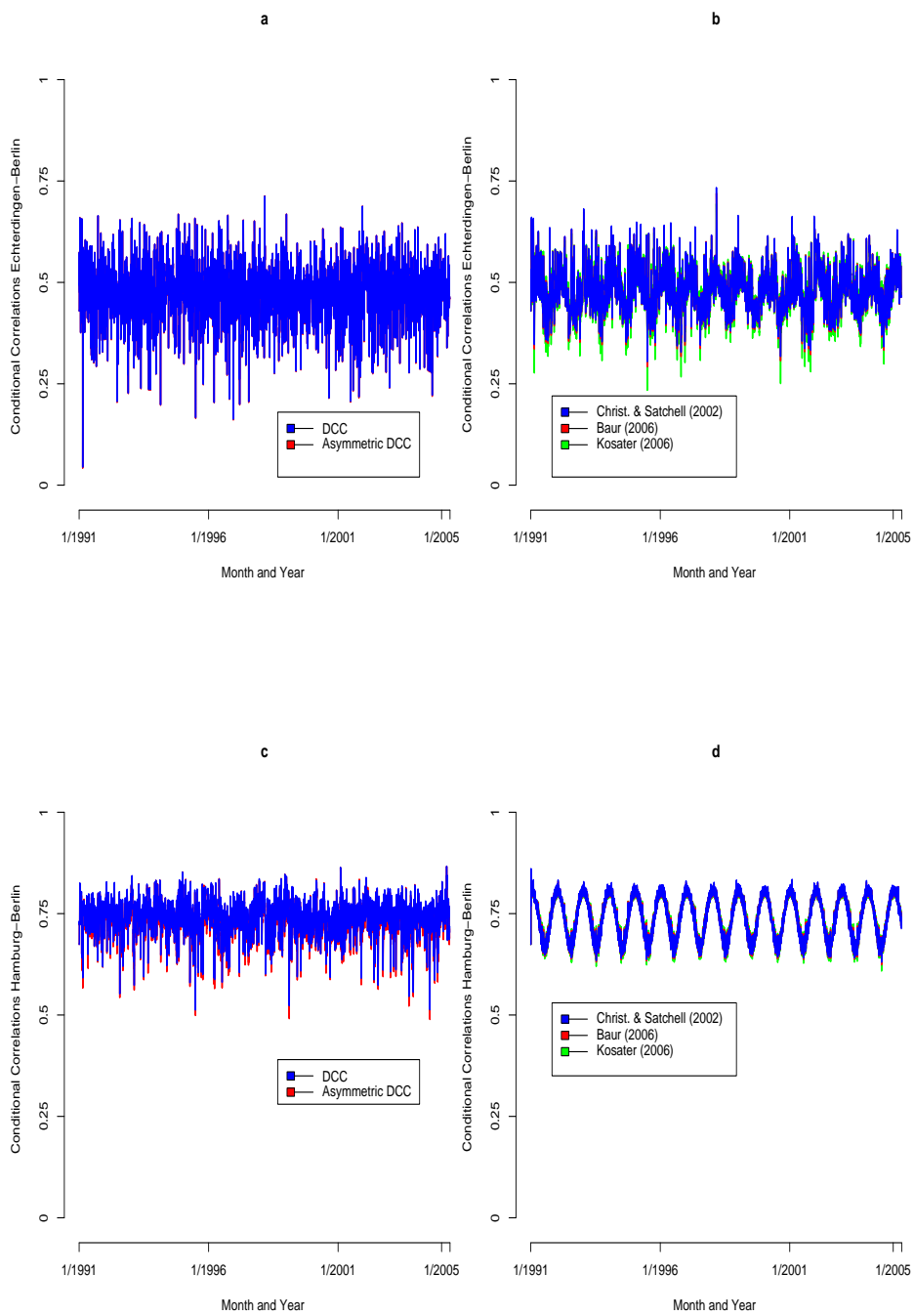


Figure 4.4.1: Conditional correlations estimated by QML: DCC and Asymmetric DCC Echterdingen-Berlin (a), FDC Echterdingen-Berlin (b), DCC and Asymmetric DCC Hamburg-Berlin (c), FDC Hamburg-Berlin (d).

## 4.5 Forecasting Conditional Correlations

In this section, we discuss forecasting of conditional correlations with the dynamic conditional correlation models which have been introduced in section 4.4.

Following Engle (2002) the h-step ahead forecast  $Q_{t+h}^f$  is,

$$Q_{t+h}^f = (1 - \phi - \psi)\bar{Q} + \phi E[\mathbf{u}_{t+h-1}\mathbf{u}_{t+h-1}' | \mathcal{F}_t] + \psi Q_{t+h-1}, \quad (4.5.1)$$

where  $E[\mathbf{u}_{t+h-1}\mathbf{u}_{t+h-1}' | \mathcal{F}_t] = R_{t+h-1}$  and  $R_{t+h-1} = (Q_{t+h-1}^*)^{-1}Q_{t+h-1}(Q_{t+h-1}^*)^{-1}$ . Engle and Sheppard (2001) point out that the h-step ahead forecast of the correlation cannot be directly solved to provide a convenient method for forecasting. Hence, they suggest two forecasts, each requiring a different set of approximations. The first technique is to approximate  $E[\mathbf{u}_{t+i}\mathbf{u}_{t+i}' | \mathcal{F}_t] \approx Q_{t+i}$ . Consequently, we obtain the following h-step ahead forecast for the symmetric DCC model,

$$Q_{t+h}^f = E[Q_{t+h} | \mathcal{F}_t] = \sum_{i=0}^{h-2} (1 - \phi - \psi)\bar{Q}(\phi + \psi)^i + (\phi + \psi)^{h-1}Q_{t+1}. \quad (4.5.2)$$

The second technique is based on the approximations  $\bar{Q} \approx \bar{R}$  and  $E[Q_{t+1} | \mathcal{F}_t] \approx E[R_{t+1} | \mathcal{F}_t]$ . This approximation enables us to forecast the correlation  $R_{t+h}$  exploiting the relationship,

$$R_{t+h}^f = E[R_{t+h} | \mathcal{F}_t] = \sum_{i=0}^{h-2} (1 - \phi - \psi)\bar{R}(\phi + \psi)^i + (\phi + \psi)^{h-1}R_{t+1}. \quad (4.5.3)$$

Engle and Sheppard (2001) conduct some Monte Carlo experiments to assess the forecasts of the two methods. They find that neither of the techniques outperforms the other. Therefore, they suggest to take the second technique which directly forecasts  $R_t$ , since this method is easier to implement.

The outlined results of Engle and Sheppard (2001) only hold for the symmetric DCC model. Albeit the asymmetric extension suggested by Capiello et al.(2003) performs poorly, it may be useful for other temperature time series. Therefore, we outline our forecasting procedure with the asymmetric DCC model in the next subsection.

### 4.5.1 Forecasting Correlations in Asymmetric DCC Models

We put forward to recursively compute the h- step ahead forecast, where  $h \geq 2$ , as follows,

$$Q_{t+h}^f = \left( \bar{Q} - \phi\bar{Q} - \psi\bar{Q} - vE[\eta_t\eta_t'] \right) + \phi E[\mathbf{u}_{t+h-1}\mathbf{u}_{t+h-1}' | \mathcal{F}_t] + \psi Q_{t+h-1} + vE[\eta_{t-h+1}\eta_{t-h+1}' | \mathcal{F}_t] \quad (4.5.4)$$

$$Q_{t+h}^f = \left( \bar{Q} - \phi\bar{Q} - \psi\bar{Q} - vE[\eta_t\eta_t'] \right) + (\phi + \psi + 0.5 \cdot v) Q_{t+h-1}. \quad (4.5.5)$$

Here, we add some explanation why the above relation holds. We assume that the  $u_{i,t}, i \in \{1, 2\}$  are symmetric around 0. Therefore it holds,

$$E[\eta_{t-h+1}\eta_{t-h+1}' | \mathcal{F}_t] = 0.5 \cdot E[\mathbf{u}_{t+h-1}\mathbf{u}_{t+h-1}' | \mathcal{F}_t] + 0.5 \cdot 0 \approx 0.5 \cdot Q_{t+h-1}. \quad (4.5.6)$$

## 4.5.2 Forecasting Correlations in the Flexible Dynamic Correlation Models.

Due to the transformation which ensures that correlations are in the interval between -1 and 1, the forecasting procedure is not straightforward. For the sake of simplicity, we suggest to assume,

$$E[u_{1,t+h-1}u_{2,t+h-1}|\mathcal{F}_t] \approx r_{12,t+h-1}^* . \quad (4.5.7)$$

Consequently, we can further deduce,

$$E[\eta_{1,t-h+1}\eta_{2,t-h+1}|\mathcal{F}_t] = 0.5 \cdot E[u_{1,t+h-1}u_{2,t+h-1}|\mathcal{F}_t] + 0.5 \cdot 0 \quad (4.5.8)$$

$$E[\eta_{1,t-h+1}\eta_{2,t-h+1}|\mathcal{F}_t] \approx 0.5 \cdot r_{12,t+h-1}^* . \quad (4.5.9)$$

Finally, we can recursively compute forecasts as follows,

$$\begin{aligned} r_{12,t+h}^{*,f} &= \omega_{12} + \lambda_{c,1}^* \cos(2\pi \frac{d_{t+h}}{365}) + \lambda_{s,1}^* \sin(2\pi \frac{d_{t+h}}{365}) + \phi E[u_{1,t+h-1}u_{2,t-1}|\mathcal{F}_t] \\ &\quad + \psi r_{12,t+h-1}^* - \nu E[\eta_{1,t-1}\eta_{2,t-1}|\mathcal{F}_t] \end{aligned} \quad (4.5.10)$$

$$\begin{aligned} r_{12,t+h}^{*,f} &= \omega_{12} + \lambda_{c,1}^* \cos(2\pi \frac{d_{t+h}}{365}) + \lambda_{s,1}^* \sin(2\pi \frac{d_{t+h}}{365}) \\ &\quad + (\phi + \psi - 0.5 \cdot \nu) r_{12,t+h-1}^* . \end{aligned} \quad (4.5.11)$$

The actual forecast  $r_{12,t+h}^f$  is then calculated by applying one of the transformation functions proposed by Christodoulakis and Satchell (2002), Baur (2006) or Kosater (2006), see equations (4.4.11-4.4.13).

In figure 4.5.1, we present point forecasts and forecasted 99% two-sided confidence intervals for temperature from Hamburg for the HDD period from 11/01/2004 until 03/31/2005 based on the 31<sup>st</sup> of October 2004 as the forecast origin. We have carried out the study with estimates from quasi maximum likelihood estimation of the different five bivariate GARCH models to prove that they yield very similar results with respect to forecasts of the conditional mean and the conditional variance, respectively.

Why do we opt for data from Hamburg ? In the univariate study, standardized residuals of the temperature time series from Hamburg exhibited the largest departure from normality throughout all four considered univariate models. Therefore, we expect the data from Hamburg to be the biggest challenge. Indeed, we can see that more than 1% of the actual data exceeds the confidence bounds. However, we should bear in mind that also the confidence bounds themselves are only forecasts. By this, the results are quite encouraging.

Finally, figures 4.5.2 and 4.5.3 present the estimated conditional correlations for the forecast period together with the point forecasts for the five dynamic conditional correlation models of interest.

The conditional correlations provided by the flexible dynamic correlation models are less volatile around their long-run mean than those provided by the dynamic conditional correlation models of Engle (2002) and Capiello (2003). This is especially true for the pair Hamburg-Berlin and a consequence of the choice of the transformation function. Despite the good in-sample fit for the pair Echterdingen-Berlin, the model based on the transformation suggested by Kosater (2006) in

this thesis yields the worst forecasts of the conditional correlations. The forecasted long-run level is too high. The model based on the Fisher transformation of Christodoulakis and Satchell (2002) seems to perform best with regard to forecasting the trend of conditional correlations.

The figures 4.5.2 and 4.5.3 indicate that conditional correlations may notably deviate from the long-run mean. Consequently, confidence intervals for the point forecasts of conditional correlations may help in practical work.

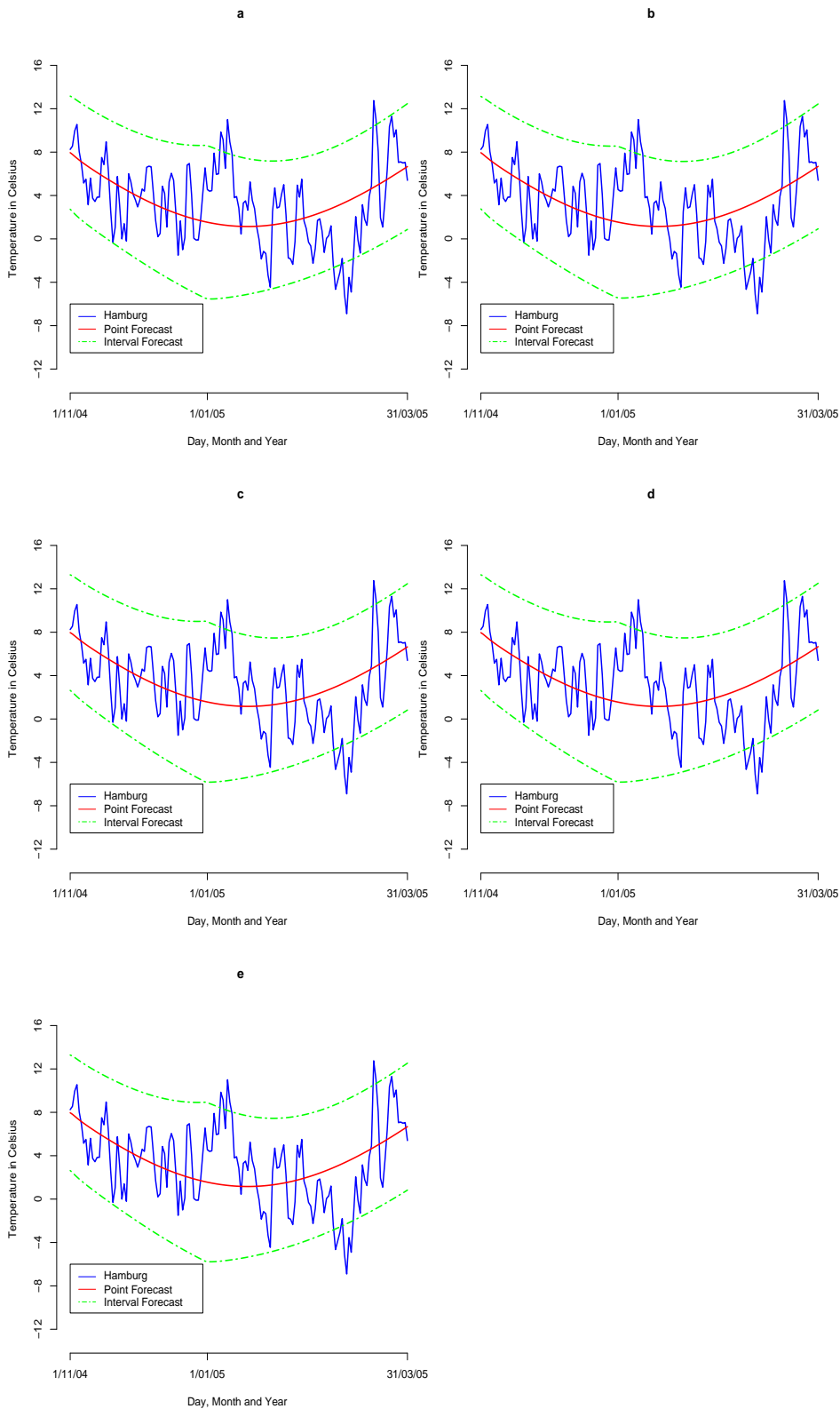


Figure 4.5.1: Point and interval forecasts ( 99 %) for the HDD period 11/01/2004 until 03/31/2005 for Hamburg from : the symmetric DCC (a), the asymmetric DCC (b), FDC of Christodoulakis and Satchell (2002) (c), FDC of Baur (2006) (d), FDC of Kosater (2006)(e).

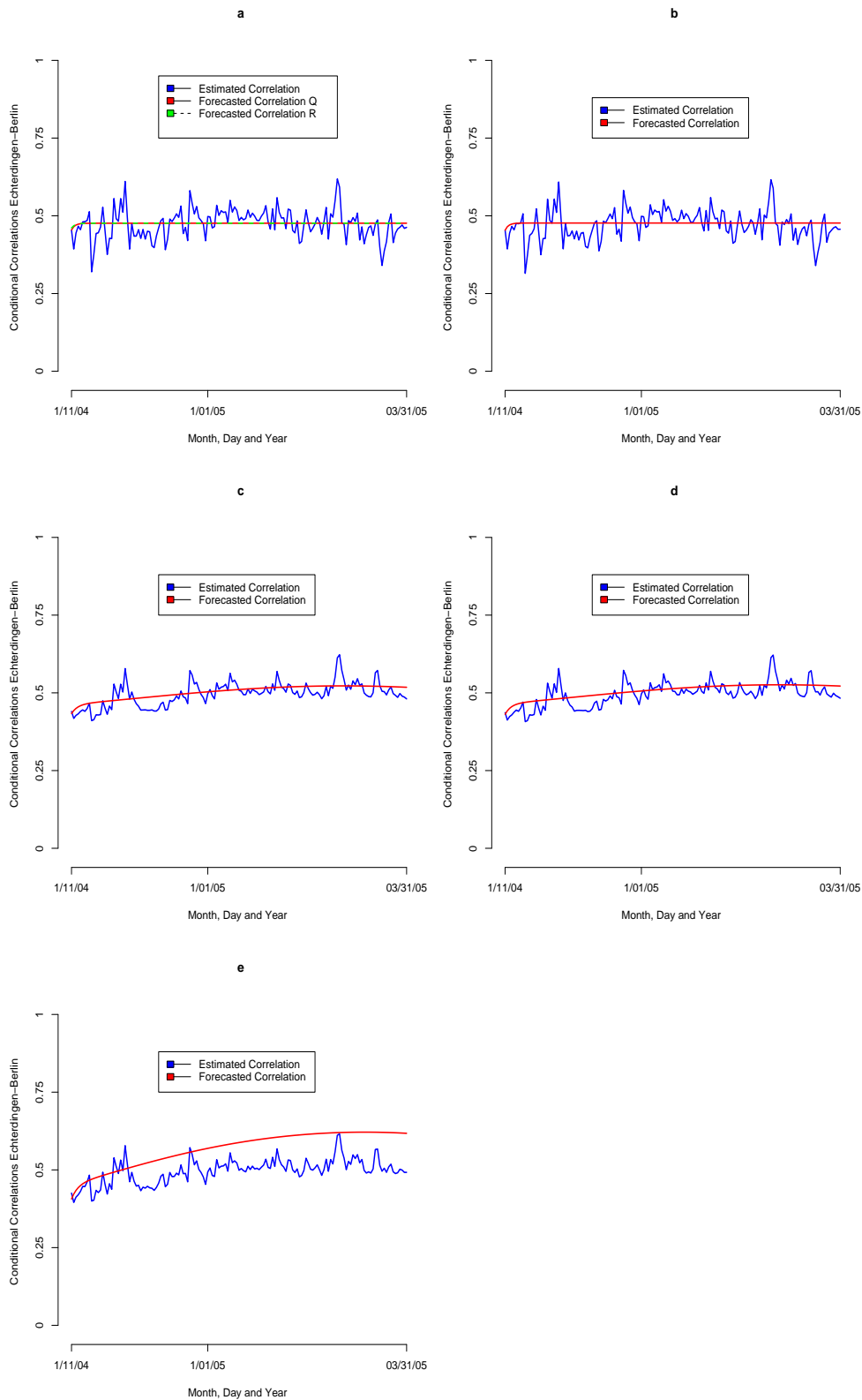


Figure 4.5.2: Point forecasts of the conditional correlations for the HDD period 11/01/2004 until 03/31/2005 for Echterdingen-Berlin from : the symmetric DCC (Forecast Q corresponds to equation (4.5.2) and Forecast R corresponds to equation (4.5.3) ) (a), the asymmetric DCC (b), FDC of Christodoulakis and Satchell (2002) (c), FDC of Baur (2006) (d), FDC of Kosater (2006) (e).

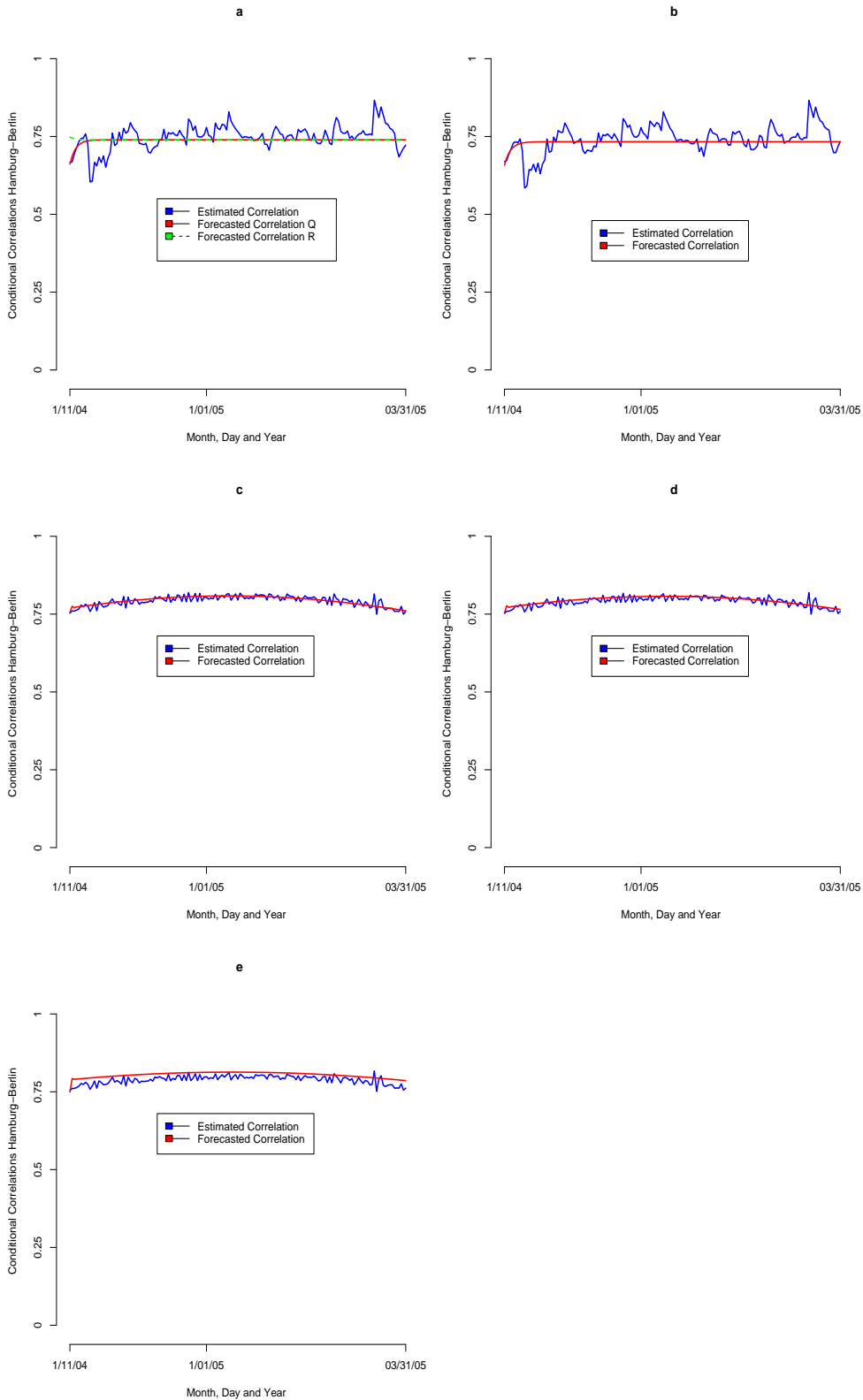


Figure 4.5.3: Point forecasts of conditional correlations for the HDD period 11/01/2004 to 03/31/2005 for Hamburg-Berlin from : the symmetric DCC (Forecast Q corresponds to equation (4.5.2) and Forecast R corresponds to equation (4.5.3))(a), the asymmetric DCC (b), FDC of Christodoulakis and Satchell (2002) (c), FDC of Baur (2006) (d), FDC of Kosater (2006)(e).

## 4.6 Cross-City Hedging

In this section, we want to discuss how the presented methodology can be used. We do this from the angle of an electricity supplier who wants to hedge his volume risk at non-traded locations such as Echterdingen or Hamburg constructing a hedge based on HDDs or CDDs computed and accumulated on the temperature measured in Berlin. Recall, HDDs and CDDs are computed as follows,

$$HDD(t_1, t_2) = \sum_{t=t_1}^{t_2} \max(18.33^\circ - Y_{1,t}, 0), \quad (4.6.1)$$

$$CDD(t_1, t_2) = \sum_{t=t_1}^{t_2} \max(Y_{1,t} - 18.33^\circ, 0), \quad (4.6.2)$$

where  $t_1$  denotes the beginning while  $t_2$  marks the end of the accumulation period and  $Y_{1,t}$  is the daily average temperature measured at the traded station in Berlin. Let  $Y_{2,t}$  be the non-traded location which, in our case, is Echterdingen or Hamburg. For the sake of simplicity and according to our preceding assumptions, we assume that  $Y_{1,t}$  and  $Y_{2,t}$  are conditional bivariate normal distributed according with,

$$\begin{pmatrix} Y_{1,t} \\ Y_{2,t} \end{pmatrix} = \begin{pmatrix} E[Y_{1,t}|\mathcal{F}_{t-1}] \\ E[Y_{2,t}|\mathcal{F}_{t-1}] \end{pmatrix} + \begin{pmatrix} \epsilon_{1,t} \\ \epsilon_{2,t} \end{pmatrix} \quad (4.6.3)$$

and

$$\begin{pmatrix} \epsilon_{1,t} \\ \epsilon_{2,t} \end{pmatrix} \sim \mathbf{N} \left( \begin{pmatrix} 0 \\ 0 \end{pmatrix}, \begin{pmatrix} h_{11,t} & h_{12,t} \\ h_{21,t} & h_{22,t} \end{pmatrix} \right).$$

The assumption of bivariate normality is to some extent heroic but not completely unrealistic given our univariate studies. Furthermore, it offers the advantage that the distribution of  $\{Y_{1,t}|Y_{2,t} = y_{2,t}\}$  is a univariate normal distribution,

$$\{Y_{1,t}|y_{2,t}\} \sim N \left( E[Y_{1,t}|\mathcal{F}_{t-1}] + r_{12,t} \frac{\sqrt{h_{11,t}}}{\sqrt{h_{22,t}}} (y_{2,t} - E[Y_{2,t}|\mathcal{F}_{t-1}]), h_{11,t}(1 - r_{12,t}^2) \right). \quad (4.6.4)$$

The relation in equation (4.6.4) enables the electricity supplier to construct forecast intervals for  $Y_{1,t}$  if he can predict how  $Y_{2,t}$  evolves at  $t$ . In the preceding section we have seen that the electricity supplier can predict  $Y_{2,t}$  with forecast intervals obtained from a time series model.

For example, she may expect the temperature to be  $6.1^\circ$  on a certain day  $t$ . Using the bivariate GARCH model, she immediately obtains that with probability  $\alpha$ , temperature  $Y_{1,t}$  will lie in the interval  $I_{1,t,\alpha} = [Y_{1,t,low}; Y_{1,t,high}]$ . Henceforth, she can estimate the relation between temperature realizations  $y_{2,t}$  at the non-traded locations and HDDs or CDDs based on temperature in Berlin on a daily scale.

More precisely, let us consider a conditional HDD based on  $Y_{1,t}$  and conditioned on  $Y_{2,t} = y_{2,t}$ . Moreover, let  $Z_t^* = 18.33^\circ - \{Y_{1,t}|Y_{2,t} = y_{2,t}\}$ . In addition, we denote,

$$Z_t = \begin{cases} 0 & \text{if } Z_t^* \leq 0, \\ Z_t^* & \text{if } Z_t^* > 0. \end{cases} \quad (4.6.5)$$

Obviously,  $Z_t$  corresponds to the value of a daily HDD( $t_1, t_1$ ). Moreover, we obtain

$$\begin{aligned} Prob(Z_t = 0) &= Prob(\{Y_{1,t}|Y_{2,t} = y_{2,t}\} \geq 18.33^\circ) \\ &= 1 - \Phi_{Norm}(18.33^\circ). \end{aligned} \quad (4.6.6)$$

$$\begin{aligned}
\text{Prob}(0 \leq Z_t \leq z_t) &= \text{Prob}(18.33^\circ - z_t \leq \{Y_{1,t}|Y_{2,t} = y_{2,t}\} \leq 18.33^\circ)(4.6.7) \\
&= \Phi_{Norm}(18.33^\circ) - \Phi_{Norm}(18.33^\circ - z_t).
\end{aligned}$$

Note that  $\Phi_{Norm}(x)$  is the value at quantile  $x$  of the cumulative conditional normal distribution given in equation (4.6.4).

Hence, equations (4.6.6) and (4.6.7) directly provide probabilities for the daily HDD( $t_1, t_1$ ) given a temperature realization  $y_{2,t}$  at a non-traded location.

In addition, the tick size, which is the amount attached to each HDD or CDD, has to be fixed for each contract. The electricity supplier may know that temperature at Echterdingen is on average  $4.1^\circ$  in winter. Moreover, she may also know that every additional degree above this average temperature is accompanied by a loss of 5000 Euro on average.

Unfortunately, she has to compute a tick size with respect to the temperature dynamics in Berlin. Tick sizes are determined by a least square regression of load on temperature to examine how temperature on average affects demand for electricity. As a result, we obtain a relation between load and temperature which enables us to fix a tick size. The tick size for load at Echterdingen and temperature in Berlin can be determined, analogously.

Although to the best of our knowledge constant tick sizes are typical of temperature contracts, we think that a time-varying tick size may be more realistic. Demand and therefore load exhibit different patterns of seasonality such as inter-daily, weekly and yearly seasonality. As a result, unexpected temperature values can have a very different impact on electricity demand depending on the hour or the type of day, for example. Time-varying tick sizes, however, allow more accurate hedging and can be very easily included in the bivariate GARCH framework. Additionally, daily load information could be brought into play to determine time-varying tick sizes.

## 4.7 Summary

Volumetric risk has become a crucial issue in competitive electricity markets. Especially in the USA, energy companies seek to hedge their volumetric risk. Weather derivatives are attractive instruments which allow to protect from volumetric risk due to unforeseen weather conditions.

In this thesis, we focus on temperature derivatives since over 90 % of weather contracts are struck on heating degree days or cooling degree days that are transformations of daily average temperature. Exchange-based trading mainly takes place at the Chicago Mercantile Exchange, abbreviated CME. To ensure liquidity, contracts at the CME can only be negotiated on temperature from few selected cities. Consequently, market participants who wish to hedge their volumetric risk at non-traded locations cannot buy tailor-made contracts. Hence, they have to correlate their risk with the risk at tradeable cities. Consequently, the correlation between temperature time series from traded locations with temperature from non-traded locations is of special interest.

After a thorough analysis, we have found dynamic conditional correlation models, DCC, to be most appealing among the plethora of competing multivariate

GARCH models for our purposes.

Our main challenge is to integrate seasonality into bivariate GARCH models. DCC models allow for an utmost flexibility in modelling the conditional variance and conditional correlation dynamics, respectively. In addition, the flexible dynamic correlation models even allow to model yearly seasonality of conditional correlations. Moreover, we also present how correlation dynamics can be predicted. Finally, we discuss how our presented methodology may be used by an investor to construct a hedge for a non-traded location.

We think that further research with correlation dynamics should concentrate on the DCC model class, with a special focus on seasonality. The univariate study has revealed that a simple ARMA-GARCH cannot completely capture temperature dynamics. Therefore, in further research the ability of regime-switching models in modelling and forecasting daily average temperature should be investigated.

# Chapter 5

## Conclusion

The subject of this thesis has been the application of non-linear time series models to power risk management.

The first part of this work is sacrificed to the modelling of daily average prices baseload and peakload at the spot market of the European Energy Exchange, EEX. After the presentation of two established models, these models are extended by the introduction of day-dependent spikes. With the inclusion of day-dependent spikes, we take into account that large sized upward spikes are not to be expected on days when demand is usually low.

Additionally, the long- run forecasting ability of the extended models is compared with the original models and a linear model. As a result, we obtain that the extended models clearly outperform the original models as well as the linear model in terms of long-run forecasting. These results have been summarized and recently published in the article of Kosater and Mosler (2006). Moreover, De Jong (2006) confirmed that models with day-dependent spikes are worthwhile in modelling spot prices in several electricity markets in Europe and the USA.

Finally, model extensions of the models with day-dependent spikes are presented which take into account autoregressive conditional heteroscedasticity dynamics.

In the second part, the relation between weather, represented by temperature and wind velocity, and hourly electricity prices from the EEX in Leipzig is investigated. Furthermore, it is assessed whether the relation between weather and prices can be successfully exploited for short-term forecasting. The study is carried out with the Markov regime-switching model with day-dependent and independent spikes. As a result, a strong relationship between weather and hourly prices is detected, on one hand. On the other hand, the significance of this relation for forecasting is confined to certain hours. Some earlier results on the topic which is discussed in the second part have been published in Kosater (2006).

In the third part, cross-city hedging with weather derivatives is addressed. Weather derivatives can be bought by electricity suppliers to protect from revenue uncertainties due to unexpected weather conditions. The special focus is on temperature derivatives. Since temperature contracts at the Chicago Mercantile Exchange can only be negotiated for weather variables measured at few selected locations, electricity supplier have to correlate their risk at non-traded locations with the risk at tradeable locations.

Here, the usefulness of bivariate GARCH models with dynamic conditional correlations in modelling the correlation between non-traded and traded temperature time series is examined.

Due to their flexibility in modelling the conditional variance and conditional correlation dynamics, the study is carried out with dynamic conditional correlation models. Moreover, forecasting of conditional correlation dynamics is discussed. The discussion on constructing a cross-city hedge with the support of bivariate GARCH models with dynamic conditional correlations concludes the third part.

With regard to the first part, the suggested models with autoregressive conditional heteroscedasticity could be tested on a wider set of electricity markets. In addition, the usefulness of more sophisticated Markov regime-switching ARMA-GARCH models could be examined.

Furthermore, we think that aspects of multivariate analysis hold promise for future work. The European electricity markets tend towards their unification. Multivariate approaches which take into account correlations between the different markets may be an asset for portfolio management and risk management.

With respect to the second part, the study could be extended to examine the impact of weather on electricity spot prices on a wider set of international electricity spot markets. Moreover, weather variables such as precipitation could be taken into consideration. With regard to the Scandinavian exchange Nord Pool, we expect the impact of precipitation to be very important, since the share of hydro power on total generation capacity is around 51%.

As aforementioned, load and the reserve margin should be incorporated in a good model specification. The general impact of weather on prices should be specified more precisely taking into account the four seasons or even the different months of the year. Finally, the relation between spot prices and wind velocity may be worthwhile to examine.

To conclude, with correlation dynamics should concentrate on the DCC model class, with a special focus on seasonality. The univariate study has revealed that a simple ARMA-GARCH model cannot completely capture temperature dynamics. Therefore, in further research the ability of regime-switching models in modelling and forecasting daily average temperature should be investigated.

# Bibliography

- [1] ANDERSON L, MARCUS B, DAVISON M, ANDERSON K : Development of a hybrid model for electrical power spot prices.*IEEE Transactions on Power Systems*, 17(2) (May 2002), 257-264.
- [2] ANGELES CARNERO M, KOOPMAN JS, OOMS M : Periodic heteroskedastic RegARFIMA models for daily electricity spot prices. *Journal of the American Statistical Association*, 2007, forthcoming.
- [3] BABA Y, ENGLE RF, KRAFT D, KRONER KF: Multivariate simultaneous GARCH. San Diego, Department of Economics. Working paper. 1991.
- [4] BAILLIE RT, BOLLERSLEV T: Prediction in dynamic models with time dependent conditional variances.*Journal of Econometrics*,52 (1992), 91-113.
- [5] BAUR D.: A flexible dynamic correlation model.*Advances in Econometrics ( Part A ) : Econometric analysis of financial and economic time series*, 20 (2006).
- [6] BAUWENS L, LAURENT S, ROMBOUTS JVK: Multivariate GARCH models : A survey.*Journal of Applied Econometrics*, 21 (2006), 79-109.
- [7] BERNDT EK, HALL RE, HAUSMAN JA : Estimation and inference in nonlinear structural models. *Annals of Economic and Social Measurement*, 3 (1974), 653-665.
- [8] BHANOT K: Behaviour of power prices: implications for the valuation and hedging of financial contracts. *Journal of Risk*, 2(3) 2000, 43-62.
- [9] BIERBRAUER M, TRÜCK S, WERON R : Modeling electricity prices with regime switching models.*Lecture Notes in Computer Science*, 3039 (2004), 859-867.
- [10] BOLLERSLEV, T : Generalized conditional heteroskedasticity. *Journal of Econometrics*, 81 (1986), 307-327.
- [11] BOLLERSLEV T: Modelling the coherence in short-run nominal exchange rates: A multivariate generalized ARCH model.*Review of Economics and Statistics*, 72 (1990), 498-505.
- [12] BOLLERSLEV T, ENGLE RF, WOOLDRIDGE JM: A capital asset pricing model with time-varying covariances.*Journal of Political Economy*, 96 (1988), 116-131.

- [13] BROCKWELL AE, RAMBHARAT BR, SEPPI DJ : A threshold autoregressive model for wholesale electricity prices. *Journal of the Royal Statistical Society Series C*, 54(2) (2005), 287-299.
- [14] BRODY DC, SYROKE J, ZERVOS M: Dynamic pricing of weather derivatives. *Quantitative Finance*, 2 (2000), 189-198.
- [15] BUNN D : Forecasting loads and prices in competitive power markets. *Proc. IEEE*, 88(2) (2000), 163-169.
- [16] BURGER M, KLAR B, MÜLLER A, SCHINDLMAYER G: A spot market model for pricing derivatives in electricity markets. *Quantitative Finance* 4 (2004), 109-122.
- [17] CAI J: A Markov model of switching-regime ARCH. *Journal of Business and Economic Statistics*, 12 (1994), 309-316.
- [18] CAMPBELL, S.& DIEBOLD FRANCIS X.: Weather Forecasting for Weather Derivatives , *Journal of the American Statistical Association*, 100 (2005), No. 469, 6-16.
- [19] CAO M, LI A, WEI J: Watching the weather report. *Canadian Investment Review*, 17(2) (2004), 27-33.
- [20] CAO M, WEI J: Pricing the weather. *Risk*, 67 (May 2000), 67-70.
- [21] CAO & WEI : Weather Derivatives valuation and market price of weather risk *The Journal of Futures Markets*, 24 (2004), No. 11, 1065-1089.
- [22] CAPIELLO L, ENGLE RF, SHEPPARD K: Asymmetric Dynamics in the correlations of global equity and bond returns. European Central Bank. Working Paper No. 204. 2003.
- [23] CHEN C, LIU LM: Joint estimation of model parameters and outlier effects in time series. *Journal of the American Statistical Association*, 88 (1993), 284-297.
- [24] CLEMENTS MP, KROLZIG HM. A comparison of the forecast performance of Markov-Switching and Treshold Autoregressive models of US GNP. *Econometrics Journal* 1 (1998) , C47 - C57.
- [25] CLEWLOW L, STRICKLAND C. Energy Derivatives - Pricing and Risk Management. *Lacima Publications* 2000. London.
- [26] CHRISTODOULAKIS GA, SATCHELL SE: Correlated ARCH: Modelling the time-varying correlation between financial asset returns. *European Journal of Operations Research*, 139 (2002), 351-370.
- [27] CUARESMA JC, HLOUSKOVA J, KOSSMEIER S, OBERSTEINER M : Forecasting electricity spot prices using linear univariate time series models. *Applied Energy*, 77 (2004), 87-106.
- [28] DAVIS, M.: Pricing Weather Derivatives by marginal value *Quantitative Finance*, 1 (2001), 1-4.

- [29] DE JONG C: The nature of power spikes: A regime-switch approach. *Studies in Nonlinear Dynamics and Econometrics*, 10(3) (2006).
- [30] DE JONG C, HUISMAN R : Option pricing for power prices with spikes. *Energy Power and Risk Management*, 7 (2003), 12-16.
- [31] DIEBOLD FX, HAHN J, TAY AS: Multivariate density forecast evaluation and calibration in financial risk management: High-frequency returns on foreign exchange. *The Review of Economics and Statistics*, 81(4) (1999), 661-673.
- [32] DISCHEL B: Black-Scholes won't do. *Risk*, October 1998, 8-9.
- [33] DUFFIE D, GRAY S: Volatility in Energy Prices *Managing Energy Price Risk*, Robert Jameson, ed., Risk Publications, London. 1995.
- [34] ENGLE RF : Autoregressive conditional heteroscedasticity with estimates of the variance of United Kingdom inflation. *Econometrica*, 50 (1982), 987-1007.
- [35] ENGLE RF: Dynamic conditional correlation - A simple class of multivariate Garch models. *Journal of Business and Economic Statistics*, 20 (2002), 339-350.
- [36] ENGLE RF, KRONER KF. Multivariate simultaneous generalized arch. *Econometric Theory*, 11 (1995), 122-150.
- [37] ENGLE RF, MEZRICH J: Garch for groups. *RISK*, 9 (1996), 36-40.
- [38] ENGLE RF, NG VK: Measuring and testing the impact of news on volatility. *Journal of Finance*, 48 (1993), 1749-1788.
- [39] ENGLE RF, SHEPPARD K: Theoretical and empirical properties of dynamic conditional correlation multivariate Garch. UCSD. Discussion Paper No. 2001-15. 2001.
- [40] ESCRIBANO A, PENA I, VILLAPLANA P : Modelling electricity prices: International evidence. Universidad Carlos III de Madrid. Working paper. 2002.
- [41] ETHIER R, MOUNT T : Estimating the volatility of spot prices in restructured electricity markets and the implications for option values. Cornell University, Ithaca New York. Working Paper. 1998.
- [42] EViews 5.1. Quantitative Micro Software, LLC. *Irvine California*. 1994-2004.
- [43] FEDERICO T, LERCH F : Gefühlter Wind. *Marktplatz Energie*, 5 (2002), 10-15.
- [44] FILARDO AJ : Business-cycle phases and their transitional dynamics. *Journal of Business & Economic Statistics*, 12 (1994), 299-308.
- [45] FILARDO AJ : Choosing information variables for transition probabilities in a time-varying transition probability Markov switching model. Federal Reserve Bank of Kansas City. Working Paper 98-09. 1998.
- [46] FRANCES PH, VAN DIJK D: Forecasting stock market volatility using nonlinear GARCH models. *Journal of Forecasting*, 15 (1996), 229-235.

- [47] FRANSES PH, NEELE J, VAN DIJK D: Modeling asymmetric volatility in weekly Dutch temperature data. *Environmental Modelling & Software* , 16 (2001), 131-137.
- [48] FRANSES PH, VAN DIJK D: Non-linear time series models in empirical finance. *Cambridge University press*, Cambridge, 2000.
- [49] GLOSTEN LR, JAGANNATHAN R, RUNKLE D: On the Relation between the Expected Value and the Volatility of the Nominal Excess Return on Stocks. *Journal of Finance*, 48 (1993), 1779-1801.
- [50] GRAY SF: Modelling the conditional distribution of interest rates as a regime-switching process. *Journal of Financial Economics*, 42 (1996), 27-62.
- [51] HAAS M, MITTNIK S, PAOLELLA M: A new approach to Markov switching Garch models. *Journal of Financial Econometrics*, 2(4) (2004), 493-530.
- [52] HAFNER CM, FRANSES PH: A generalized dynamic conditional correlation model for many assets. Erasmus University Rotterdam. Econometric Institute Report EI 2003-18.2003.
- [53] HAFNER CM, VAN DIJK D, FRANSES PH: Semi-Parametric modelling of correlation dynamics. *Advances in Econometrics ( Part A ): Econometric analysis of financial and economic time series*, 20 (2006).
- [54] HAMILTON JD : A new approach to the economic analysis of nonstationary time series and the business cycle. *Econometrica*, 57 (1989), 357-384.
- [55] HAMILTON JD : Analysis of time series subject to change in regime. *Journal of Econometrics*, 45 (1990), 39-70.
- [56] HAMILTON JD, SUSMEL R: Autoregressive conditional heteroscedasticity and changes in regime. *Journal of Econometrics*, 64 (1994), 307-333.
- [57] HUISMAN R, MAHIEU R : Regime jumps in electricity prices. *Energy Economics*, 25 (2003), 425-434.
- [58] JARQUE CM, BERA AK: A Test for normality of Observations and regression residuals. *International Statistical Review* , 55(2) (1987), 163-172.
- [59] JOHNSON B, BARZ G: Selecting Stochastic Processes for Modelling Electricity Prices. *Energy modelling and the Management of Uncertainty*, (London: Risk Books ). 1999, 3-22.
- [60] JONDEAU E, ROCKINGER M: The copula-GARCH model of conditional dependencies: An international stock-market application. *Journal of International Money and Finance*, 2005.
- [61] KIM CJ : Dynamic linear models with Markov-switching. *Journal of Econometrics*, 60 (1994), 1-22.
- [62] KNITTEL CR, ROBERTS MR : An empirical examination of deregulated electricity prices. *Energy Economics*, 27(5) (2005), 791-817.

- [63] KOSATER P: Does weather affect German hourly power prices ? *Proceedings of the European Electricity Market EEM-06 Conference* Warszawa, (2006), 279-286.
- [64] KOSATER P, MOSLER K : Can Markov regime-switching models improve power price forecasts ? Evidence from German daily power prices. *Applied Energy*, 83(9) (2006), 943-958.
- [65] KRONER KF, NG VK: Modeling asymmetric comovements of asset returns. *The Review of Financial Studies*, 11(4) (1998), 817-844.
- [66] LUCIA JJ, SCHWARTZ ES : Electricity prices and power derivatives: Evidence from the Nordic Power Exchange. *Review of Derivatives Research*,5 (2002), 5-50.
- [67] MISIOREK A, TRÜCK S, WERON R (2006): Point and interval forecasting of spot electricity prices: Linear vs. non-linear time series models. *Studies in Nonlinear Dynamics and Econometrics*,10(3) (2006).
- [68] MISIOREK A, WERON R : Forecasting spot electricity prices with time series models. *Proceedings of the European Electricity Market EEM-05 Conference* Łódź, (2005), 133-141.
- [69] MOUNT TD, NING Y, CAI X : Predicting price spikes in electricity markets using a regime-switching model with time-varying parameters. *Energy Economics*, 28 (2006), 62-80.
- [70] NELSON DB: Conditional Heteroskedasticity in Asset Returns: A new approach. *Econometrica*, 59 (1991), 347-370.
- [71] PATTON A:Modelling time-varying exchange rate dependence using the conditional copula. University of California, San Diego. Discussion Paper 01-09.2001.
- [72] PELLETIER D: Regime switching for dynamic correlations. *Journal of Econometrics*, 131 (2006), 445-473.
- [73] PILIPOVIC D: *Energy Risk : Valuing and Managing Energy Derivatives*. McGraw- Hill. 1998.
- [74] PIRRONG, C. & JERMAKYAN, M. Valuing Power and Weather Derivatives on a Mesh Using Finite Difference Methods *Energy Modelling & the Management of Uncertainty*. Risk Books. 1999.
- [75] ROSENBLATT M: Remarks on a multivariate transformation. *Annals of Mathematical Statistics*, 23 (1952), 470-472.
- [76] SENTANA E: Quadratic ARCH models. *Review of Economic Studies*, 62 (1995), 639-661.
- [77] SILVENNOINEN A, TERÄSVIRTA T: Multivariate autoregressive conditional heteroskedasticity with smooth transitions in conditional correlations. Stockholm School of Economics. SSE/EFI Working Paper Series in Economics and Finance No. 577.2005.

- [78] TAYLOR JW, BUIZZA R: Comparing Temperature Density Forecasts from GARCH and Atmospheric Models. *Journal of Forecasting*, 23 (2004), 337-355.
- [79] TAYLOR JW, BUIZZA R: Density forecasting for weather derivatives pricing. *International Journal of Forecasting*, 22 (2006), 29-42.
- [80] TOL RJS: Autoregressive conditional heteroscedasticity in daily temperature measurements. *Environmetrics*, 7 (1996), 67-75.
- [81] TORRO H, MENEU V, VALOR E: Single factor stochastic models with seasonality applied to underlying weather derivatives variables. *Journal of Risk Finance*, Summer 2003.
- [82] TSE YK, TSUI AKC: A multivariate GARCH model with time-varying correlations. *Journal of Business and Economic Statistics*, 20 (2002), 351-362.
- [83] VAN DER WEIDE R: GO-GARCH: A multivariate generalized orthogonal GARCH model. *Journal of Applied Econometrics*, 17 (2002), 549-564.
- [84] WERON R., Market price of risk implied by Asian-style electricity options. *Energy Economics*, 2006, submitted.
- [85] ZENG, L. Pricing Weather Derivatives *Journal of Risk Finance*, Spring 2000